COLLAGE OF TECHNOLOGY AND BUILT ENVIRONMENT

SCHOOL OF BUILT ENVIRONMENT

EVALUATING STREET ORIENTATION FOR PEDESTRIAN THERMAL COMFORT THE CASE OF METEHARA TOWN

By

Rorisa Eshetu Debele

A Thesis Submitted for Graduate Studies of Addis Ababa University for the

Partial Fulfilment of the Degree of Master of Science in Urban Design and

Development.

Addis Ababa, Ethiopia

April, 2025

Addis Ababa University

School of Graduate Studies

This is to certify that the thesis prepared by Rorisa Eshetu, entitled: "**Evaluating street orientation for pedestrian thermal comfort the case of Metehara town"** and submitted in partial fulfillment of the requirements for the degree of Masters of Science in Urban Design and Development complies with the regulations of the university and meets the accepted standards concerning originality and quality.

Signed by the Examining Committee:

Advisor: Nebyou Yonas (Ass.Prof) Signature ___________ Date ______

External Examiner: Alazar Assefa (PhD) Signature ___________ Date______

Internal Examiner: Tibebu Assefa (PhD) Signature ___________ Date______

Chairperson: Abunu Arega (PhD) Signature ___________ Date______

Department Head _____________________ Signature ___________ Date______

Declaration

I hereby declare that all information in this document has been obtained and presented in accordance with academic rules and ethical conduct. I also declare that, as required by these rules and conduct, I have fully cited and referenced all materials and results that are not original to this study.

Rorisa Eshetu

Signature: _____________

This is to confirm that the thesis work is complete and the candidate is ready for examination.

Advisor: Nebyou Yonas (Ass.Prof)

Signature: _____________

Abstract

Urban design plays essential role in designing pedestrian thermal comfort, especially in regions going through high temperatures. This research investigates the evaluation of street orientation on pedestrian thermal comfort in Metehara Town, Oromia, Ethiopia, through a systematic examination of climatic variables and urban geometry during the hottest months of the year April, May and June of the town. The study utilizes a combined methodology integrating field measurements of air temperature and relative humidity alongside wind speed and solar radiation analysis collected from global weather datasets. Additionally, the study integrates thermal indices of mean radiant temperature and universal thermal climate index to evaluate outdoor thermal conditions extensively. A pedestrian survey obtaining thermal sensation, comfort perception, and meteorological preferences is carried out to verify subjective experiences. The study employs bioclimatic chart, shadow length and sky view factor analyses to examine optimal street configurations. Findings involve that street orientation effectively influences thermal exposure with north-south, east-west and northeast-southwest and northwest-southeast streets exhibit different microclimatic characteristics. In addition, the importance of integrating climate-responsive urban design strategies such as vegetation coverage, reflective surfaces and optimized urban geometry to enhance pedestrian thermal comfort. This study provides a framework for urban planners and policymakers to formulate street design strategies that prioritize pedestrian's thermal comfort supporting to sustainable urban development in arid and semi-arid climates.

Key words: Thermal comfort, street orientation, urban design, pedestrian comfort, shadow length and Metehara town

Acknowledgment

First of all, I would like to express my deepest gratitude to the Almighty God for his care and guidance throughout my journey especially in completing this work. Glory to his Almighty for his care and smoothening challenges in doing this paper.

I want to express my profound gratitude to my family for their constant encouragement all along with my study. Their support has been my pillar of strength.

I extend my sincere thanks to my advisor Dr. Nebyou Yonas for his diligent support, guidance, and encouragement right from the beginning of the research up to the realization of this paper. He also gives me new insight and inspiration toward thesis and academics relating to the current urban challenges.

I am particularly grateful to the Metehara town land administration for providing me data and information. I would also like to thanks my friends and classmate who encouraged me in my paper accomplishment.

Finally, I would like to acknowledge all those who have supported me to complete this study, directly or indirectly. Thank you all.

TABLE OF CONTENTS

List of Tables

List of Figures

Acronyms

ASHRAE	American Society of Heating, Refrigeration and Air-Conditioning Engineers
E-W	East- West
GIS	Geographic Information System
H/W	Height to Width ratio
ISO	International organization for standardization
KWh/m^2	Kilowatt -Hour per Meter square
LOS	Level of service
MRT	Mean radiant temperature
N-S	North- South
NASA	National American Satellite Agency
RH	Relative humidity
SVF	Sky View Factor
TCV	Thermal comfort vote
UTCI	Universal thermal climate index
W	Shadow width
W/m^2	Watt per meter square

CHAPTER ONE

INTRODUCTION

1.1. Background of the Study

City streets are functioning like blood system of human anatomy. Traditional and contemporary architectures make a lot efforts to design urban streets according to climate, quantitative information about the best possible street design, based on scientific methods, in order to regulate the climate comfort is still required (Asimakopoulos, et al., 2001). Streets play a crucial role in shaping microclimatic conditions by affecting solar exposure, wind flow, and shading (Johansson, 2020). In regions with high temperatures, poorly oriented streets can lead to excessive heat accumulation, reducing pedestrian activity and overall urban livability (Ali-Toudert & Mayer, 2006). Understanding the relationship between street layout and thermal comfort is essential for creating climate-responsive urban environments that enhance walkability and public well-being (Oke et al., 2017).

Thermal comfort is the condition of mind that expresses satisfaction with the thermal environment (ASHRAE, 2013). Outdoor thermal comfort of cities mainly depends on air temperature, humidity, wind speed and solar radiation. The orientation of streets, size and related plants and street side buildings plays great role in adjusting the outdoor thermal comfort (Mayer H., 1987). Pedestrian thermal comfort in urban environments is influenced by various interacting factors including air temperature, solar radiation, wind dynamics, metabolic heat production and clothing insulation. Although air temperature is the temperature of the air surrounding the human body. Some of the scholars found that the effect of air temperature alone on pedestrian thermal comfort is insignificant (Matzarakis and Endler, 2010).

Ethiopia, as a country with diverse climatic conditions ranging from highland temperate zones to lowland arid regions faces increasing urban heat stress particularly in its rapidly expanding towns (Fesseha, 2020). Despite growing urbanization Ethiopian cities often lack integrated climate adaptive street design making pedestrian mobility challenging in warm dry regions like Metehara town (Zerihun, 2019).

In Ethiopia, there is a limited study of pedestrian thermal comfort in cities about sun path, street and building orientation relationship. However, the government of Ethiopia is urging city development by making more efficient use of urban land. A great deal of attention has been placed on an ideal opportunity to develop a sustainable community with mixed use of urban land. Most of the planners and designers are initiated to design a city with its social, economic, cultural and aesthetic values depending on the topographic and other parameters of the area.

Metehara town located in Ethiopia's warm-dry climate zone characterized by high temperatures, low humidity and excessive solar exposure particularly in peak hours of the day (Berhanu et al., 2018). The town dominant North-South (N-S) and East-West (E-W) street orientations shape urban thermal conditions but pedestrian discomfort persists due to insufficient shading, poor airflow and heat retaining materials (Teshome & Taye, 2022).

Urban street orientation plays a critical role in shaping pedestrian thermal comfort, particularly in warm-dry climates like Metehara. The town experiences high solar radiation and limited precipitation making outdoor thermal conditions a significant factor in urban planning (Asmamaw, 2019). Street orientation influences solar exposure, wind flow and shading patterns all of which contribute to the microclimate pedestrians' experience (Komi Bernard, 2023). Properly aligned streets can mitigate heat stress by optimizing shade and ventilation; while poorly oriented streets may exacerbate thermal discomfort, increasing reliance on artificial cooling solutions (Naznanin & Amir Ghosouri, 2020).

This study aims to address this gap by evaluating the thermal performance of different street orientations and their implications for pedestrian well-being. Understanding the microclimatic interactions between urban form and climate factors can contribute to developing effective strategies for mitigating urban heat stress and enhancing walkability.

1.2.Problem Statement

Metehara town located in Ethiopia warm dry climate zone faces increasingly acute challenges in ensuring pedestrian thermal comfort particularly during the hottest months of April, May and June. With average daytime temperatures exceeding 36°C and solar radiation reaching intolerable levels, the town's built environment often fails to provide walkable public spaces. Pedestrians routinely navigate between residential areas, workplaces and the sugar factory often shown to high average temperatures and inadequate shading incase existing street orientations fail to sufficiently mitigate heat exposure leading to thermal discomfort and potential health risks.

The absence of climate responsive street designs in Metehara town worsen pedestrian discomfort particularly in areas lacking strategic plantation and optimal shading. Streets with improper orientation experience prolonged solar radiation exposure, reduced airflow and minimal cooling effects. A critical contributor to this discomfort is the lack of sufficient shading along the streets. Throughout Metehara main pedestrian corridors shading mechanisms whether from buildings, structures and vegetation are largely absent or ineffectively configured. During peak sun hours walkways are open to extended direct solar radiation. Pedestrians moving through these streets frequently encounter intolerable heat which discourages walking.

Green infrastructure which could offer natural cooling through solar interception and evapotranspiration remains sparse or entirely absent in many parts of the town. The limited presence of urban greenery not only reduces shading potential but also reduce humidity regulation within pedestrian zones. Without such ecological buffers Metehara town walkways become area of amplified dryness and heat further intensifying discomfort during the hottest periods of the day.

Ventilation within pedestrian streetscapes is also compromised due to obstructive building geometries and poor spatial planning. In several segments of the urban fabric air circulation is obstructed by built forms that block prevailing winds limiting the cooling effect that could otherwise increase thermal stress. These disruptions lead to high heat and stagnant conditions that exacerbate the impact of high solar exposure.

During midday hours when solar altitude is highest and thermal stress peaks pedestrian zones across Metehara town absorb and reradiate heat beyond tolerable thresholds. Despite being essential pathways for economic and social activity these streets routinely discourage movement due to their harsh environmental conditions.

1.3.Objective

General objective:

To identify thermally comfortable street orientation for pedestrian in Metehara town.

Specific objectives:

1. To understand perception of pedestrians about the thermal comfort of streets.

2. To assess the thermal comfort performance of existing street orientations for pedestrians.

1.4. Research Question

General question:

Which street orientation provides better thermal comfort for pedestrians in Metehara town?

Specific questions:

1. What are the perception of pedestrians about thermal comfort of the streets?

2. Which existing street orientation have good performance for the pedestrian's thermal comfort?

1.5. Significance of the Study

This study provides to climate responsive urban design by systematically evaluating pedestrian thermal comfort in relation to street orientation in Metehara town, Ethiopia. Academically it contributes to urban climate research by integrating meteorological analysis with urban planning strategies offering a methodological framework for optimizing street orientation to improve pedestrian thermal comfort. According to governmental perspective it supports evidence based policy development for climate resilient cities guiding municipal planning toward sustainable urban expansion. Professionally it gives scientific basis for urban designers, architects and planners with practical strategies to reduce heat stress through shading techniques, ventilation corridors and reflective materials. Publicly, it enhances pedestrian mobility, improves outdoor comfort and fosters community awareness about climate-responsive urban design. By addressing the challenges of thermal discomfort in Metehara town this research provides actionable strategies for creating sustainable, livable and pedestrian friendly urban spaces in warm dry climates.

1.6. Scope of the Study

This study is temporally bound to the three hottest months in Metehara town April, May and June during which pedestrian thermal comfort is significantly impacted by elevated temperatures and intense solar radiation. The thesis is time bound restricting data collection to the period between 10:00 AM and 16:00 PM at the time of thermal stress elevated. Additionally, the scope systematically limited to selected streets identified based on their orientation, vegetation cover and microclimatic conditions. By delimiting the investigation to this critical period the research aims to provide empirically grounded insights into the temporal dynamics of urban thermal comfort and facilitating evidence based design strategies for climate responsive urban design in Metehara town.

1.7. Limitation of the Study

The limitations of this study primarily related to field measurement instruments and the availability of meteorological data which collectively challenged the accuracy and scope of the findings. Due to instrumentation issues only the air temperature and relative humidity were directly recorded, while key meteorological parameters such as wind speed and solar radiation were taken from secondary sources. Additionally, the Ethiopia Meteorology Agency does not provide fully recorded climatic data necessitating reliance on external databases and estimations, which may introduce minor inconsistencies in the analysis. These constraints affected the precision of microclimatic assessments and limited the ability to capture localized atmospheric variations. Despite these challenges, the study systematically combines primary and secondary data to evaluate street orientation and pedestrian thermal comfort.

CHAPTER TWO

LITERATURE REVIEW

2.1. Theoretical Review

2.1.1. Urbanization

"Cities are increasingly expanding their boundaries and populations and from the climatological point of view human history is defined as the history of urbanization" (M. Santamouris, 2001). Urbanization has significantly altered the thermal conditions of cities, leading to environmental challenges such as the urban heat island (UHI) effect. Rapid urban growth has transformed natural landscapes into impervious urban surfaces, increasing regional and global temperatures (Balling, 1992). The concentration of human activities in cities creates localized heat accumulation, impacting thermal comfort for pedestrians and residents (Oke, 1982). Understanding the relationship between urban expansion and microclimate variations is essential in designing sustainable cities that mitigate thermal stress (Santamouris, 2001).

Urban climate studies across Africa highlight the complex interactions between rapid urbanization and climate variability emphasizing the exacerbation of heat stress, altered precipitation patterns and urban heat island (UHI) effects due to unplanned expansion (Xueqin Li. & Martin, 2022). The lack of climate sensitive urban planning has led to increased thermal discomfort particularly in densely populated cities with limited vegetation cover and poor ventilation corridors (Henderson, 2016). Studies indicate that street orientation, shading strategies and microclimate interventions play a crucial role in mitigating urban heat stress especially in warm climate area; yet many African cities lack integrated frameworks to address these concerns systematically (Kamgnia Dia, 2021).

2.1.2. Urban Design

Urban design is the design of towns and cities, streets and spaces; and also that involves the design of buildings, groups of buildings, spaces and landscapes, and establishing frameworks and procedures that will deliver successful development by different peoples over time. Urban design plays a fundamental role in shaping pedestrian thermal comfort by influencing environmental parameters such as solar radiation, air temperature, humidity, and wind speed (De Jong, 2013).

Effective urban design integrates street orientation, shading strategies, and material selection to enhance thermal conditions in outdoor spaces (Golany, 1996).

Streets, forming a significant portion of urban environments, vary in geometry, height-to-width ratios, and orientation, which affect solar exposure and airflow patterns (Sanaieian et al., 2014). Narrow streets provide shade by limiting direct solar radiation, whereas wider streets can be optimized through shading devices and greenery to improve thermal comfort (Littlefair, 2000). Traditional urban layouts often incorporate climate-responsive designs, yet modern urban development's frequently overlook thermal comfort considerations (Emmanuel, 2005).

2.1.3. Thermal Comfort

Thermal comfort is defined as the condition in which individuals experience satisfaction with the thermal environment, influenced by physiological and psychological factors (ASHRAE, 2017). The human body regulates heat through processes such as radiation, convection, and evaporation, which are affected by air temperature, humidity, wind speed, and solar exposure (Givoni, 1998). Urban design parameters significantly influence thermal sensation, necessitating strategies that balance heat dissipation and shading (Lin, Matzarakis & Hwang, 2010). Bioclimatic urban planning integrates thermal comfort indices to assess and optimize pedestrian environments (Toy & Yilmaz, 2010). The Universal Thermal Climate Index (UTCI) and Mean Radiant Temperature (MRT) serve as key indicators for evaluating microclimate conditions and their implications on human well-being (Taleghani, 2020).

ASHRAE Standard 55 establishes guidelines for acceptable thermal conditions in occupied spaces, considering environmental factors such as air temperature, mean radiant temperature, humidity, and air velocity. These parameters collectively determine the thermal sensation experienced by individuals. For instance, air temperature alone does not fully define comfort, as radiant heat from surrounding surfaces significantly influences perceived warmth. Mean Radiant Temperature (MRT), which accounts for the thermal radiation emitted by surrounding surfaces, plays a crucial role in outdoor thermal comfort assessments. Thermal sensation scale has seven grades: hot, warm, slightly warm, neutral, slightly cool, cool, and cold with each grade assigned a numerical value, from +3 to-3, in respective order.

Outdoor space is important for cities as this provides daily pedestrian flow and different outdoor activity contribution to urban livability and vitality (Chen and Ng, 2011). Ensuring that people are comfortable in outdoor spaces is essential to a better quality of urban life (Tapies and Schmith, 2014). The urban microclimate determines the quality of outdoor space for the users (Tapies and Schmith, 2014). Pedestrians are directly exposed to their immediate environment in terms of variation of air temperature, humidity, wind speed, and solar radiation. Therefore, people's sensation of thermal comfort is greatly affected by the local microclimate (Chen and Ng, 2011).

In urban settings, thermal comfort is influenced by microclimatic conditions shaped by urban design elements such as street orientation, shading, vegetation, and material properties. The Urban Heat Island (UHI) effect, caused by heat absorption and retention in built environments, exacerbates thermal discomfort, particularly in densely populated areas. Streets with high height-to-width ratios (H/W) provide better shading and reduce solar exposure, improving pedestrian comfort. Conversely, wide streets with minimal shading experience higher thermal loads, increasing heat stress (ASHRAE, 2017).

2.1.4. Pedestrian Thermal Comfort

A Thermally Comfortable Pedestrian Route (TCPR) is defined as one that can be walked from start to finish without a risk of increasing human body core temperature and/or perceived discomfort. Pedestrian thermal comfort refers to the environmental conditions that influence the thermal sensation and overall well-being of pedestrians in outdoor urban spaces. It is a critical factor in urban design, affecting walkability, social interaction, and public health (ASHRAE, 2013).

Various parameters contribute to pedestrian thermal comfort, which can be broadly categorized into meteorological and human-related factors. The four environmental variables affecting the thermal comfort of the pedestrian are air temperature, solar radiation, relative humidity, and wind speed. In addition, two personal variables influence pedestrian thermal comforts are clothing and the level of activity (Enteria et al. 2019). However, other personal factors related to adaptation and acclimatization have proven to affect thermal sensation.

i) Air temperature

Air temperature is a measure of how hot or cold the air is (Hakimiefaez, 2010). Air temperature is a fundamental determinant of pedestrian thermal comfort, influencing heat exchange between the human body and the surrounding environment. Studies indicate that air temperature alone has a limited effect on pedestrian thermal comfort unless combined with other climatic factors such as humidity and wind speed (Matzarakis & Endler, 2010).

The air temperature determines the convective heat exchange between the skin and ambient temperature. Both the body's convective heat loss and its dry respiration heat loss decrease with increasing air temperature (Johansson, 2006). The effect of air temperature on the comfort is straight forward: raising temperature always results in correspondent in thermal sensation (Givoni, 1992). The condition of humidity and wind speed modifies the magnitude of temperature effect but doesn't change its trend. The pedestrian thermal comfort is generally maintained when temperatures are below 35^{o}c. beyond this value walking becomes uncomfortable and heat stress increases (Litman T., 2023).

ii) Humidity

The relative humidity is the ratio of the amount of water vapor in the air to the amount of water vapor that the air could hold at the specific temperature and pressure. The recommended level of outdoor humidity in warm dry climate is in the range of 30-60% in air-conditioned buildings (Amir Ghosouri, 2020). Relative humidity affects the body's ability to regulate temperature through evaporative cooling. High humidity levels reduce sweat evaporation, intensifying heat stress, while low humidity can lead to dryness and discomfort (Givoni, 1998). This is because, although the evaporative capacity of the air diminishes with increasing humidity, the body compensates for this by spreading the sweat over a larger area of skin, thus maintaining the required evaporation rate.

iii) Wind speed

Wind speed is defined as the rate of air movement at a point without regard to direction. According to ASHRAE (2010), it is the average speed of the air to which the body is exposed with respect to location and time. Commonly the body exposed to uniform wind speed but some spaces might provide strongly no uniform air velocity that cannot be considered uniform. Therefore, the designer shall decide the proper average, especially including airspeeds incident on unclothed body parts that have greater cooling effect and potential for local discomfort.

Wind speed plays a crucial role in dissipating heat and enhancing pedestrian comfort. Increased air movement improves convective cooling, reducing thermal discomfort in hot climates. However, excessive wind speeds can lead to discomfort in colder environments (Johansson, 2006). Wind speed comfort depends on temperature, humidity, and clothing. As the temperature increases the wind speed increase to restore thermal comfort (Givoni, 1998). Strong air movement is thus a disadvantage in cold climates but has a clear advantage in hot climates. Comfortable wind speeds for pedestrians typically range between 1m/s to 5 m/s depending on local conditions and urban design (H.W. Fricke, 2015).

iiv) Solar radiation

Solar radiation significantly impacts pedestrian thermal comfort by increasing heat absorption and elevating mean radiant temperature (MRT). Direct exposure to sunlight can lead to thermal discomfort, especially in urban environments with limited shading, as surfaces absorb and radiate heat, intensifying outdoor temperatures (Mayer, 1987).

Solar radiation is one of the most significant environmental factors influencing pedestrian thermal comfort, as direct exposure to solar radiation increases radiant heat absorption and elevates mean radiant temperature (MRT), leading to potential heat stress (Krüger & Pearlmutter, 2015). Effective urban shading strategies, such as tree canopies and built structures, can mitigate solar radiation impacts, reducing surface temperatures and improving pedestrian comfort (Johansson et al., 2012). In warm dry climates, tolerable solar radiation levels range between 500 – 800w/m^2 for pedestrian comfort depending on shading, wind flow and surface materials (Mahina Jain, 2018).

iv) Mean Radiant Temperature (MRT)

Mean Radiant Temperature (MRT) is a critical factor in evaluating pedestrian thermal comfort, as it accounts for the combined effects of shortwave and longwave radiation from surrounding surfaces and the sky. Unlike air temperature, MRT directly influences the heat exchange between pedestrians and their environment, making it a key determinant of outdoor thermal sensation (Fiala et al., 2012). The intensity of MRT varies depending on street orientation, shading, and material properties generally providing lower MRT levels and reducing thermal discomfort (Johansson, 2012).

In warm dry urban environments, mean radiant temperature (MRT) values below 40 - 45 °C are generally tolerable for adapted pedestrians especially when aligned with moderate wind speeds and relative humidity (Krüger & Pearlmutter, 2015). Even small increases in MRT can significantly affect noticed thermal comfort due to its strong influence on the human thermal balance (Fanger, 1970). According to ISO 7726 (1998), MRT should be measured with an accuracy of ±2 °C for comfort assessments. Proper urban design strategies, such as shading, reflective materials and vegetation, can mitigate excessive MRT improving pedestrian thermal comfort and reducing heat stress.

v) Clothing Insulation

Clothing insulation influences the body's ability to regulate temperature. Lighter clothing enhances heat dissipation, while heavier clothing retains warmth, affecting pedestrian thermal comfort in different seasons (ASHRAE, 2013). Clothing insulation further plays a crucial role in regulating heat exchange between the human body and the environment. Lightweight, breathable clothing enhances evaporative cooling, while heavier, less permeable fabrics increase thermal retention, affecting pedestrian thermal sensation in both hot and cold climates (Bröde et al., 2012).

According to ASHRAE, (2017) Standard 55 the Clo unit quantifies clothing insulation. ASHRAE considers dynamic thermal environments incorporating factors like solar radiation, wind speed and metabolic activity to determine tolerable comfort levels. In extreme heat conditions typical Clo values range from 0.2 Clo for minimal clothing (e.g. shorts and a sleeveless shirt) to 0.5 Clo for light summer attire (e.g. T-shirt and trousers), and up to 0.8 Clo for moderate layering suited to evening cooling. These values help define thermal comfort thresholds, ensuring pedestrians experience acceptable heat stress levels while navigating urban spaces.

vi) Metabolic Rate

The level of physical activity affects heat generation within the body. Walking or exercising increases metabolic heat production, impacting thermal comfort levels (de Dear & Brager, 1998). Metabolic rate also contributes to pedestrian thermal comfort by determining internal heat production, with higher metabolic activities, such as walking, leading to increased body heat generation and susceptibility to thermal stress, while lower metabolic rates correspond to reduced heat production altering thermal perception (Fiala et al., 2012).

2.1.5. Urban Design and Pedestrian Thermal Comfort

Urban design significantly influences pedestrian thermal comfort by shaping microclimatic conditions within cities. The spatial configuration of streets, building orientations, vegetation, and open spaces dictates exposure to solar radiation, wind flow, and surface heat retention, thereby determining pedestrian thermal experiences (Santamouris, 2012). Street orientations, for instance, control solar access and shading patterns, with north-south streets generally offering better shade potential compared to east-west streets, which experience prolonged solar exposure (Littlefair, 2000). Furthermore, urban geometry, including height-to-width (H/W) ratios, impacts airflow patterns, shading effectiveness, and heat dissipation, directly affecting pedestrian comfort levels (Givoni, 1998).

Urban design strategies aimed at pedestrian comfort must be evaluated using scientifically validated thermal indices. The Mean Radiant Temperature (MRT) assesses radiative heat exchange between pedestrians and urban surfaces, making it a critical metric in shade and material selection (Fanger, 1982). Another widely applied index, the Universal Thermal Climate Index (UTCI), incorporates air temperature, humidity, wind speed, and radiation effects to gauge pedestrian heat stress levels (Taleghani, 2020). Applying these indices enables urban planners to optimize shading mechanisms, ventilation corridors, and surface reflectivity for pedestrian-friendly environments (Matzarakis & Mayer, 2007).

Effective shading solutions, such as tree canopies, arcades, and pergolas, mitigate excessive solar radiation, improving microclimatic conditions in pedestrian zones (Andreou, 2013). Vegetation plays a dual role in cooling pedestrian spaces, both by blocking solar exposure and facilitating evapotranspiration for ambient temperature reduction (Emmanuel & Johansson, 2006). In contrast, high-albedo urban surfaces minimize heat retention, with reflective pavements and façades lowering thermal loads in dense urban environments (Shishegar, 2013). A combination of these strategies ensures optimal pedestrian thermal comfort by regulating localized heating effects and enhancing cooling efficiency (Middel & Ariane, 2016).

For climate-responsive pedestrian thermal comfort, urban environments must integrate adaptive shading networks, optimized street orientations, and sustainable surface materials. Strategic tree placement and dynamic shading elements contribute to long-term urban heat mitigation (Kim & Baik, 2005). Additionally, water-based cooling solutions, including artificial lakes and misting systems, support evaporative cooling processes (Johansson, 2006). By aligning urban design with bioclimatic principles, cities can create walkable, heat-resilient pedestrian spaces, fostering urban livability in response to climate change challenges (Santamouris, 2012).

2.1.6. Street Orientation

Street orientation is an important parameter that determines the solar access and wind speed in urban canyons and is therefore significant in determining the thermal comfort level inside walks (Yang,Qian, and Lau, 2013). Streets oriented north-south tend to receive balanced sunlight distribution throughout the day. Shading elements such as buildings and vegetation on the east and west sides can significantly reduce thermal stress (Johansson et al., 2012). This orientation generally benefits from better airflow, particularly when aligned with prevailing wind directions, improving pedestrian thermal comfort (Hegazy & Qurnfulah, 2020).

East-west oriented streets often experience intense solar exposure throughout the day, especially on the south-facing facades. The higher height-to-width (H/W) ratios help mitigate heat stress by increasing shading (Emmanuel & Johansson, 2006). However, these streets may require additional shading elements like trees, arcades, or reflective materials to reduce mean radiant temperature (MRT) (Krüger & Pearlmutter, 2015).
Streets oriented northeast-southwest (NE-SW) and northwest-southeast (NW-SE) exhibit variable thermal conditions, depending on the season and time of day. In warm climates, NE-SW streets tend to receive greater morning and afternoon sun, while NW-SE streets experience prolonged midday exposure (Littlefair, 2000). Optimizing building height and vegetation along these orientations can improve pedestrian comfort by controlling direct solar radiation (Masoud, 2021). When the wind flow is oblique to the canyon axis, a spiral vortex develops along the length of the canyon; this flow is not perfectly reflected by building walls. To address this issue, Givoni proposed street widening to improve ventilation in urban canyons. When the wind direction is parallel to the street axis, an obstacle-free passageway is developed so that the prevailing wind penetrates into the urban canyon. However, the friction between building walls and different surfaces delays the approaching wind flow (Ahmad, Khare, and Chaudhry, 2005).

2.1.7. Universal Thermal Climate Index (UTCI)

The Universal Thermal Climate Index (UTCI) is a scientifically validated tool designed to assess outdoor thermal conditions, particularly for pedestrian environments. Unlike basic air temperature measurements, UTCI accounts for multiple climatic factors, including air temperature, mean radiant temperature (MRT), wind speed, and relative humidity, to determine the perceived thermal stress experienced by pedestrians (Taleghani, 2020). This index is widely applied in urban climate studies to evaluate thermal discomfort levels and guide climate-responsive urban design strategies (Matzarakis et al., 2007).

UTCI values classify pedestrian thermal stress into distinct heat and cold stress categories, assisting urban planners in quantifying comfort zones (Błażejczyk et al., 2013). These classifications include:-

Above +46^{o}c: extreme heat stress
+38 to +46^{o}c: very strong heat stress
+32 to +38^{o}c: strong heat stress
+26 to +32^{o}c: moderate heat stress
+9 to +26^{o}c: no thermal stress
+9 to +0^{o}c: slight cold stress
0 to -13^{o}c: moderate cold stress
-13 to -27^{o}c: strong cold stress
-27 to -40^{o}c: very strong cold stress
Below -40^{o}c: extreme cold stress

UTCI classifications help determine pedestrian vulnerability to heat and cold extremes, supporting the design of thermally adaptive urban spaces (Middel & Ariane, 2016). UTCI provides an accurate scientific framework for assessing pedestrian thermal comfort, integrating climatic parameters to evaluate urban heat stress dynamics. By incorporating shade structures, airflow optimization, reflective materials, green infrastructure, and water features, urban planners can effectively reduce pedestrian heat stress, creating livable, climate-adaptive spaces (Santamouris, 2012).

2.1.8. Bioclimatic Chart

The bioclimatic chart is an essential tool for analyzing the interaction between meteorological parameters, such as temperature, humidity, wind speed, and solar radiation, to assess human thermal comfort. Developed as part of bioclimatic design principles, the bioclimatic chart provides insights into thermal regulation strategies based on varying climatic conditions (Givoni, 1992). The quantitative bioclimatic chart illustrates how comfort thresholds shift due to environmental factors, identifying corrective measures like increasing wind speed, adjusting humidity levels, or modifying radiation exposure to restore thermal equilibrium (Katafygiotou & Serghides, 2014).

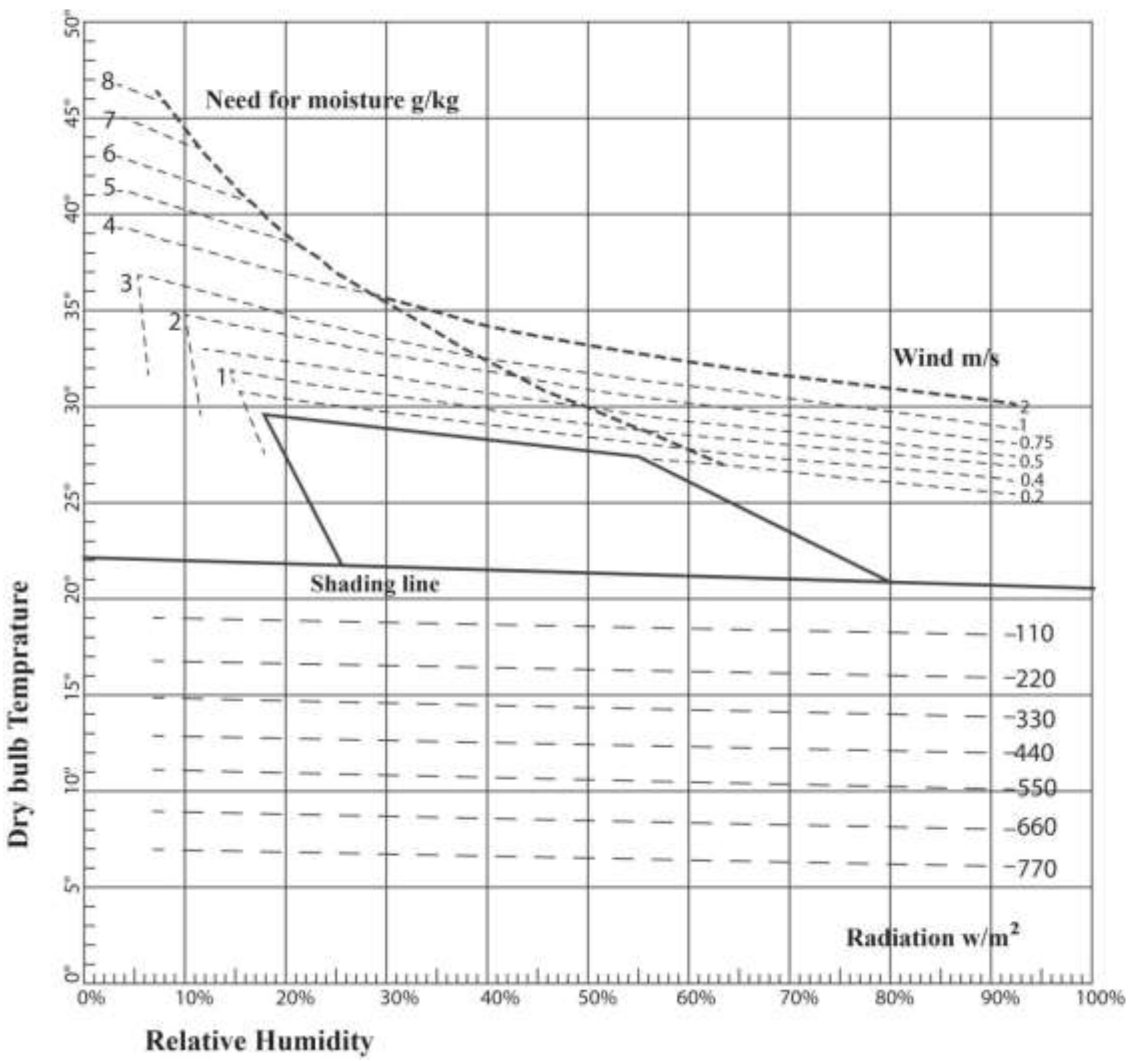

Figure 2.1 Quantitative bioclimatic chart (Source: Katafygiotou and Serghides, 2014)

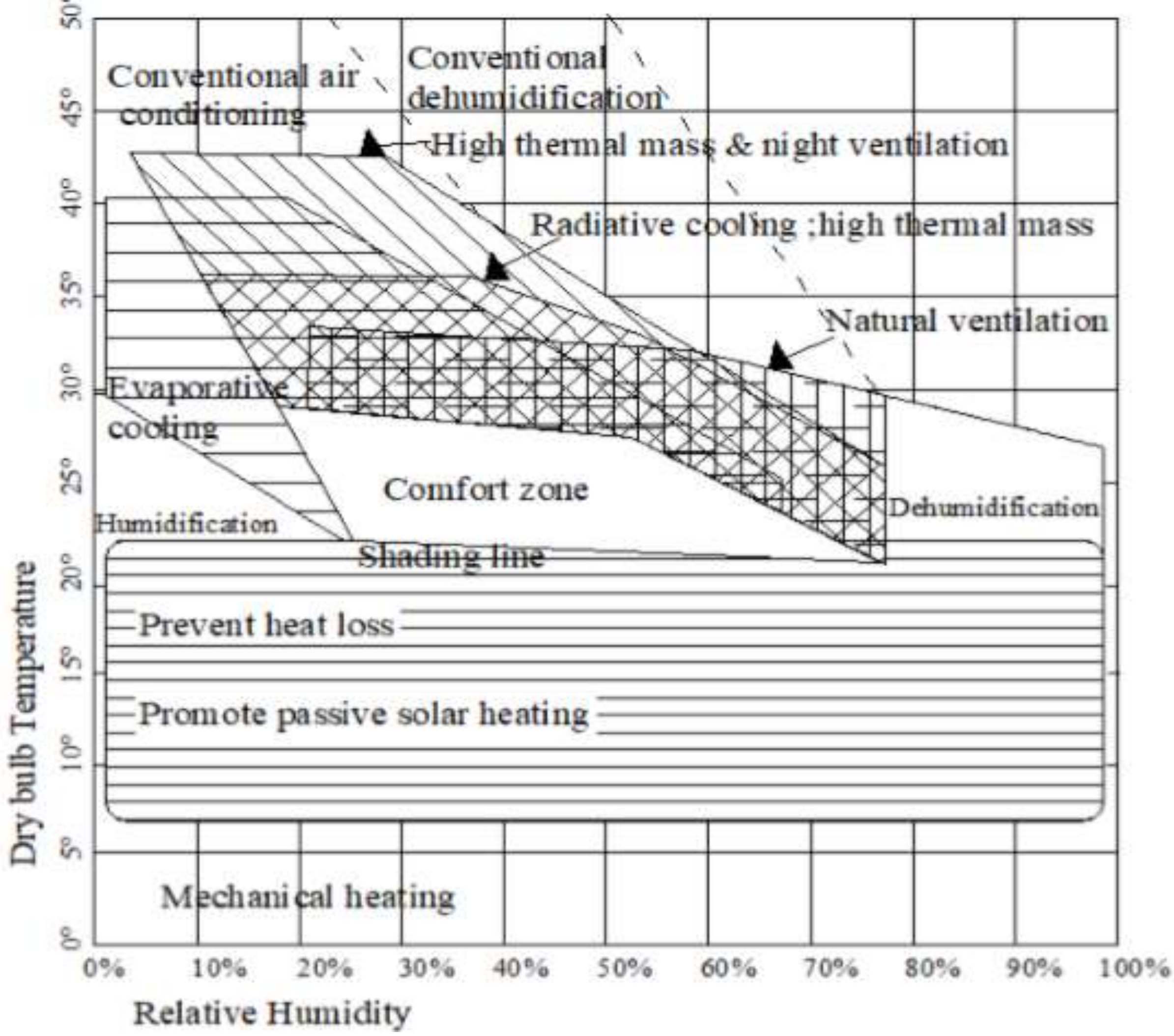

Figure 2.2 Qualitative bioclimatic chart (Source: Katafygiotou and Serghides, 2014)

In warm-dry climates, excessive solar radiation can elevate mean radiant temperature (MRT), leading to heat stress, requiring solutions such as shading, evaporative cooling, and reflective surfaces to mitigate thermal discomfort (Krüger & Pearlmutter, 2015). The qualitative bioclimatic chart categorizes design strategies based on climate adaptation, emphasizing the importance of natural ventilation, high thermal mass materials, and passive cooling techniques to optimize outdoor thermal conditions (Olgyay, 1963). A comprehensive bioclimatic analysis enables urban planners and architects to tailor design interventions that balance shading, airflow optimization, and humidity regulation, improving pedestrian thermal comfort in urban environments (Bröde et al., 2012).

2.1.9. Sun Path and Solar Shadow

The sun path and solar shadows are important concepts in urban planning, architecture, and environmental design. The sun path refers to the apparent movement of the sun across the sky throughout the day and year, influenced by latitude and seasonal variations. Understanding the sun path is crucial for optimizing solar access, shading strategies, and thermal comfort in urban environments (Marsh, 2015). The solar altitude and azimuth angles determine the intensity and direction of sunlight, affecting pedestrian thermal comfort and urban microclimates (Khodakarami, 2020).

Solar shadow analysis evaluates the impact of shading elements such as buildings, trees, and urban canopies on pedestrian thermal comfort. Shadows vary in length and direction depending on the time of day and season, influencing heat exposure and cooling potential in outdoor spaces (Ghosouri, 2020). The formula for shadow length, $L = h / \tan(\alpha)$, where h is the object height and α is the solar altitude angle, helps quantify shading effectiveness (Kumar, 2023). Properly designed shading structures can reduce solar radiation exposure by up to 90%, significantly improving pedestrian comfort (Lee & Cheung, 2019).

The movement of the sun across the sky influences urban microclimates by altering solar radiation exposure throughout the day and year. Buildings, trees, and other urban structures create dynamic shadow patterns, impacting pedestrian thermal comfort by reducing direct solar radiation and modifying mean radiant temperature (MRT) (Khodakarami, 2020). The efficiency of shading depends on solar altitude, azimuth angle, and the geometry of surrounding urban forms. Studies indicate that urban streets with high height-to-width (H/W) ratios provide greater shade coverage, reducing surface temperatures by up to 10°C, enhancing pedestrian thermal comfort in hot climates (Lee & Cheung, 2019). Incorporating solar shadow analysis into urban planning helps optimize shading strategies, improve walkability, and mitigate urban heat island effects by ensuring adequate shade structures that adapt to seasonal variations (Ghosouri, 2020).

2.1.10. Shading effect and H/W ratio

Controlling solar radiation is the most important factor affecting outdoor thermal comfort, especially in hot seasons (Middel and Ariane, 2016). Investigated outdoor thermal comfort within the two urban squares of Naghshe-Jahan and Jolfa in the hot arid climate of Isfahan, Iran. Using field measurements and questionnaires, they found out that Jolfa has more comfortable hours mainly due to the shading effect of its walls (Kariminia et al, 2016).

Most studies on the effect of urban canopy shading on outdoor thermal comfort were conducted in warm seasons. Some canopies reduce the amount of sunlight in winter and increase thermal discomfort. Therefore, the effect of shading on thermal comfort should be examined in both warm and cold seasons (Mohammad Taleghani, 2020). Studied the impact of sidewalk materials on raising the local temperature in summer in Nis (Serbia; temperate climate). They showed that temperature differences between the shaded and unshaded surfaces were up to 20 °C (Djekic, J, 2018).

Shading by buildings is an important strategy for creating thermally comfortable conditions for pedestrians in urban canyons. In several studies, various proportions of building height to street width (H/W) were investigated with respect to thermal comfort (Andreou, E., 2013). A height to width ratio in warm climates, higher H/W ratios closer to 1.0 are often recommended. This because taller buildings relative to street width provide more shading, reducing exposure to direct solar radiation and lowering the mean radiant temperature (MRT), which significantly impacts thermal comfort (Meng Han, 2024). However, achieving the ideal ratio depends on other factors like street orientation, vegetation and wind flow (Amir Ghosouri, 2020).

Studies that directly measure bioclimatic condition and outdoor thermal comfort have reported a clear correlation between pedestrian thermal comfort and aspect ratio and emphasized the need to consider the possible consequences of aspect ratio on thermal radiation in cities (Lin,Matzarakis, and Hwang2010). Shading has been reported as the main source of reduced level of discomfort in cities; increased shade and H/W ratio can significantly reduce UTCI (Emmanuel, Rosenlund, and Johansson 2007). Narrow streets with buildings provide better shading for sidewalk pedestrians than wide streets. (Matzarakis, Rutz, and Mayer 2007).

2.1.11. Sky View Factor

Sky View Factor (SVF) is a critical parameter in urban climatology representing the fraction of the sky visible from a specific point. It significantly influences radiative exchange, microclimate, and thermal comfort in urban settings. Studies have demonstrated that SVF affects mean radiant temperature (MRT) and urban heat island (UHI) intensity by modulating incoming shortwave and outgoing long wave radiation (Oke, 1988). This effect significantly influences pedestrian thermal comfort. Lower SVF values, commonly found in narrow street canyons, reduce daytime solar exposure leading to localized heat retention. (Johansson, 2004). Various empirical formulas have been developed to calculate SVF based on urban geometry allowing researchers to estimate its impact on thermal conditions without relying on simulation tools (Ali-Toudert & Mayer, 2006).

SVF is increasingly linked to vegetation presence, as tree canopies modify sky exposure and thermal conditions demonstrating the importance of integrating greenery into urban planning (Wong, 2010). By refining SVF calculations and incorporating asymmetrical shading effects, urban designers can enhance pedestrian thermal comfort, particularly in warm dry climates where solar access and shading are critical factors (Bouyer et al., 2011).

2.1.12. Urban Landscape and Pedestrian Thermal Comfort

The urban landscape plays a fundamental role in shaping pedestrian thermal comfort by influencing local microclimatic conditions. As urban areas continue to expand, designing climate-responsive landscapes is essential to enhance walkability, reduce heat stress, and create thermally resilient environments (Johansson, 2006). This section systematically explores how urban landscape elements influence pedestrian thermal comfort through scientific principles and evidence-based strategies.

Vegetation and Green Infrastructure: Trees, shrubs, and green façades serve as passive cooling elements, reducing radiant heat exposure and improving local humidity levels (Andreou, 2013). Vegetation enhances thermal comfort by facilitating evapotranspiration and reducing ground temperatures.

Water Bodies and Cooling Effects: Urban lakes, fountains, and misting systems lower ambient temperatures through evaporative cooling. The presence of water bodies can create microclimates that enhance pedestrian thermal comfort, especially in regions with high solar radiation exposure (Emmanuel & Johansson, 2006).

Street and Urban Surface Materials: Pavements, façades, and building materials significantly influence heat retention and dissipation. High-albedo surfaces reflect solar radiation and prevent excessive heat buildup, thereby reducing thermal discomfort for pedestrians (Shishegar, 2013).

Urban Geometry and Wind Flow Optimization: The orientation and layout of urban spaces determine airflow efficiency, which helps disperse heat and improve ventilation in pedestrian pathways (Kim & Baik, 2005). Narrow, shaded streets enhance cooling effects, while wide open spaces may intensify thermal discomfort without proper shading (Givoni, 1998). Sidewalk location on either E-W or N-S oriented streets, locate sidewalks as closely as possible to the building to maximize building shade for as much of the day as possible and provide ease of access to building entrances. Locating walks adjacent to buildings also may minimize walking distance. Providing a buffer between the sidewalk and the roadway creates space for trees and other shade structures while increasing the perceived safety and comfort of people walking (Gehl, J., and Svarre, B., 2013).

Shade Structures and Passive Design: Constructing canopies, pergolas, and arcades in pedestrian areas to provide adequate shading and mitigate heat stress (Littlefair, 2000). And also, **Microclimate Management**: Urban landscape can create microclimates that enhance thermal comfort by strategically placing elements that influence local temperature, humidity, and wind patterns (Aljawabra, F., & Nikolopoulou, M. 2010).

By integrating these strategies, urban designers can create more comfortable pedestrian environments. Quantifying a thermally comfortable pedestrian to be considered thermally comfortable, residents should be able to walk 20 minutes (about one mile) from origin to destination without risk of heat illness or personal discomfort from heat exposure. This 20-minute standard derives from walkability standards in public health literature and municipal sustainability goals (Ariane, 2016).

2.2. Case Study: Pedestrian Thermal Comfort in Jeddah, Saudi Arabia

Jeddah, a coastal city in Saudi Arabia, experiences hot and humid climatic conditions, making pedestrian thermal comfort a critical urban design challenge (Masoud, 2021). The city's urban morphology, street orientation, and shading strategies significantly influence outdoor thermal conditions, directly impacting pedestrian well-being (Hegazy & Qurnfulah, 2020).

Urban expansion in Jeddah has intensified the urban heat island (UHI) effect, leading to increased thermal discomfort for pedestrians (Masoud, 2021). Research indicates that compact urban forms with narrow streets and high-rise buildings provide better shading and reduce direct solar exposure, which improves pedestrian thermal comfort (Hegazy & Qurnfulah, 2020). The study combining quantitative and qualitative approaches to assess thermal conditions. Methodologies used in this study is field measurements by instruments, observational and questionnaire survey, urban morphology analysis, thermal comfort indices, sky view factor analysis and numerical simulations.

Street orientation plays a crucial role in regulating solar exposure and mitigating heat stress in urban environments (Johansson, 2006). A study using ENVI-met simulations revealed that north-south oriented streets receive less direct solar radiation than east-west oriented streets, which experience higher thermal loads due to prolonged sun exposure (Hegazy & Qurnfulah, 2020). Proper street orientation helps mitigate heat stress by optimizing shading and airflow, thus enhancing pedestrian comfort (Littlefair, 2000).

Shading elements such as trees, arcades, and urban canopies are effective in improving pedestrian thermal comfort in Jeddah (Masoud, 2016). Research findings indicate that tree-lined streets reduce surface temperatures by up to 5°C, creating a more favorable microclimate for pedestrians (Littlefair, 2000). Additionally, sky view factor (SVF) analysis suggests that higher building density contributes to better shading, effectively reducing mean radiant temperature (MRT) (Mayer, 1987).

Natural ventilation is another key factor influencing pedestrian thermal comfort in Jeddah (Johansson, 2006). Studies show that street orientation and urban geometry affect wind flow patterns, which directly impact cooling efficiency (Hegazy & Qurnfulah, 2020). Streets aligned with prevailing wind directions facilitate better airflow, reducing heat accumulation and improving pedestrian thermal conditions (Johansson, 2006). However, dense urban layouts can obstruct wind movement, leading to localized heat stress and reduced air circulation (Littlefair, 2000).

The findings from Jeddah emphasize the importance of climate-responsive urban design in mitigating pedestrian thermal discomfort. Strategies such as optimizing street orientation, enhancing shading elements, improving urban ventilation, and using reflective materials can significantly enhance pedestrian thermal comfort (Masoud, 2021). Implementing these strategies promotes sustainable urban environments and ensures thermally comfortable pedestrian spaces, particularly in hot climates (Hegazy & Qurnfulah, 2020).

2.3. Summary of Literature Review

The literature review highlights the role of street orientation on shading plays a critical role in mitigating thermal stress, with studies emphasizing the effectiveness of tree canopies, building form and high height to width ratios in lowering mean radiant temperature (MRT) and Universal Thermal Climate Index (UTCI) particularly when guided by Sky View Factor (SVF) thresholds below 0.5. pedestrian perception of comfort is deeply influenced by subjective experiences, including clothing insulation, activity levels and adaptive preferences as well as microclimatic elements such as air temperature and wind flow underscoring the need to prioritize human centered design principles validated through tools like comfort votes and meteorological preference scales. Street orientation itself directly impacts thermal performance street orientation. These effects are well captured through bioclimatic charts and quantitative metrics derived from Cohen’s conventions, offering a scientifically grounded approach for evaluating and improving thermally comfortable urban design.

CHAPTER THREE

MATERIALS AND METHODS

3.1. Descriptions of the Study Area

Geographically, Metehara town is located in central part of Ethiopia in the East Shewa zone of Fentale woreda in Oromia region, at a distance of 192km from Addis Ababa and 96km from Adama city. The town is bounced in the east by Awash Park; in the west by Beseka Lake; in the north by Fentale Mountain and in the south by Methara sugar factory. It is located at 08°54′N latitude and 39°55′E longitude with an elevation of 947meters above sea level.

According to the traditional climate zone of Ethiopia the climate in Metehara town is kola (lowland) (MOA, 2000). According to Koppen climate classification system, the climate in Metehara town is hot semi-arid (steppe) climate, characterized by hot, sometimes extremely hot, summers, warm to cool winters and with some minimum precipitation. According to data from NASA (1993-2023) the annual average temperature in Metehara town exceeds 26.92 ^{o}c, and the highest monthly average temperature for the year occurs in June (29 ^{o}c), the lowest monthly average temperature occurs in December (24 ^{o}c) and the monthly average relative humidity is between 48% and 78%.

Metehara urban planning is influenced by rapid population growth, industrial the presence of Metehara sugar factory and environmental concerns particularly related to Lake Beseka and the Awash River. Metehara town street system is structured to support both local mobility and the regional connectivity. Metehara is accessible the Addis Ababa to Djibouti railway, which enhances the town is the hub of transport. The town street layout dominant North-South (N-S) and East-West (E-W) street orientations.

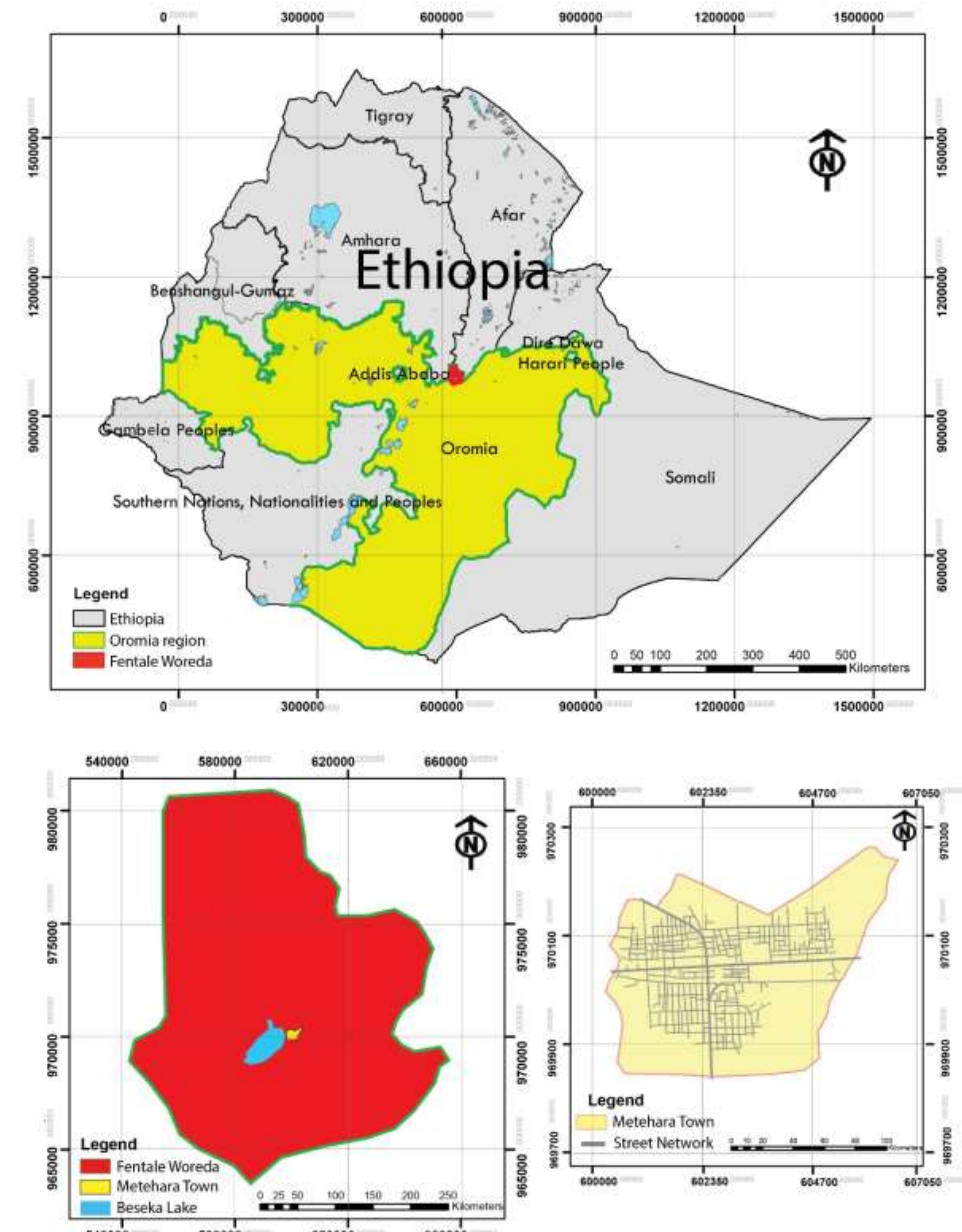

Figure 3.1 Location map

3.2. Research Design

The study was undertaken in orderly and sequential manner starting from problem statement to conclusion and recommendation of the study.

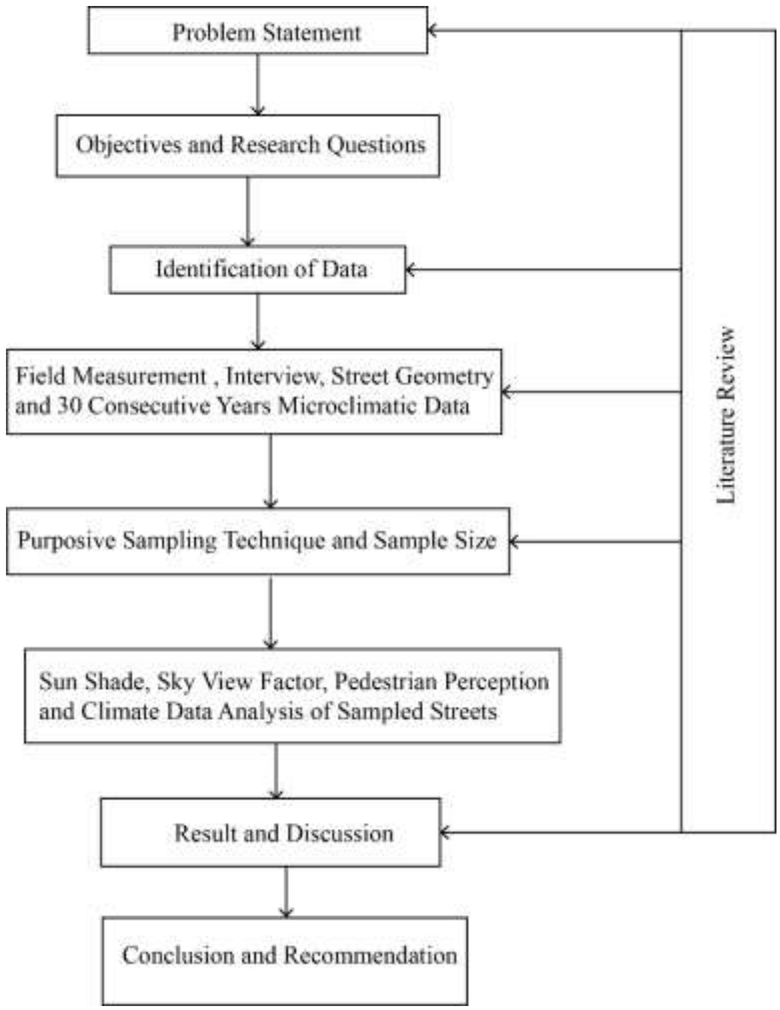

Figure 3.2 Research design

3.3. Method of Data Collection

3.3.1. Type and Source of Data

In this study a mixed method approach data type was used. Data source is anything that gives direct evidence about the data, site or phenomena that are studying. The data these monthly and hourly temperature, wind speed, relative humidity and solar radiation recorded for 30 consecutive years from 1993 to 2023 was obtained from the Ethiopia meteorology Agency and the website of global weather data for SWAT and NASA surface meteorology. In addition, the data was collected from surveys, interview of the pedestrian and collected by personal measuring of the air temperature and relative humidity of the pedestrian street.

i. Feld Measurement

In the field measurement experiments, meteorological parameters, including air temperature (Ta) and relative humidity (RH) were measured by using a hygrometer (Co. KGaA, Titisee-Neustadt, Germany, 2019). The instruments comply with the ISO 7726 standard. All instruments were set up 1.5 m above ground level (Zhang, T., 2019) and the meteorological parameters were recorded every minute. In order to exclude the influence of surrounding buildings on the measured data, the instruments were located a minimum of two meters away from nearby buildings.

Table 3.1 Instrument used for measure the air temperature and relative humidity

Parameters	**Instrumentation**	**Range**	**Accuracy**
Temperature	Temperature & humidity meter(hygrometer)	−50◦C to +70 ◦C (-58◦F to +158◦F)	±1 ◦C (1.8◦F)
Relative humidity	Temperature & humidity meter(hygrometer)	10%RH to 99%RH	±5%RH

ii. Interview Questionnaires

The questionnaires are divided into two sections. The first section gathers personal information including gender, age, activity level and clothing. The second section evaluates three key aspects: the overall comfort vote, preference for meteorological parameters and thermal acceptability. The overall comfort vote uses a 3-point scale (−1, discomfort; 0, neutral and 1, comfortable). Thermal acceptability vote follows a 7-point scale (−3, extremely unacceptable; −2, unacceptable;-1, slightly unacceptable; 0, neutral; 1, slightly acceptable; 2, acceptable and 3, extremely acceptable). Finally, preferences for meteorological parameters are indicated using a 3-point scale (−1, 0 and 1 representing weaker/lower, unchanged and stronger/higher respectively) reflecting respondents desired conditions.

3.4. Sampling Technique and Sample Size

In order identify the thermal comfort of the pedestrian, it is need to gather and compile quantitative micro climatic data about hourly temperature, humidity, wind speed, solar radiation and also street orientation and plant type availability. For analyzing the physical conditions of streets of Metehara town, representative sample streets are need to identify. These streets were screened out using purposive sampling. To select the streets for study were by grouped using cardinal direction.

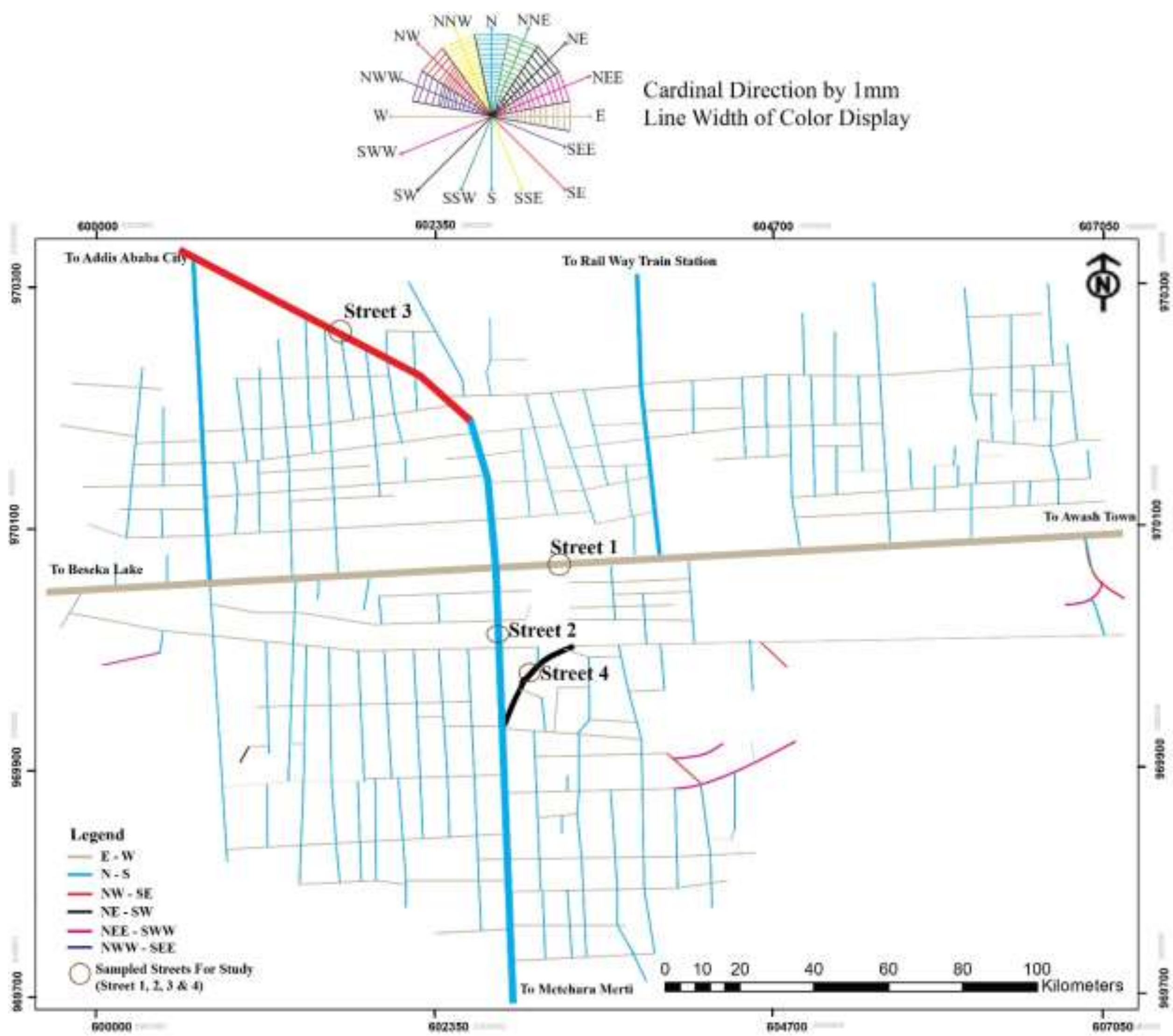

Figure 3.3 Streets orientations of Metehara town by cardinal direction and selected streets

From the total of 197 streets identified on figure 3.3; 49.5% of streets are oriented to N-S, 47.6% are oriented to E-W, 1% are oriented to NW - SE, 0.3% of streets are oriented to NE-SW, 0.45%

of streets are oriented to NEE-SWW and 0.15% of streets are oriented to NWW-SEE. Generally 98.1% of existing streets in Metehara town are oriented to N-S and E-W.

For the study as show in figure 3.3; the large size streets were chosen. The parameters are orientation, street width, street side plantation and volume of pedestrian. Based on those parameters four (4) streets out of the existing streets are systematically and purposively sampled to check thermal comfort of the pedestrian.

Table 3.2 Sampled street geometry and description

Name	Street orientation	Street width	Building height	Satelite image of selected street	Street section
Street-1	E-W	20m	G+0 on the north side of street G+2 on the south side		
Street-2	N-S	20m	G+0 both side		
Street-3	NW-SE	20m	G+0 both side		
Street-4	NE-SW	15m	G+0 both side		

The selected streets are sampled to check thermal comfort of the pedestrian, one of the parameter for these sampled streets are selected depend on volume of the pedestrian. In this study, in order to use a large sample size, to reduce sampling bias, and to make sure that the results will be representative large number of pedestrian volume streets with their orientation will be used to collect information on the pedestrian thermal comfort of the selected streets. Therefore, to obtain representative information from the selected streets are important to recorded number of pedestrians for 15 minutes at each streets and days of the week.

Table 3.3 Recorded number of pedestrians

Rol.no	**Days**	**Recorded number of pedestrians for 15 minutes each day in 3 meter width pedestrian walkway**			
		Street 1	Street 2	Street 3	Street 4
1	Monday	32	29	15	1]4
2	Tuesday	35	34	18	12
3	Wednesday	27	31	19	7
4	Thursday	33	27	11	13
5	Friday	21	19	15	6
6	Saturday	29	21	21	11
7	Sunday	21	17	9	7
Total		198	178	108	70
Flow rate (ped/min/m)		0.63	0.56	0.34	0.22
LOS		A	A	A	A

To compare pedestrian thermal comfort across four selected street orientations according to pedestrians perception a sample size estimation was conducted according to Cohen's (1988) the formula to determine and calculate the sample size of pedestrian based on one-way ANOVA Cohen's effect size.

$$n = (k - 1)\,(Z_{1-\beta} + Z_{1-\alpha/2})^2 / k.f^2$$

Where: n = sample size per group (per street), k = number of groups, f= Cohen's effect size (ratio of between group SD ($\boldsymbol{\sigma}_{between}$) to within group SD ($\boldsymbol{\sigma}_{within}$)), $Z_{1-\beta}$= Z-score for desired power (0.84 for 80% power) and $Z_{1-\alpha/2}$ = Z-score for confidence level (1.96 for 95% confidence).

The table above (table 3.3) shows group means were derived from 15 minute pedestrian flow rates recorded over seven consecutive days: Street 1 = 0.63, Street 2 = 0.56, Street 3 = 0.34 and Street 4 = 0.22 pedestrians per minute per meter (ped/min/m). The within group standard deviation calculated from daily recorded within each street, approximately 0.3 ped/min/m reflecting the average variation in flow rate over time for each street. The between group standard deviation calculated from the variation among the four street means, approximately 0.165 ped/min/m.

$$\text{Cohen's effect size (f)} = \boldsymbol{\sigma}_{between} / \boldsymbol{\sigma}_{within}$$

$$f = 0.165/0.3 \approx 0.55,$$

This value represents a large effect size according to Cohen's (1988) benchmarks. Using this value along with k = 4 (4 selected streets orientation), f = 0.55, $Z_{1-\beta}$ = 0.84 (for 80% power) and $Z_{1-\alpha/2}$ = 1.96 (for 95% of confidence)

$$n = (4-1)\,(0.84 + 1.96)^2 / 4 \cdot (0.55)^2 = 23.52/1.21 = 19.4 \approx 20 \text{ sample size per street}$$

Then the total sample size is 4 x 20 = 80 pedesterians

3.5. Analysis and Method of Data Analysis

3.5.1. Analysis of Pedestrian Interview Questionnaires

The Analysis of pedestrian interview data involves identifying patterns and themes related to pedestrian perceptions and experiences. This can be done through qualitative analysis, such as coding and thematic analysis or by using statistical methods to analyze numerical data.

The interview questions responses also analyzed through the comparative analysis of streets to determine thermal comfort performance the streets for pedestrians. Data was analyzed by visual representation; charts and graphs created by using software's such as Excel, SPSS and illustrator.

3.5.2. Sun path and Sun Shade Analysis

Sun shade analyses are an important tool for studying thermal comfort of the pedestrian at different street orientation. Sun shade was analyzed through the equations;

Sun shade length (L) = H/tan θ ………………………………………….………….. (1)

Where H = height of buildings or trees

θ = Sun altitude

Modeling of street orientation graphics analysis has been performed using AutoCAD and illustrator software's.

For analyzing sun shade of the site first of all we must be find declination, latitude, hour angle, altitude and azimuth angle of the sun of the town. Therefore the solar analysis was made using the following three equations as described in the following three equations.

Step -1: calculating the declination (σ) which is the same for all locations

σ =23.45*sin(360/365 (N+284))………………………………………………………….. (2)

Where N= Julian yean starting from January 1

Step-2: Calculate the altitude (A) of the sun using the following formula

Altitude=sin^ (sin σ sin ɵ +cos σ cos ɵ cos ɯ)…………………….…………………….... (3)

Where, σ=latitude of the location; ω= hour angle (which is ω=cos^(-tanϴ tanσ)

Step-3: calculate the Azimuth of the sun for each hour

AZI = arcsin [(cosσ*sinω)/cosALT] and to get the day length = 2/15ω……………..…… (4)

3.5.3. Sky View Factor (SVF) Analysis

To find SVF and analyze it effectively, methods depending on the data, tools and complexity of the urban environment by using the following key formulas;

Symmetrical urban canyon according to Oke (1981)

$$SVF = 1/ 1 + (H/W)^2 \text{……………………………………………………………. (1)}$$

Where: - H is average building height

- W is street width

Used when both side height are same

Asymmetrical canyon (two different heights) according to Grimmond (1999)

$$SVF = ½ [\cos^2 (\arctan (H_1/W)) + \cos^2 (\arctan (H_2/W))] \text{……………….. (2)}$$

Where:- H1, H2 are building heights on each side

-W is street width; used for uneven urban geometry

Vegetation adjustment according to Lindberg & Grimmond (2010)

$$SVF_{adjusted} = SVF_{geometric} \times T_f \text{…………………………………………………….. (3)}$$

Where: T_f is tree canopy transmissivity (typically, dense tree canopy using T_f = 0.3 - 0.5 and sparse trees with gaps use T_f = 0.7 – 0.9).

By using the above three formulas the SVF was plays a critical role in examining shading effects on pedestrian thermal comfort across different street orientations.

3.5.4. Environmental Parameters Analysis

These parameters were analyzed using both long-term archival data and field measurements to assess their impact on thermal conditions along various street orientations.

Air Temperature trends were compared across streets to determine the intensity of thermal exposure. Temperature variations were analyzed over critical hours (10:00 AM–4:00 PM). Relative Humidity variations were assessed to understand evaporative cooling effects and their implications on pedestrian comfort. Wind Speed analysis were conducted to evaluate the capacity of air movement to dissipate heat. Spatial differences were analyzed to determine the influence of urban geometry on airflow. Solar Radiation data were examined to quantify heat stress potential, integrating long-term records and observational data.

The actual wind speed pedestrians experience at ground level often differs from NASA power data, which is typically measured at a standard meteorological height (around 10 meters or higher). The difference depends on several factors. Surface Roughness like buildings, trees and street geometry and also street orientation cause wind speed to decrease compared to open areas. Wind speed reduces closer to the ground due to friction, so pedestrians typically experience lower speeds than what NASA POWER data reports. Using standard wind profile equations estimate for pedestrian level wind speed can be found using the logarithmic wind profile equation.

$$U(z) = U_{ref} \times (\ln(Z/Z_0) / \ln(Z_{ref} / Z_0))$$

Where: U (z) is the pedestrian level wind speed

U_{ref} is the NASA power wind speed at reference height Z_{ref} typically 10m

Z is pedestrian height (1.5–2m)

Z_O is the surface roughness length (varies by terrain ~0.1m-1m for urban areas)

Data were graphically represented using histograms charts to highlight diurnal and seasonal patterns. These visualizations elucidated critical insights into the microclimatic variations among the sampled streets.

3.5.5. Mean Radiant Temperature Analysis

The mean radiant temperature (MRT) is one of the important factors for evaluating street for pedestrian thermal comfort. This is defined as the uniform ambient temperature in an imaginary enclosure, where the radiant heat transfer from the human body to an enclosure surface is equal to the no uniform temperature heat transfer to an actual enclosure surface. According to Fanger (1982), Mean radiant temperature analyses are an important tool for studying thermal comfort of the pedestrian at different street orientation.

Mean radiant temperature have been analyzed through the Formula;

$$MRT = \left(\frac{GHI \cdot \frac{A_p}{A_s} + \sigma \cdot T_a^4}{\sigma} \right)^{1/4}$$

Where; MRT: mean radiant temperature (^{o} c or k)

GHI: global horizontal irradiance (w/m^2)

A_p /A_s: Ratio of the projected area to the surface area of the human body that is directly exposed to the radiant heat source. A_s is total surface area of the human body. Which is in contact with the surrounding air and radiant heat sources (taken as 0.7)

Ta: air temperature (k)

σ: Stefan Boltzmann constant (5.67 x 10^{-8} w/m^{2}k^4)

The mean radiant temperature numerical result of all street orientation was analyzed by using line chart on excel software.

3.5.6. Universal Thermal Climate Index Analysis

The Universal Thermal Climate Index analyzed by using the Antonello Di Nunzios, 2020 online UTCI calculator of selected street orientations and geometrics. The UTCI considers the combined effects of air temperature, wind speed, relative humidity and mean radiant temperature of the streets. The result of the calculator was analyzed by using line chart of the Excel software and through descriptive statistics, comparative analysis and graphical representation. The analysis of UTCI is depending on the scale that is divided in to ten thermal stress categories according to Bernd Tinz, (2012).

3.5.7. Developing Bioclimatic Chart

Bioclimatic chart involves interpreting climate data to assess thermal comfort and identify suitable design strategies. Understand the axes bioclimatic charts typically plot temperature (x-axis) against relative humidity (y-axis). Some versions also incorporate solar radiation and wind speed. Comfort zones identify the thermal comfort range, often represented as a shaded or enclosed area. This zone indicates conditions where people feel comfortable without additional heating or cooling. The climate data plot points (monthly averages for selected three months) onto the chart. This helps visualize how often conditions fall within or outside the comfort zone. Design strategies based on the analysis, select appropriate urban or architectural interventions such as vegetation integration, material selection, or street orientation to enhance thermal comfort.

The comfort zone temperature is defined between 21 ^{O}C and 27.8 ^{O}C and is changeable based on the season. The relative humidity is defined between 30% and 65% with acceptable limits of 20–78% (Katafygiotou and Serghides, 2014). The values of the mean minimum and maximum temperatures are paired with the maximum and minimum relative humidity, respectively. The line is created by connecting two variables and representing the various months to reflect the outdoor condition.

3.6. Method of Data Interpretation

The analyzed data was interpreted as tables, charts, graphs and maps. Software like autoCAD, GIS and excel were used to interpret the data in different ways.

3.7. Summary of the Methodology

Table 3.4 Summary of the research methodology

No	Specific objectives	Types of data	Data collection methods & instruments	Data analysis Methods
1	To understand perception of pedestrians about the thermal comfort of streets.	Pedestrians subjective experience, preference and overall concerns	Interview method Using mobile phone for recording and A4 size paper and pen	Evaluating perception of pedestrians across street orientation comparison
2	To assess the thermal comfort performance of existing street orientations for pedestrians.	Building height, trees availability, street width, walkway shade and street orientation and also Temperature, relative humidity, wind speed and solar radiation	Site observation, 30 years consecutively data of NASA power. Field measurement by Hygrometer  A4 size paper and pen	Shading by using formula calculating solar shadow and sky view factor value across street orientation, Compare microclimate data variotions across hours and street orientation, MRT by formula and UTCI online calculation by using grapphs & texts

CHAPTER FOUR

RESULT AND DISCUSSION

4.1. Perception of Pedestrians Thermal Comfort

The perception investigated pedestrian thermal sensation in Metehara town, considering four distinct street orientations: East-West (Street-1), North-South (Street-2), Northwest-Southeast (Street-3), and Northeast-Southwest (Street-4). The evaluation integrated respondents overall thermal comfort votes, thermal acceptability votes, and preference for meteorological parameters during critical hours (10:00 AM–16:00PM) of the day.

4.1.1. Activity Level and Clothing Insulation of Pedestrians

Among the 80 valid interview questionnaires, during the survey period; light exercising 48.21% and Sitting 44.643% were the primary activity and also standing 7.147%. The activity levels are converted to metabolic rates according to the ASHRAE 55 standard (Figure 4.1). According to the statistics for the clothing status of the respondents and the clothing insulation value estimation table compiled to the ISO 7730 standard (2005), the clothing resistance of people in Metehara town is fluctuated between 0.1 clo and 1.5 clo with changing trends in the mean clothing insulation consistent with the mean air temperature during the surveying periods of the day (10:00 AM – 16:00 PM) (Figure 4.2). Therefore activity levels and clothing insulation in Metehara town pedestrian thermal comfort have a minor influence, because in extreme heat level of activity is overshadowed by radiant heat and air temperature means it has smaller impact. In addition, in consistently of warm climates of the town, pedestrians tend to wear light and breathable clothing.

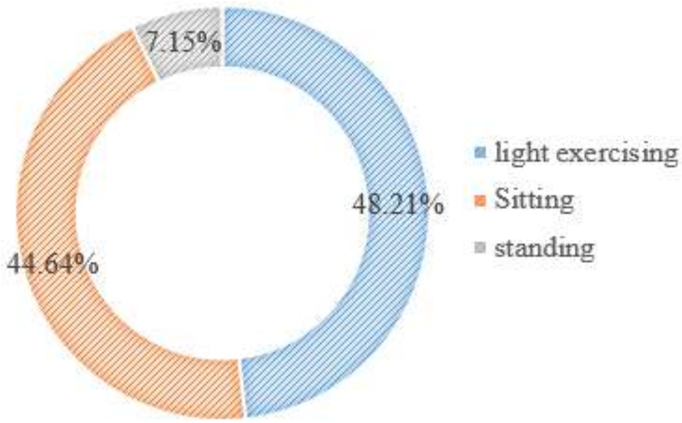

Figure 4.1 Distribution of activity levels in the survey

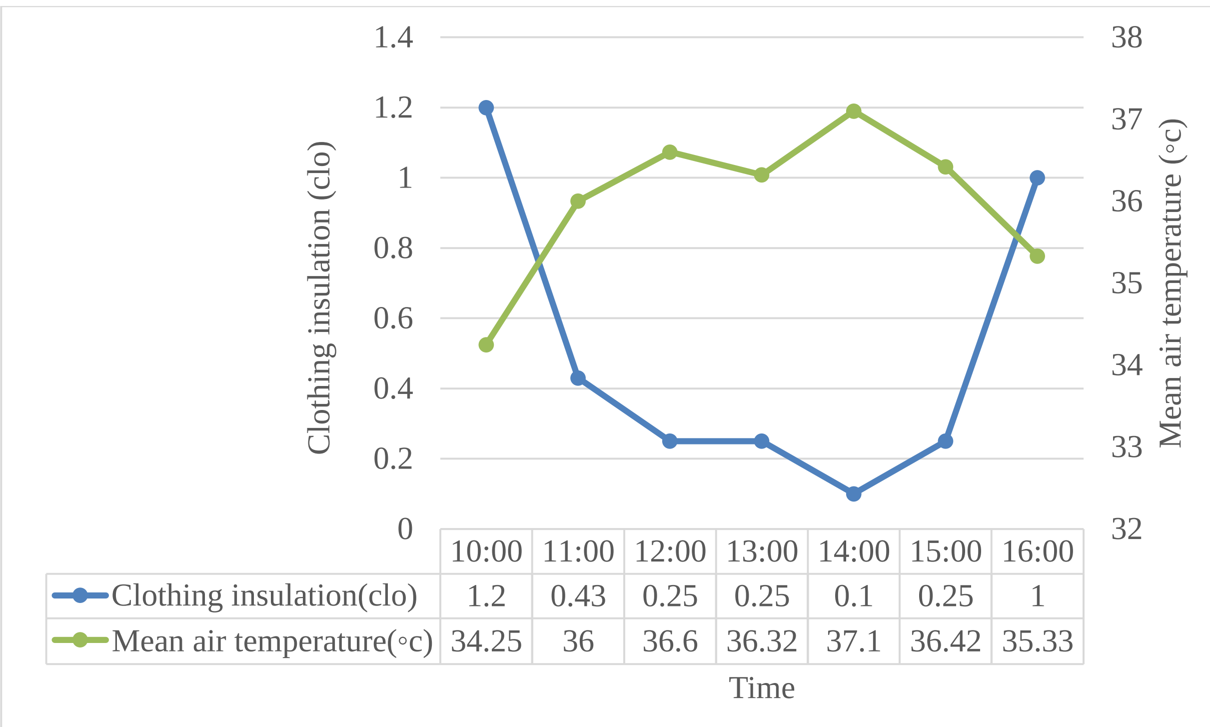

	10:00	11:00	12:00	13:00	14:00	15:00	16:00
Clothing insulation(clo)	1.2	0.43	0.25	0.25	0.1	0.25	1
Mean air temperature(◦c)	34.25	36	36.6	36.32	37.1	36.42	35.33

Figure 4.2 Clothing insulation of pedestrian and mean air temperature relation during surveying periods

4.1.2. Overall Thermal Comfort Vote

Overall comfort is influenced by many factors, such as the thermal air temperature, humidity, wind speed, solar radiation, clothing, activity level and personal factors. Figure 4.3 shows the percentage of subjects at each street orientation voting for each overall comfort level. Among the street 1 and

2 “Neutral” vote are (20% for both) while “Uncomfortable” is the most frequent vote 75% for street-1, 55% for street-2, 85% for street-3 and 90% for street-4. While at 10:00am and 16:00pm the most common overall comfort vote is neutral. This suggests that the town air condition at those three hottest (April, May and June) is not comfortable for walking on the selected streets; because the people’s needs shade.

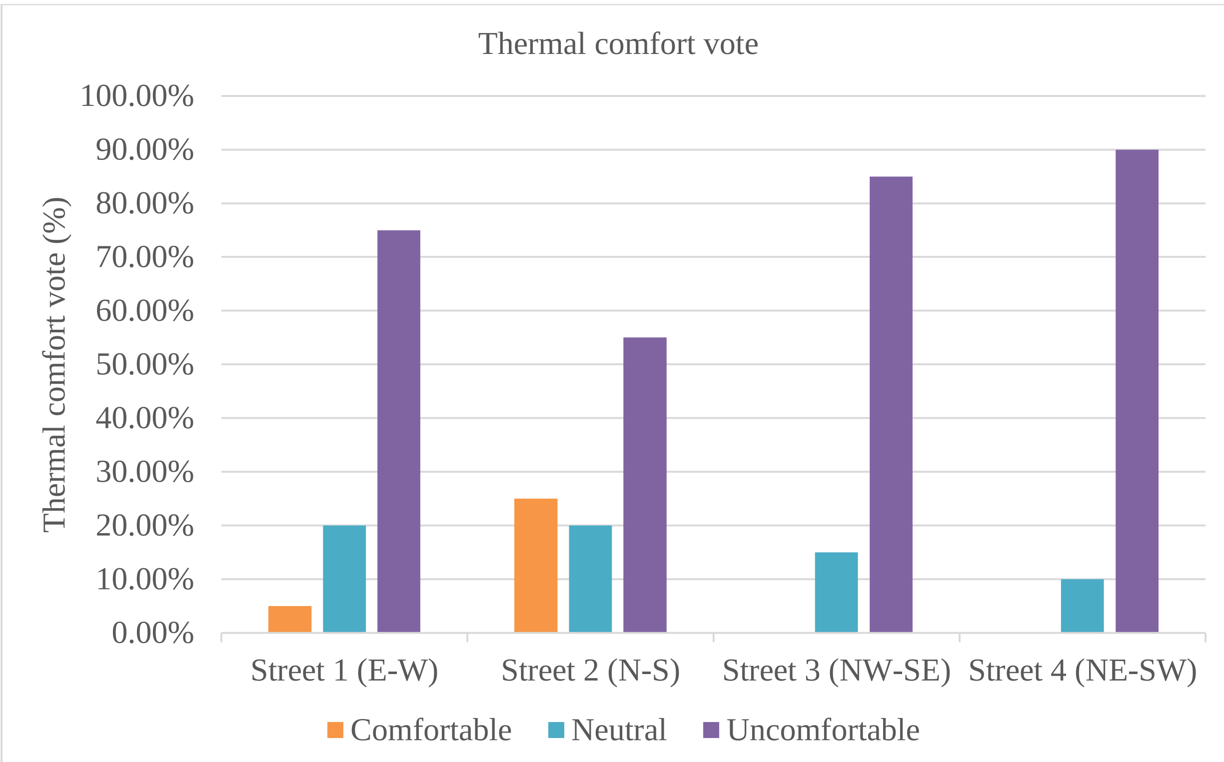

Figure 4.3 Thermal comfort vote percentage of respondents for the selected street orientation

Overall Thermal Comfort Vote (TCV) response a significant majority across all streets reported discomfort. Streets-1, 3 and 4 with minimal shade and elevated temperatures, were especially unfavorable. Neutral comfort levels were briefly noted in early morning and late afternoon (10:00 and 16:00 respectively), but the streets remained largely uncomfortable during midday hours.

4.1.3. Thermal Acceptability Vote

The distribution of thermal acceptability vote of the respondents at different street orientation shows on Figure 4.4 below. Mostly the respondents depend on their shading of the street. For the street that has no shade, they voted from extremely unacceptable (-3) to unacceptable (-2), because the air temperature and solar radiation on these street (street-3 and street-4) were high but low relative humidity and also lower air velocity on street-4, this leads to discomfort of the pedestrian. Accordingly, the street that have some shade from trees and buildings and also street that have well air velocity during the peak hours of the day the respondents vote unacceptable (-2) to acceptable (2), most of the respondents vote for slightly unacceptable (-1) and slightly acceptable (1) on orientation of (street-2). In addition, for street-1 orientation the respondents mostly vote for extremely unacceptable (-2) to unacceptable (-2).

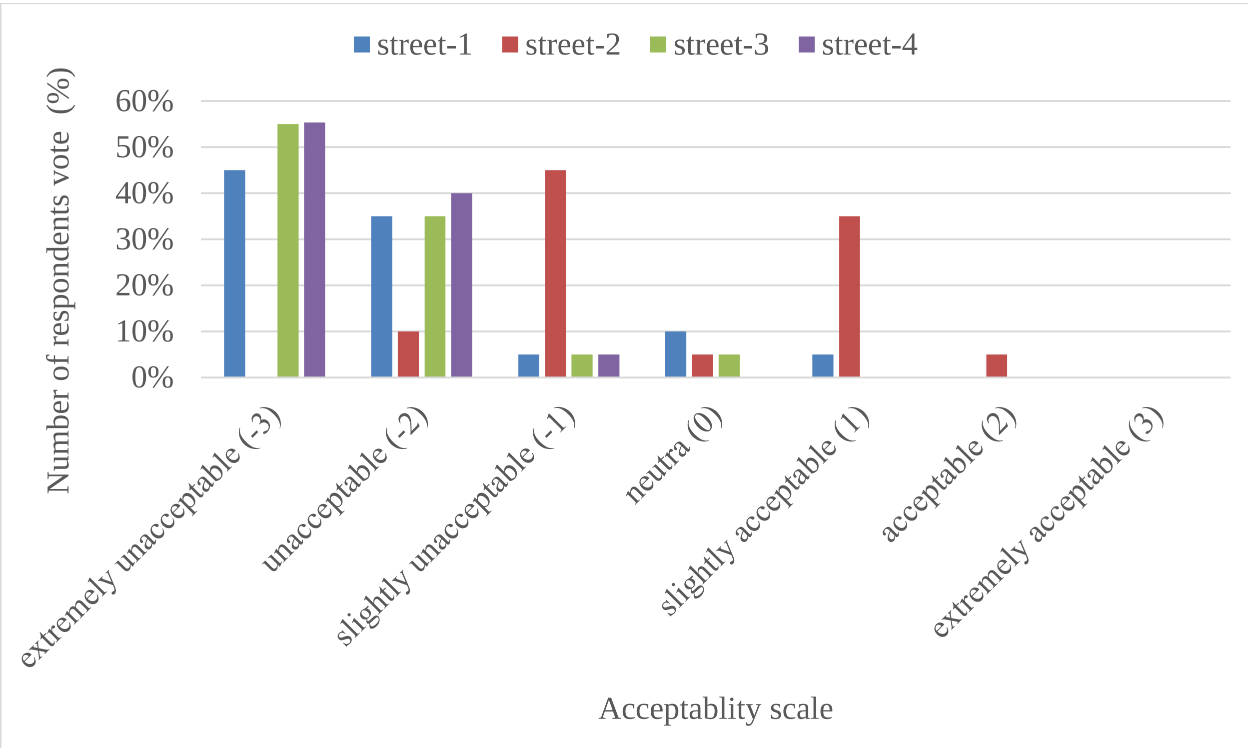

Figure 4.4 Thermal acceptability vote percentage of respondents for the selected streets orientation

In general, as considering the respondents vote that all selected streets are thermally uncomfortable for pedestrian except slightly acceptable street-2 orientation (N-S) during the periods of harsh sun. Street-4 received the most unfavorable votes, reflecting poor shading and inadequate cooling effects. The respondent’s thermal acceptability vote figure 4.4 show that the climatic need of pedestrians is shade during peak hours of the day.

4.1.4. Preference Vote of Meteorological Parameters

Pedestrian thermal comfort is not solely affected by a single meteorological parameter but by a series of parameters. Figure 4.5 below shows respondent's preferences for various meteorological parameters are different at each street. The majority of respondents at Street-1 51.8% and 65% desire lower air temperatures and higher relative humidity respectively and also 57% and 45% prefer weaker solar radiation and unchanged wind speed respectively. At street-2 the respondents prefer lower air temperature 41.1% and weaker solar radiation 37.2%, this is related to the more shaded street from trees on this street for most part of the day. However, at street-3 the respondents mostly demands for lower temperature and solar radiation but also to increase relative humidity and most of the respondents prefer constant wind speed. In terms of the pedestrian wind speed, the demands for wind speed to increase at street-4 are the most obvious, the stronger the desired wind speed and also the lower the air temperature and solar radiation. The respondents demand for increase humidity at all street is higher (more than 65%).

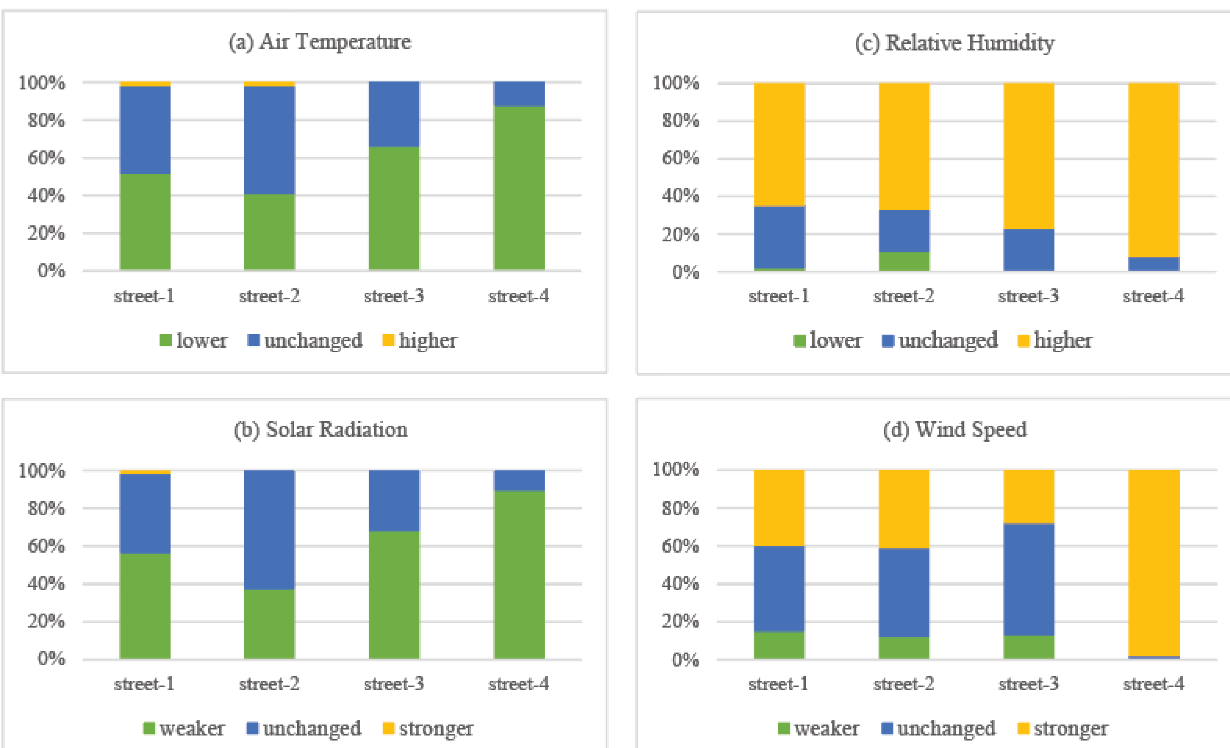

Figure 4.5 Preference vote of meteorological parameters for the selected streets (a) air temperature, (b) solar radiation, (c) relative humidity and (d) wind speed

Preference for Meteorological Parameters respondents expressed a preference for lower air temperatures and reduced solar radiation across all streets. Higher relative humidity and stronger wind speeds were desired, particularly on Streets 3 and 4, to alleviate the thermal stress caused by intense solar exposure and poor ventilation.

Overall, according to respondent's preference vote of metrological parameters (figure 4.5) above shows the pedestrians streets need for cooling by using different strategy like; street orientation for welcoming the air velocity, green infrastructure, water bodies (ponds & fountains) to maximize humidity and shading from buildings and trees. These strategy can minimize the air temperature and solar radiation of street but also it maximize their humidity and air movement.

General pedestrian perception results comparative analysis of all selected streets, Street-1 (East-West) perform poor thermal conditions, limited shade from buildings the especially south side buildings not give shade for pedestrian over the day and inadequate vegetation reduced comfort levels. Street-2 (North-South) relatively favorable thermal comfort due to better shading from trees, buildings and alignment with prevailing wind patterns. Street-3 (Northwest-Southeast) & Street-4 (Northeast-Southwest) these orientations performed poorly, with extended exposure to solar radiation and inadequate airflow. Street-4 was the least comfortable due to lower relative humidity and obstructed wind flow.

4.2. Sun Path and Solar Shadow Analysis

This study evaluates selected street orientation shading impact on pedestrian thermal comfort at the critical time (10:00 AM– 16:00 PM) of Metehara town focusing on sun path and solar shadow analysis. Sun path and solar shadow plays a crucial role in evaluating shading effect on pedestrian thermal comfort across different street orientations; this involves assessing how solar radiation interacts with the geometry of buildings, vegetation and shading through time of the day across their orientation to optimize thermal condition for pedestrians.

4.2.1. Sun Path and Shade Length

Sun path involves understanding the movement of the sun throughout the year to assess its impact on shading and pedestrian thermal comfort. The sun path diagram of Metehara is drawn as shown below Figure 4.6.

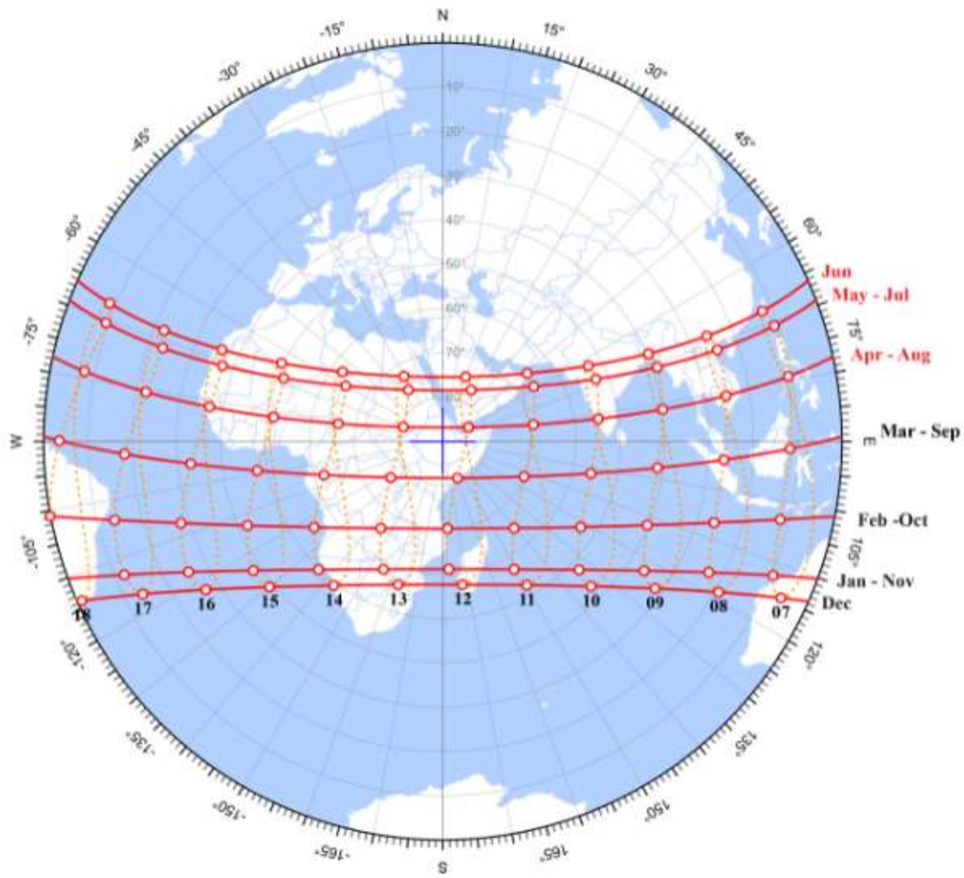

Figure 4.6 Equidistance sun path diagram of Metehara town

Using the sun path diagram above Figure 4.6 of Metehara, the shadow length is analyzed for critical hours of three months described in Table 4.1 below. The critical time in Metehara observed from 10:00 AM-16:00 PM. Shade length calculations allow to assess how much solar radiation is blocked, influencing MRT and UTCI. Variations in solar angles by (degree) for selected months on the table 4.1 below ensuring shading solutions across the seasons.

Table 4.1 Declination, Hour angel, Altitude, Azimuth and Solar shadow length of months.

Months	Unit by degree	10:00	11:00	12:00	13:00	14:00	15:00	16:00
April, 21, 2024	Declination	11.93	11.93	11.93	11.93	11.93	11.93	11.93
	Hour Angel	34.75	19.75	4.75	-10.25	-25.25	-40.25	-55.25

	Altitude(θ)	55.73	70.36	84.44	79.47	65.00	50.34	35.68
	Azimuth(β)	81.85	79.42	56.61	-72.40	-80.84	-82.01	-81.65
May, 22, 2024	Declination	20.43	20.43	20.43	20.43	20.43	20.43	20.43
	Hour Angel	34.21	19.21	4.21	-10.79	-25.79	-40.79	-55.79
	Altitude(θ)	55.06	68.18	77.79	74.47	62.59	49.04	35.09
	Azimuth(β)	66.89	56.02	18.97	-40.93	-62.29	-69.00	-71.24
June, 21, 2024	Declination	23.43	23.43	23.43	23.43	23.43	23.43	23.43
	Hour Angel	35.55	20.55	5.55	-9.45	-24.45	-39.45	-54.45
	Altitude(θ)	53.05	65.56	74.53	72.89	62.47	49.61	36.08
	Azimuth(β)	62.53	51.09	19.43	-30.79	-55.23	-64.09	-67.43
Sun shade length (SHL) = H/tan θ								
April, 21		0.6812H	0.36H	0.1H	0.19H	0.47H	0.83H	1.4H
May, 22		0.7H	0.4H	0.22H	0.28H	0.52H	0.87H	1.423H
June, 21		0.752H	0.455H	0.277H	0.31H	0.521H	0.851H	1.372H

4.2.2. Solar Shadow analysis

According to Akshay 2023 shade analysis; solar shadow analysis is a crucial step in understanding how shadows from buildings, trees, and other structures impact pedestrian thermal comfort. Here’s a brief discussion of shadow widths comparison at critical time of (10:00 – 16:00) the day for different street orientations and times of the day for three months of the year on the table 4.2 below.

Table 4.2 Selected streets shadow analysis of April, 21 (10:00 AM - 16:00 PM)

Hour	North – South	East -West	North East to South West	North West to South East
10:00	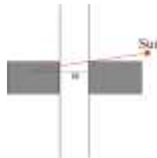 W = Sinβ*SHL W = Sin (81.85)*0.6812H W = 0.7H W= 0.7 x 3m = 2.1m	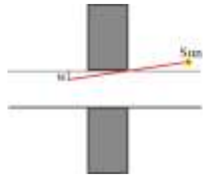 W = Cosβ*SHL W = Cos (81.85)*0.6812H W = 0.1H W = 0.3m	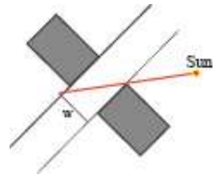 W = Sin(90 - β + 45)*SHL W = Sin(53.15)*0.6812H W = 0.55H W = 1.65m	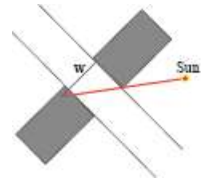 W = Cos(90 - β + 45)*SHL W =Cos(53.15)*0.6812H W = 0.41H W =1.2m
11:00	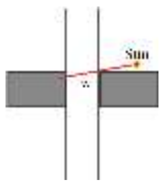 W = Sinβ*SHL W = Sin (79.42)*0.36H W = 0.354H W = 1.062m	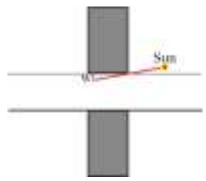 W = Cosβ*SHL W = Cos (79.42)*0.36H W = 0.07 W = 0.21m	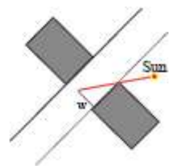 W = Sin(90 - β + 45)*SHL W = Sin(55.58)*0.36H W = 0.3H W = 0.9m	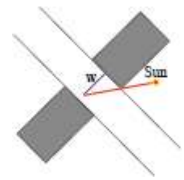 W = Cos(90 - β + 45)*SHL W = Cos(55.58)*0.36H W = 0.204H W= 0.612m
12:00	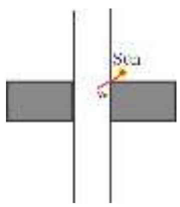 W = Sinβ*SHL W = Sin (56.61)*0.1H W = 0.1H = 0.3m	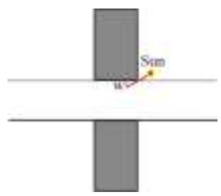 W = Cosβ*SHL W = Cos (56.61)*0.1H W = 0.055H W = 0.165m	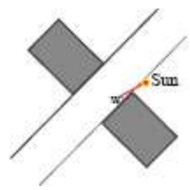 W = Sin(90 - β + 45)*SHL W = Sin(78.39)*0.1H W = 0.1H = 0.3m	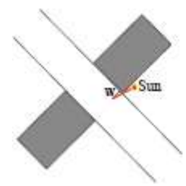 W = Cos(90 - β + 45)*SHL W = Cos(78.39)*0.1H W = 0.02H = 0.06m
13:00	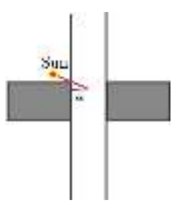 W = Sinβ*SHL W = Sin (-72.40)*0.19H W = -0.2H W = -0.6m	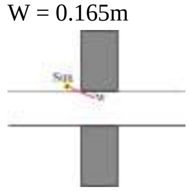 W = Cosβ*SHL W = Cos (-72.40)*0.19H W = 0.058H W = 0.174m	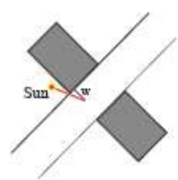 W = Sin(90 - β + 45)*SHL W = Sin(207.4)*0.19H W = -0.09H W = -027m	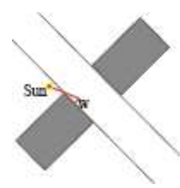 W = Cos(90 - β + 45)*SHL W = Cos(215.84)*0.47H W = -0.4H W = -1.2m
14:00	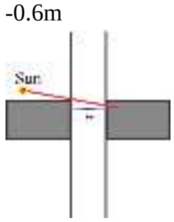 W = Sinβ*SHL W = Sin (-80.84)*0.47H W = -0.464H = -1.392m	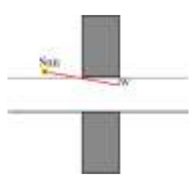 W = Cosβ*SHL W = Cos (-80.84)*0.47H W = 0.075H W = 0.225m	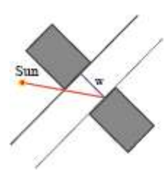 W = Sin(90 - β + 45)*SHL W = Sin(215.84)*0.47H W = -0.3H W = -0.9m	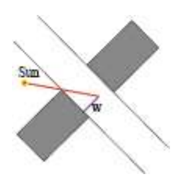 W = Cos(90 - β + 45)*SHL W = Cos(215.84)*0.47H W = -0.4H W = -1.2m

15:00	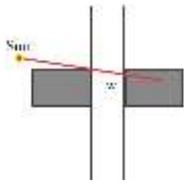 W = Sinβ*SHL W = Sin (-82.01)*0.83H W = -0.822H W = -2.466m	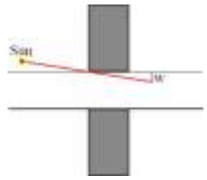 W = Cosβ*SHL W = Cos (-82.01)*0.83H W = 0.14H = 0.42m	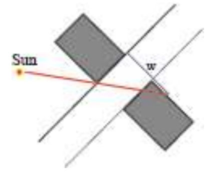 W = Sin(90 - β + 45)*SHL W = Sin(217.01)*0.83H W = -0.5H = -1.5m	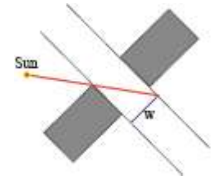 W = Cos(90 - β + 45)*SHL W = Cos(217.01)*0.83H W = -0.663H = -1.989m
16:00	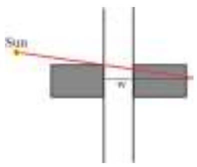 W = Sinβ*SHL W = Sin (-81.65)*1.4H W = -1.39H W = -4.17m	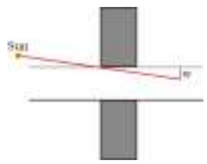 W = Cosβ*SHL W = Cos (-81.65)*1.4H W = 0.203H W = 0.609m	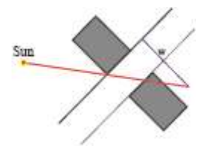 W = Sin(90 - β + 45)*SHL W = Sin(216.65)*1.4H W = -0.84H W = -2.52m	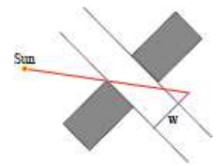 W = Cos(90 - β + 45)*SHL W = Cos(216.65)*1.4H W = -1.123H W = -3.369m

Table 4.3 Selected streets shadow analysis of May, 22 (10:00 AM - 16:00 PM)

Hour	North – South	East -West	North East to South West	North West to South East
10:00	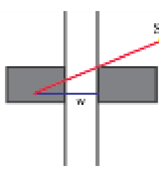 W = Sinβ*SHL W = Sin (66.89)*0.7H W = 0.644H = 1.932m	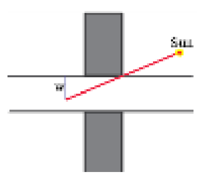 W = Cosβ*SHL W = Cos (66.89)*0.7H W = 0.3H = 0.9m	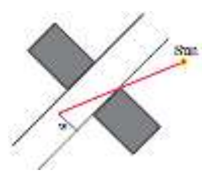 W = Sin(90 - β + 45)*SHL W = Sin(68.11)*0.7H W = 0.65H = 1.95m	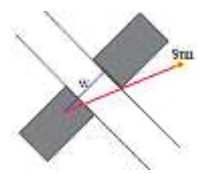 W = Cos(90 - β + 45)*SHL W = Cos(68.11)*0.7H W = 0.261H = 0.783m
11:00	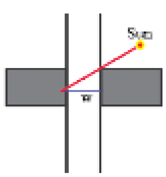 W = Sinβ*SHL W = Sin (56.02)*0.4H W = 0.332H = 0.996m	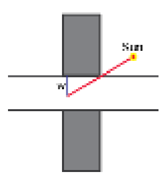 W = Cosβ*SHL W = Cos (56.02)*0.4H W = 0.224H = 0.672m	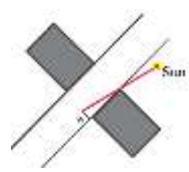 W = Sin(90 - β + 45)*SHL W = Sin(78.98)*0.4H W = 0.4H = 1.2m	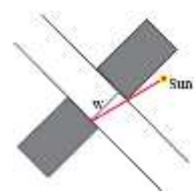 W = Cos(90 - β + 45)*SHL W = Cos(78.98)*0.4H W = 0.1H = 0.3m
12:00	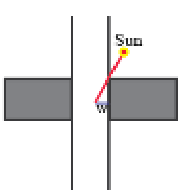 W = Sinβ*SHL W = Sin (18.97)*0.22H W = 0.1H = 0.3m	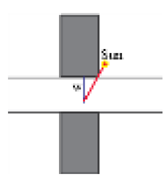 W = Cosβ*SHL W = Cos (18.97)*0.22H W = 0.21H = 0.63m	 W = Sin(90 - β + 45)*SHL W = Sin(116.03)*0.22H W = 0.2H = 0.6m	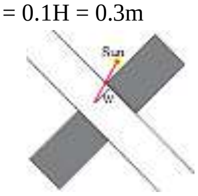 W = Cos(90 - β + 45)*SHL W = Cos(116.03)*0.22H W = -0.09H = -0.27m

13:00	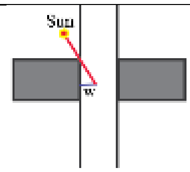 W = Sinβ*SHL W = Sin (-40.93)*0.28H W = -0.184H = -0.552m	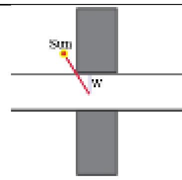 W = Cosβ*SHL W = Cos (-40.93)*0.28H W = 0.212H = 0.636m	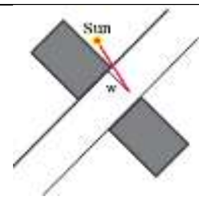 W = Sin(90 - β + 45)*SHL W = Sin(175.93)*0.28H W = 0.02H = 0.06m	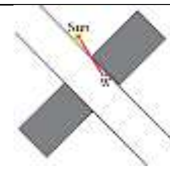 W = Cos(90 - β + 45)*SHL W = Cos(175.93)*0.28H W = -0.28H = -0.84m
14:00	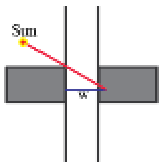 W = Sinβ*SHL W = Sin (-62.29)*0.52H W = -0.5H = -1.5m	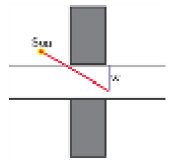 W = Cosβ*SHL W = Cos (-62.29)*0.52H W = 0.242H = 0.726m	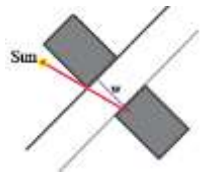 W = Sin(90 - β + 45)*SHL W = Sin(197.29)*0.52H W = -0.155H = -0.465m	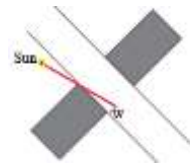 W = Cos(90 - β + 45)*SHL W = Cos(197.29)*0.52H W = -0.5H = -1.5m
15:00	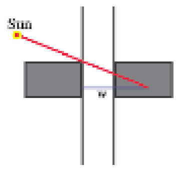 W = Sinβ*SHL W = Sin (-69.00)*0.87H W = -0.812H = -2.436m	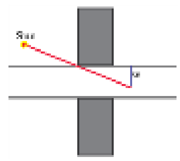 W = Cosβ*SHL W = Cos (-69.00)*0.87H W = 0.312H = 0.936m	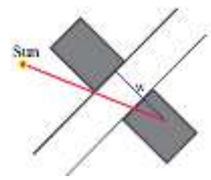 W = Sin(90 - β + 45)*SHL W = Sin(204)*0.87H W = -0.354H = -1.062m	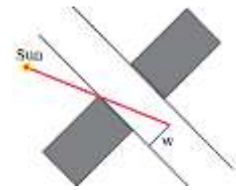 W = Cos(90 - β + 45)*SHL W = Cos(204)*0.87H W = -0.795H = -2.385m
16:00	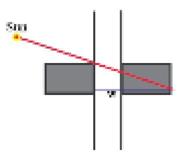 W = Sinβ*SHL W = Sin (-71.24)*1.423H W = -1.35H = -4.05m	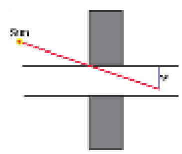 W = Cosβ*SHL W = Cos (-71.24)*1.423H W = 0.46H = 1.38m	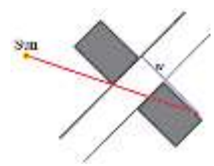 W = Sin(90 - β + 45)*SHL W = Sin(206.24)*1.423H W = -0.63H = -1.89m	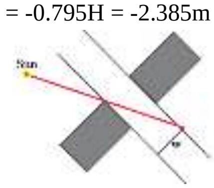 W = Cos(90 - β + 45)*SHL W = Cos(206.24)*1.423H W = -1.28H = -3.84m

Table 4.4 Selected streets shadow analysis of June, 21 (10:00 AM - 16:00 PM)

Hour	**North – South**	**East -West**	**North East to South West**	**North West to South East**
10:00	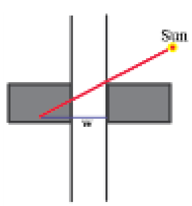 W = Sinβ*SHL W = Sin (62.53)*0.752H W = 0.67H = 2.01m	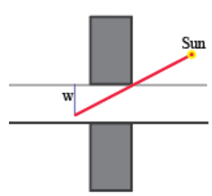 W = Cosβ*SHL W = Cos (62.53)*0.752H W = 0.35H= 1.05m	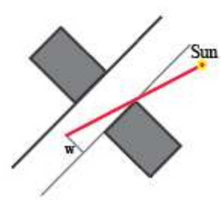 W = Sin(90 - β + 45)*SHL W = Sin(72.47)*0.752H W = 0.72H = 2.16m	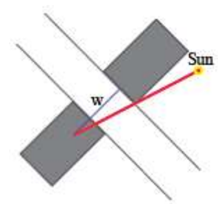 W = Cos(90 - β + 45)*SHL W = Cos(72.47)*0.752H W = 0.23H = 0.69m

11:00	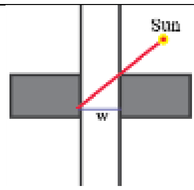 W = Sinβ*SHL W = Sin (51.09)*0.455H W = 0.354H = 1.062m	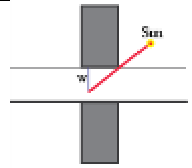 W = Cosβ*SHL W = Cos (51.09)*0.455H W = 0.29H = 0.87m	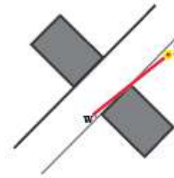 W = Sin(90 - β + 45)*SHL W = Sin(83.91)*0.455H W = 0.452H = 1.356m	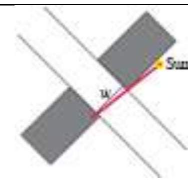 W = Cos(90 - β + 45)*SHL W = Cos(83.91)*0.455H W = 0.05H = 0.15m
12:00	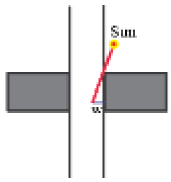 W = Sinβ*SHL W = Sin (19.43)*0.277H W = 0.092H = 0.276m	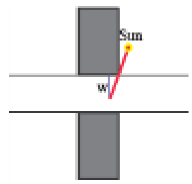 W = Cosβ*SHL W = Cos (19.43)*0.277H W = 0.261H = 0.783m	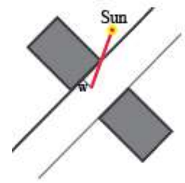 W = Sin(90 - β + 45)*SHL W = Sin(115.57)*0.277H W = 0.25H = 0.75m	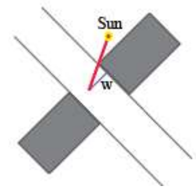 W = Cos(90 - β + 45)*SHL W = Cos(115.57)*0.277H W = -0.12H = -0.36m
13:00	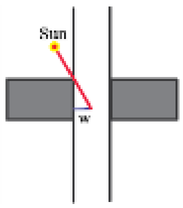 W = Sinβ*SHL W = Sin (-30.79)*0.31H W = -0.16H = -048m	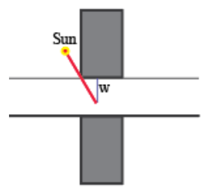 W = Cosβ*SHL W = Cos (-30.79)*0.31H W = 0.27H = 0.81m	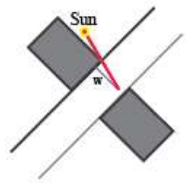 W = Sin(90 - β + 45)*SHL W = Sin(165.79)*0.31H W = 0.08H = 0.24m	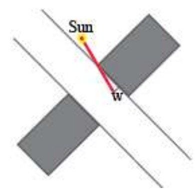 W = Cos(90 - β + 45)*SHL W = Cos(165.79)*0.31H W = -0.3H = -0.9m
14:00	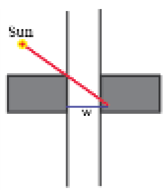 W = Sinβ*SHL W = Sin (-55.23)*0.521H W = -0.43H = -1.29m	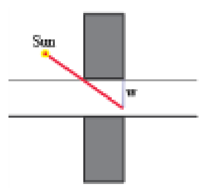 W = Cosβ*SHL W = Cos (-55.23)*0.521H W = 0.3H = 0.9m	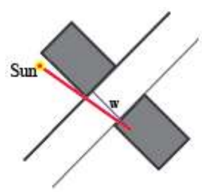 W = Sin(90 - β + 45)*SHL W = Sin(190.23)*0.521H W = -0.1H = -0.3m	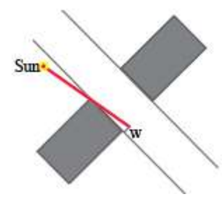 W = Cos(90 - β + 45)*SHL W = Cos(190.23)*0.521H W = -0.513H = -1.539m
15:00	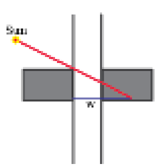 W = Sinβ*SHL W = Sin (-64.09)*0.851H W = -0.77H = -2.31m	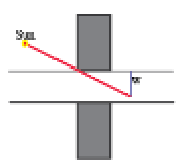 W = Cosβ*SHL W = Cos (-64.09)*0.851H W = 0.372H = 1.116m	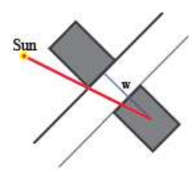 W = Sin(90 - β + 45)*SHL W = Sin(199.09)*0.851H W = -0.3H = -0.9m	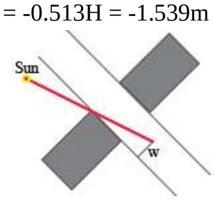 W = Cos(90 - β + 45)*SHL W = Cos(199.09)*0.851H W = -0.804H = -2.412m
16:00	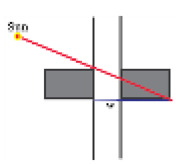 W = Sinβ*SHL W = Sin (-67.43)*1.372H W = -1.27H = -3.81m	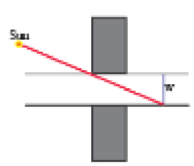 W = Cosβ*SHL W = Cos (-67.43)*1.372H W = 0.53H = 1.59m	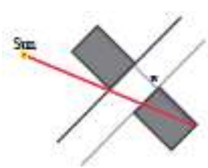 W = Sin(90 - β + 45)*SHL W = Sin(202.43)*1.372H W = -0.524H = -1.572m	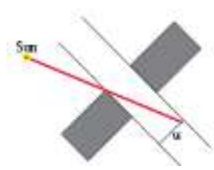 W = Cos(90 - β + 45)*SHL W = Cos(202.43)*1.372H W = -1.27H = -3.81m

On the above table 4.2, table 4.3 and table 4.4 data's are computed for the months of April, May and June of the year; the strategy of analyzing shade width is to provide shade for the pedestrian. To do so multiplying the shade by the known building height or trees will help to understand the actual effect. By doing so, it is concluded that the good shade give width is relatively preferable.

The N–S street orientation have higher shade width than the rest street orientation for those three consecutives hottest months. The street-1 (E-W) orientation have lower shade than other streets and shade of buildings are parallel to the street especially in April; in addition, on E-W street the south side buildings not give shade all over the day on those hottest months. The streets NE-SW and NW-SE orientation have higher shade width on June morning at (10:00-11:00) and afternoon at (13:00-16:00) respectively. But street orientation of NE-SW and NW-SE shade of buildings are parallel to the street morning at (11:00) and afternoon at (13:00-14:00) respectively for May and June; because of this walking on these orientated street at this time is difficult for pedestrian. Therefore, street-2 (N-S) orientation have better shade for pedestrian at the critical time of the day.

Generally for the hottest months of Metehara town (April, May and June) the at 12:00 PM o'clock when the shadow length of the buildings, trees and other things are short when compare to the other critical time of the day; so the direction of the shadow is to the west direction of the north for these months. By knowing the shadow directions and lengths, can design outdoor pedestrian spaces that provide optimal shade and improve thermal comfort for people during the hottest times of the year.

4.3. Sky View Factor Analysis of Shading

In warm dry climates, a sky view factor of less than 0.5 with careful design considerations is generally recommended for pedestrian thermal comfort promoting cooler conditions during the day and reducing heat stress. SVF between 0.3 and 0.5 is considered moderately shaded, while an SVF above 0.5 is considered less shaded and can lead to higher daytime temperatures and heat stress, according to Mohammad Taleghani (2019).

Street 1: East-West Orientation (E-W)

Building height G+0 on the north side, G+2 on the south side, street width 20m and vegetation coverage is minimal; therefore:-

SVF calculation by using the asymmetrical canyon formula:

$$SVF = ½ [\cos^2 (\arctan (3m/20m)) + \cos^2 (\arctan (9m/20m))]$$

$$SVF = ½ [(\cos^2 (8.53^o) + \cos^2 (24.23^o)] = 0.83$$

Adjusted for vegetation

$$SVF_{adjusted} = 0.83 \times 0.8 = \mathbf{0.664}$$

Sky View Factor (SVF) result indicates substantial sky exposure which increases solar radiation and heat accumulation within urban spaces leading to potential thermal stress for pedestrians. Limited shading from surrounding buildings exacerbates direct sunlight to elevate mean radiant temperature (MRT) negatively impacting pedestrian thermal comfort. Furthermore, inadequate vegetation coverage reduces the ability to mitigate thermal stress through evapotranspiration and shading.

Street 2: North-South Orientation (N-S)

Building height G+0 on both sides, street width 20m and vegetation coverage is medium; therefore:-

SVF calculation by using the symmetrical canyon formula:

$$SVF = 1/ 1 + (3m/20m)^2$$

$$SVF = 0.978$$

Adjusted for vegetation

$$SVF_{adjusted} = 0.978 \times 0.5 = \mathbf{0.49}$$

The low SVF result due to good tree canopy significantly reduces solar radiation exposure and also enhanced shading lowers MRT, improving pedestrian thermal comfort. Additionally, existence of vegetation plays a crucial role in cooling through evapotranspiration.

Street 3: Northwest-Southeast Orientation (NW-SE)

Building height G+0 on both sides, Street Width 20m and vegetation coverage is sparse; therefore:-

SVF calculation by using the symmetrical canyon formula:

$$SVF = 1/ 1 + (3m/20m)^2$$

$$SVF = 0.978$$

Adjusted for vegetation

$$SVF_{adjusted} = 0.978 \times 0.7 = \mathbf{0.685}$$

Street-3 SVF value allows substantial sky exposure leading to increased solar radiation. Limited shading results in higher MRT and thermal discomfort. And also sparse vegetation provides minimal cooling benefits.

Street 4: Northeast-Southwest Orientation (NE-SW)

Building height G+0 on both sides, street Width 15m and there is no street trees coverage; therefore:-

SVF calculation by using the symmetrical canyon formula:

$$SVF = 1/ 1 + (3m/15m)^2$$

$$SVF = \mathbf{0.96}$$

A high SVF value results in excessive solar exposure, increasing pedestrian heat stress. In addition, minimal shading leads to elevated MRT intensify discomfort and lack of vegetation further increase thermal stress. Generally, street-2 (N-S) have good shade and comfortable for pedestrian than other selected streets orientations according to sky view factor evaluation of all selected streets above.

4.4. Microclimate Analysis

Actual hourly micro climatic condition measurement was taken so as to reach the real feeling on day to day human activities. This will help to check the outdoor thermal comfort pedestrian. For checking the outdoor thermal comfort of each street, it needs on spot measurement of temperature, humidity, wind speed and solar radiation. The temperature and relative humidity of selected streets were measured using hygrometer and also wind speed and solar radiation data is taken from national solar radiation database for the typical hottest months of the year April, May and June for the period that spans from 10:00 am to 16:00 pm at an hour interval.

4.4.1. Hourly Measured Air Temperature

In warm dry climate tolerable air temperature for pedestrians generally falls within the range of $20^{o}c$ to $35^{o}c$ depending on like humidity, wind speed and solar radiation (Mohammad Teleghani, 2020). For the four selected streets the hourly air temperature was measured at one hour interval as shown in figure 4.7 for April, figure 4.8 for May and figure 4.9 for June below. It was how hourly temperature fluctuate throughout the day during (10:00 AM – 16:00 PM) for the selected street orientation street-1(East-West), street-2 (North-south), Street-3 (North West-South East) and street-4 (North East-South West); on the hottest months of the town. In April the air temperature ranges from 32^{o}C to 38^{o}C at 10:00 AM and 15:00 PM respectively. The highest temperature for street-1 and street-2 were found to be 36^{o}C at 13:00 & 14:00 and 35^{o}C at 13:00 & 14:00 respectively for the street. The highest temperature for street-3 and street-4 were also found to be 37^{o}C at 12:00 and to 38^{o}C at 15:00 respectively for the streets.

In the month of May the air temperature ranges from 33^{o}C to 39^{o}C at 10:00 am and 14:00 PM respectively. When considering the selected street orientation street-4 have recorded highest temperature and street-2 have lowest temperature when considering the street to each other. In June the hourly temperature measured for selected street were high when comparing to April and May. The air temperature ranges between 33^{o}C at 10:00 AM on street-2 and 40^{o}C at 14:00 PM on street-3.

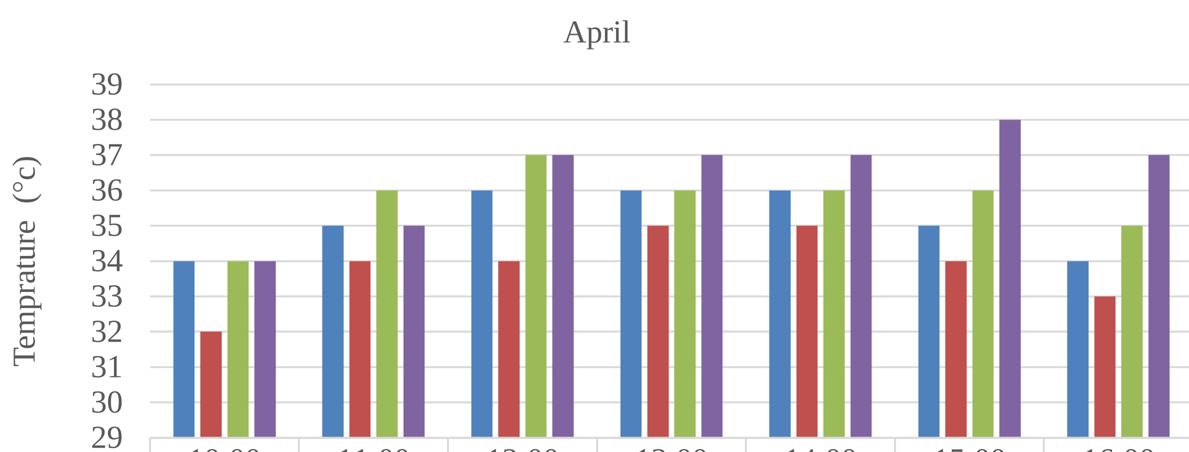

	10:00	11:00	12:00	13:00	14:00	15:00	16:00
street 1	34	35	36	36	36	35	34
street 2	32	34	34	35	35	34	33
street 3	34	36	37	36	36	36	35
street 4	34	35	37	37	37	38	37

Hour

Figure 4.7 April hourly selected streets temperature variation

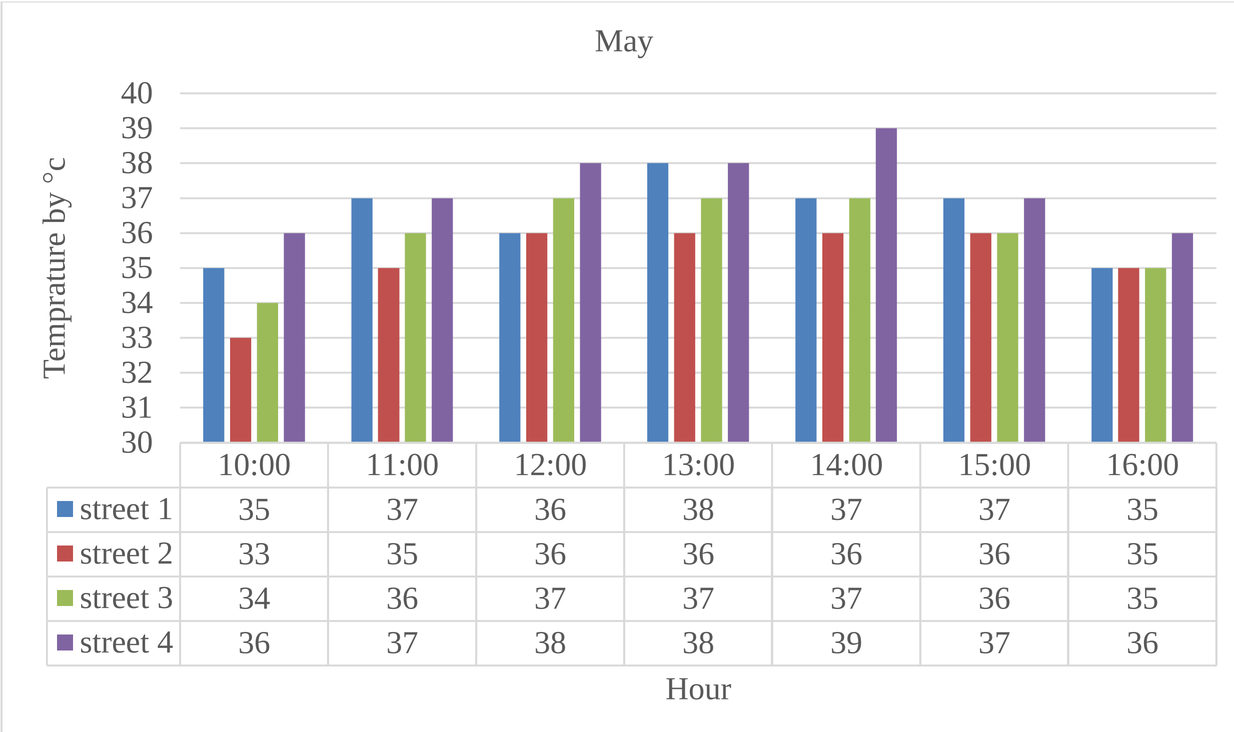

Figure 4.8 May hourly selected streets temperature variation

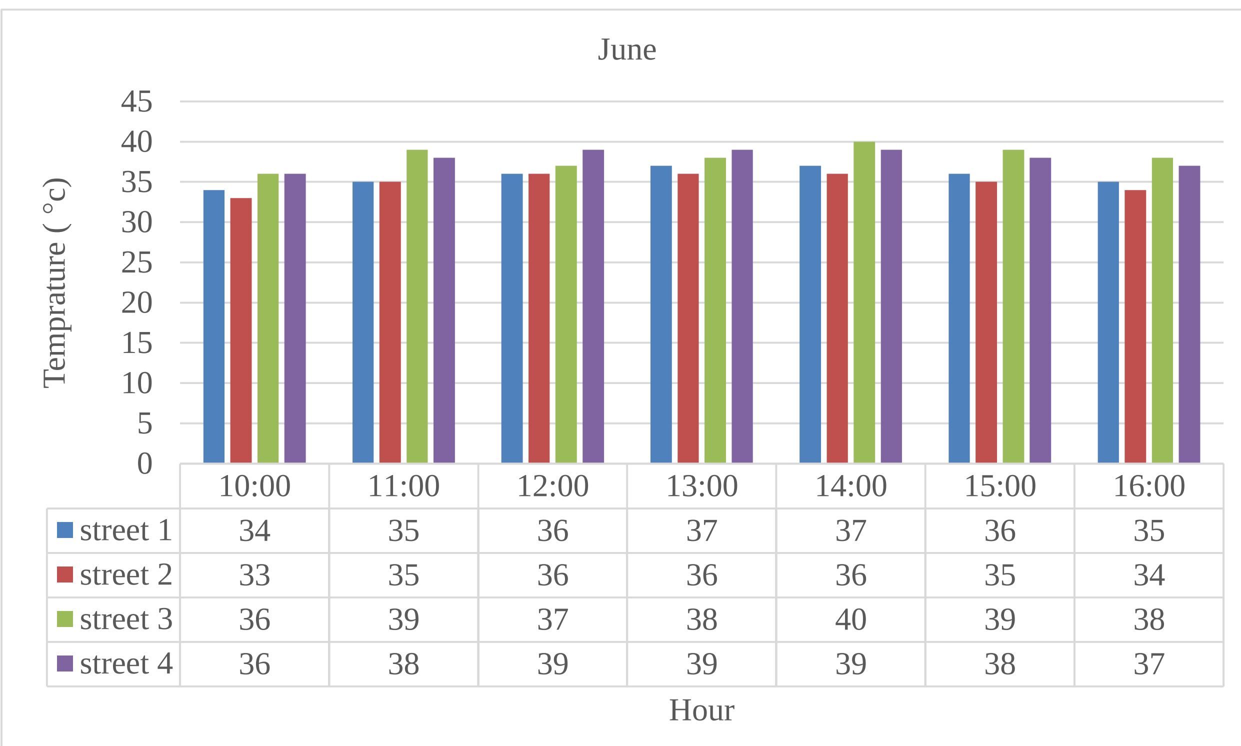

Figure 4.9 June hourly selected streets temperature variation

In general, Air temperatures consistently increased during the late morning to early afternoon hours, peaking between 12:00 PM and 14:00 PM. This temperature rise coincided with elevated solar radiation and minimal shading, contributing significantly to pedestrian thermal discomfort during this critical time of the day. Among the studied streets, the North-South (N-S) oriented street (Street-2) demonstrated relatively lower peak temperatures, attributed to enhanced airflow and shading from vegetation. Conversely, the North East-South West (NE-SW) oriented street (Street-4) exhibited the highest temperatures due to reduced shading mechanisms and impeded ventilation, thereby posing high thermal stress to pedestrians.

4.4.2. Hourly Measured Relative Humidity

According to Amir Ghosouri (2020), in warm dry climates, tolerable relative humidity for pedestrians typically falls within the range of 30% to 60% depending on air temperature and wind condition. The relative humidity data for evaluating pedestrian thermal comfort in Metehara town requires understanding how humidity variations throughout the day can impact human comfort. It was found that the relative humidity ranges between 25% at 11:00 AM on street-3 (NW-SE oriented) and 58% at 16:00 PM on street-2 (N-S oriented) for the month of April. In the months of May and June the relative humidity ranges between 20.9% at 12:00 PM on street-4 (NE-SW oriented) & 50.1% at 10:00 AM on street-2 (N-S oriented) for May and also 12.8% at 14:00 PM on street-4 (NE-SW oriented) & 39.56% at 16:00 PM on street-2 (N-S oriented) for June.

The relative humidity is generally on all selected streets typically decreases as temperature rise from 10:00 AM to 14:00 PM and at 15:00 PM – 16:00 PM relative humidity starts to rise again as temperatures begin to decrease. High relative humidity on the streets enhance the feeling of coolness but also to discomfort if combined with lower temperature. Lower humidity during high temperature can lead to a dry and hot feeling, causing significant thermal discomfort for pedestrians. The selected street orientation general relative humidity level for all hottest months (April, May & June) in the figure 4.10, figure 4.11 and figure 4.12 below showed that, street-2 (N-S) has high relative humidity while street-4 (NE-SW) has lower relative humidity.

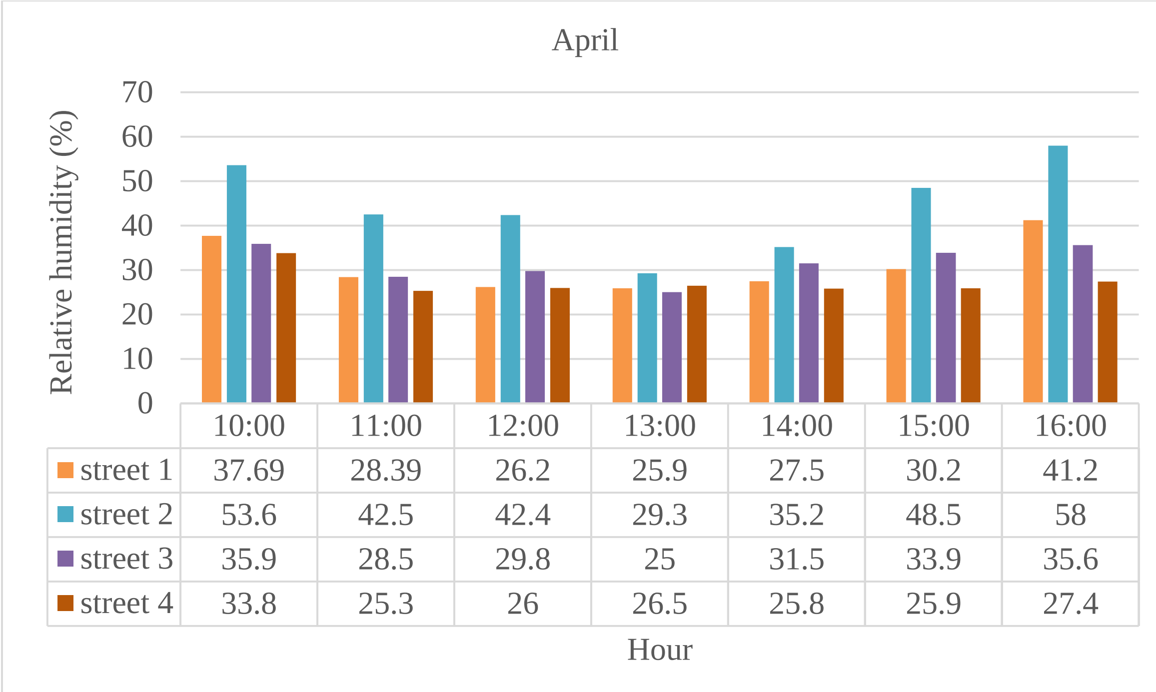

	10:00	11:00	12:00	13:00	14:00	15:00	16:00
street 1	37.69	28.39	26.2	25.9	27.5	30.2	41.2
street 2	53.6	42.5	42.4	29.3	35.2	48.5	58
street 3	35.9	28.5	29.8	25	31.5	33.9	35.6
street 4	33.8	25.3	26	26.5	25.8	25.9	27.4

Figure 4.10 April hourly selected streets relative humidity variation

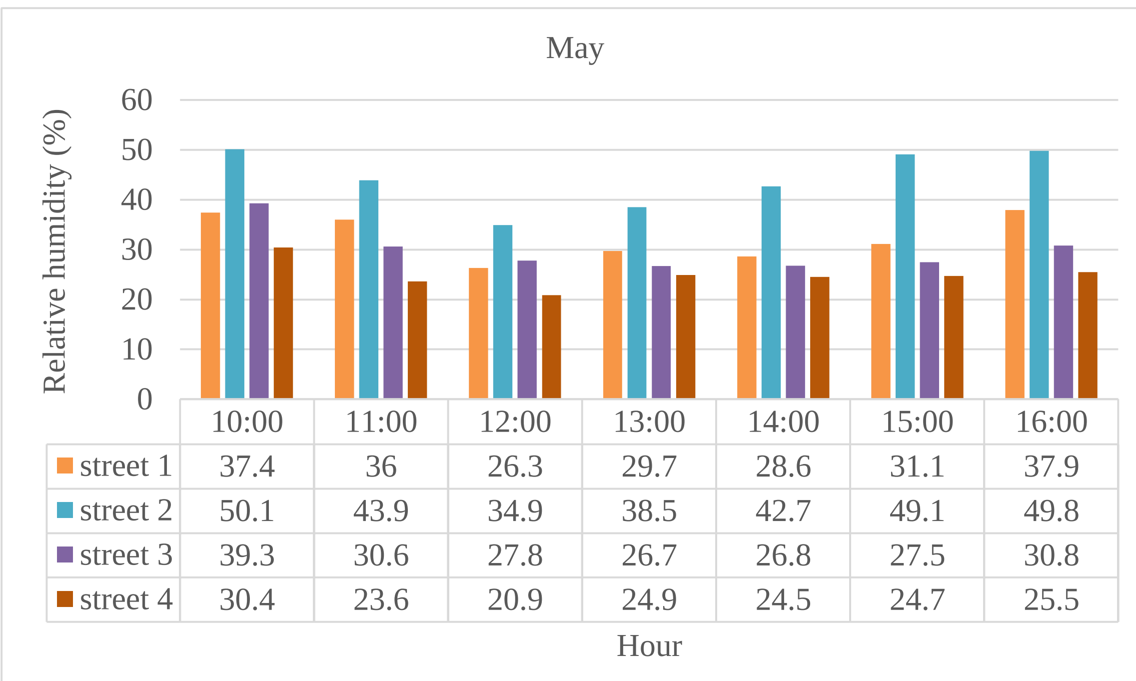

	10:00	11:00	12:00	13:00	14:00	15:00	16:00
street 1	37.4	36	26.3	29.7	28.6	31.1	37.9
street 2	50.1	43.9	34.9	38.5	42.7	49.1	49.8
street 3	39.3	30.6	27.8	26.7	26.8	27.5	30.8
street 4	30.4	23.6	20.9	24.9	24.5	24.7	25.5

Figure 4.11 May hourly selected streets relative humidity variation

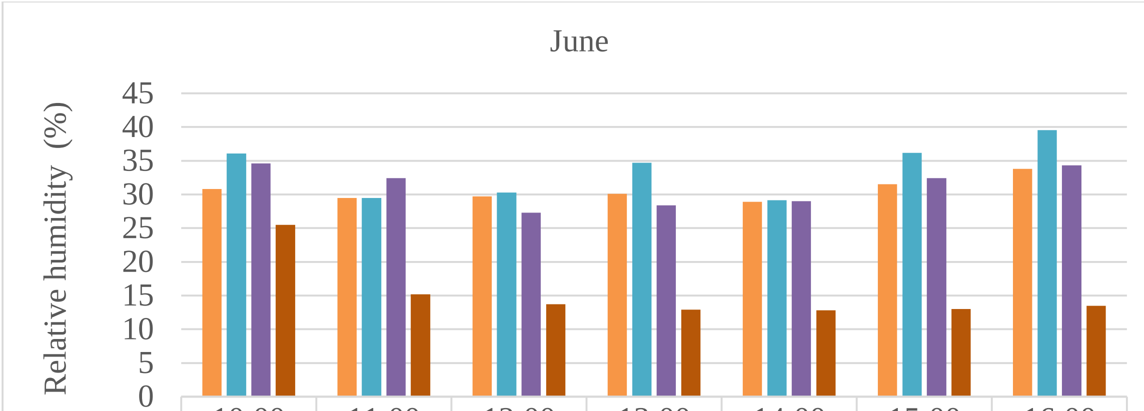

	10:00	11:00	12:00	13:00	14:00	15:00	16:00
street 1	30.8	29.48	29.7	30.11	28.9	31.5	33.8
street 2	36.1	29.5	30.3	34.7	29.16	36.19	39.56
street 3	34.6	32.4	27.3	28.4	29	32.4	34.3
street 4	25.5	15.2	13.7	12.9	12.8	13	13.5

Figure 4.12 June hourly selected streets relative humidity variation

The hourly analysis of relative humidity for the selected streets in Metehara town highlights distinct diurnal patterns and notable differences across street orientations. Relative humidity typically decreased during the late morning to early afternoon hours (10:00 AM to 14:00 PM), coinciding with peak air temperatures and intensified solar radiation. Among the streets analyzed, the North-South (N-S) oriented street (Street-2) demonstrated tolerable relative humidity levels throughout the day, supported by better shading from vegetation and optimized airflow. Conversely, the North East-South West (NE-SW) oriented street (Street-4) exhibited the lowest relative humidity, attributable to reduced vegetation cover, less shading and obstructed air movement.

4.4.3. Hourly Wind speed

According to Zhang & deng x. (2020) in warm dry climate tolerable wind speed for pedestrian thermal comfort typically range between 1 to 3.5 m/s, depending on factors such as air temperature, solar radiation and humidity. Wind speed data was obtained from NASA Power at hourly intervals for April, May, and June. Figure 4.13 illustrates wind speed variations for these months, April wind speeds gradually increased throughout the day, starting at 2.96 m/s at 10:00 AM and peaking at 5.65 m/s by 15:00 PM. In May wind speeds followed a similar pattern, ranging from 3.79 m/s at 10:00 AM to 5.84 m/s at 16:00 PM. In June the highest wind speeds were recorded, beginning at 4.78 m/s at 10:00 AM and reaching 6.2 m/s at 16:00 PM.

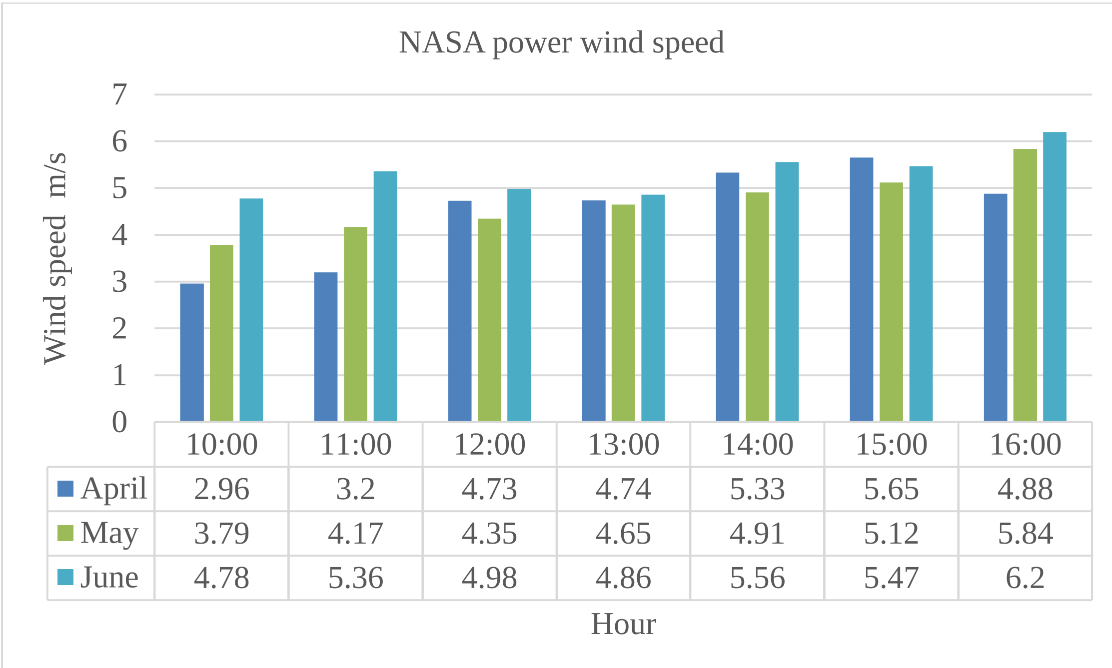

	10:00	11:00	12:00	13:00	14:00	15:00	16:00
April	2.96	3.2	4.73	4.74	5.33	5.65	4.88
May	3.79	4.17	4.35	4.65	4.91	5.12	5.84
June	4.78	5.36	4.98	4.86	5.56	5.47	6.2

Figure 4.13 NASA power wind speed variation of the hottest months

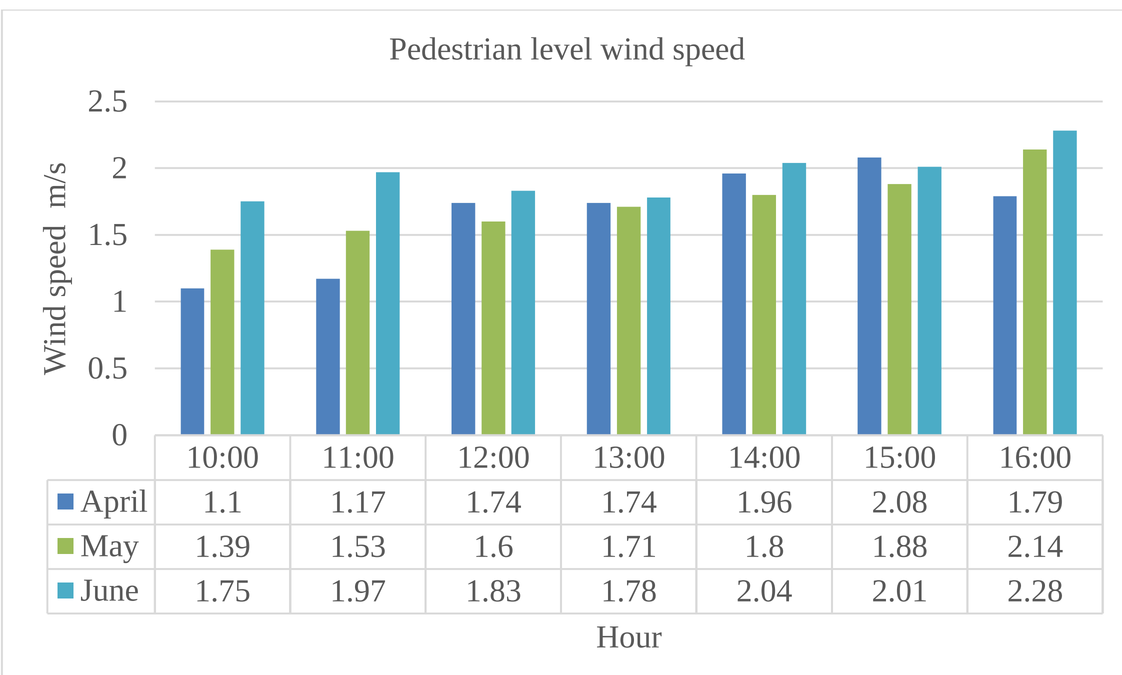

	10:00	11:00	12:00	13:00	14:00	15:00	16:00
April	1.1	1.17	1.74	1.74	1.96	2.08	1.79
May	1.39	1.53	1.6	1.71	1.8	1.88	2.14
June	1.75	1.97	1.83	1.78	2.04	2.01	2.28

Figure 4.14 Pedestrian level wind speed variation of the hottest months

The pedestrian level wind speed calculated by logarithmic wind profile equation value shows on the figure 4.14 above can be tolerable for pedestrians but it depends on the wind direction and street orientation. The data illustrates that wind speeds generally rise during the afternoon across all months, with June exhibiting the highest overall values. Higher wind speeds contribute significantly to pedestrian thermal comfort by enhancing airflow and reducing heat stress. Streets aligned with prevailing wind patterns benefit most, emphasizing the need for strategic urban planning to maximize ventilation potential. Conversely, areas with obstructed airflow should prioritize shading and vegetation to alleviate heat related discomfort in the town.

4.4.4. Wind Direction

The figures 4.15, 4.16 and 4.17 below shows the hourly wind direction taken from NASA power. The figure 4.15 below illustrates in April the predominant wind directions are from the East (E), East-Northeast (ENE), and Northeast (NE) sectors. The degree ranges include 45.7° to 91.69°, signifying strong alignment with easterly patterns. The figure 4.16 below illustrates in May wind direction shifts occur, winds remain predominantly from the ENE in the early hours (10:00–12:00) but transition to ESE at (13:00–15:00) and at 16:00, ENE winds resume. The figure 4.16 below shows in June wind directions vary significantly, ranging from the South-Southeast (SSE) to South-Southwest (SSW), with degrees spanning 152.12° to 211.62°.

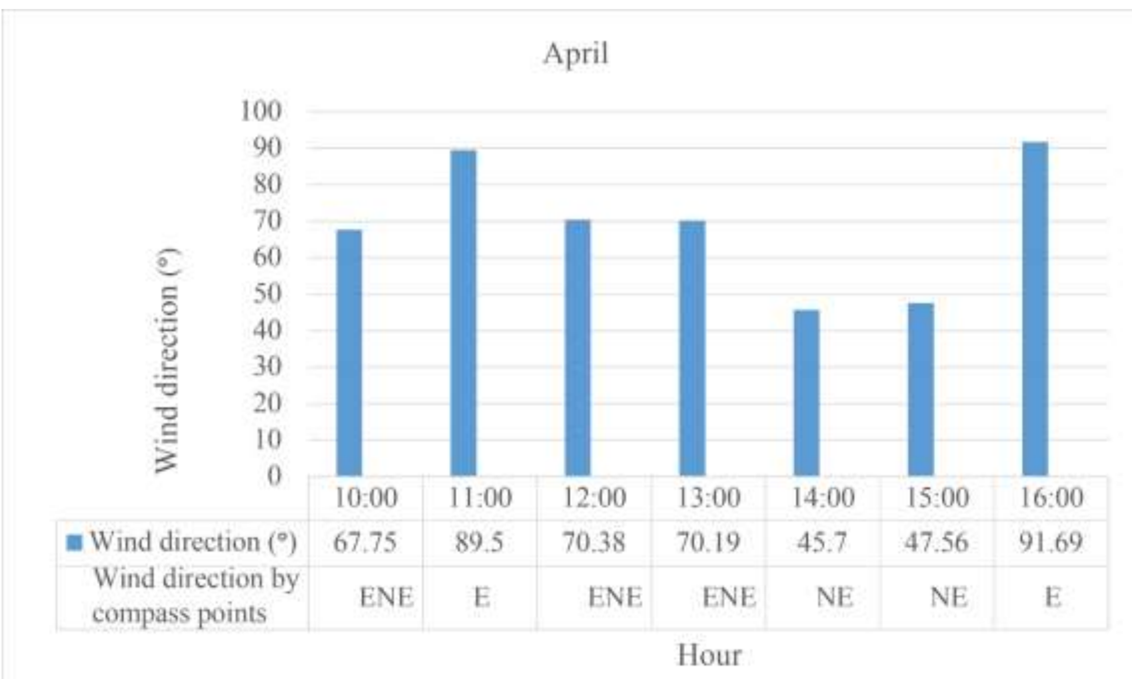

Figure 4.15 Hourly wind direction variation of April

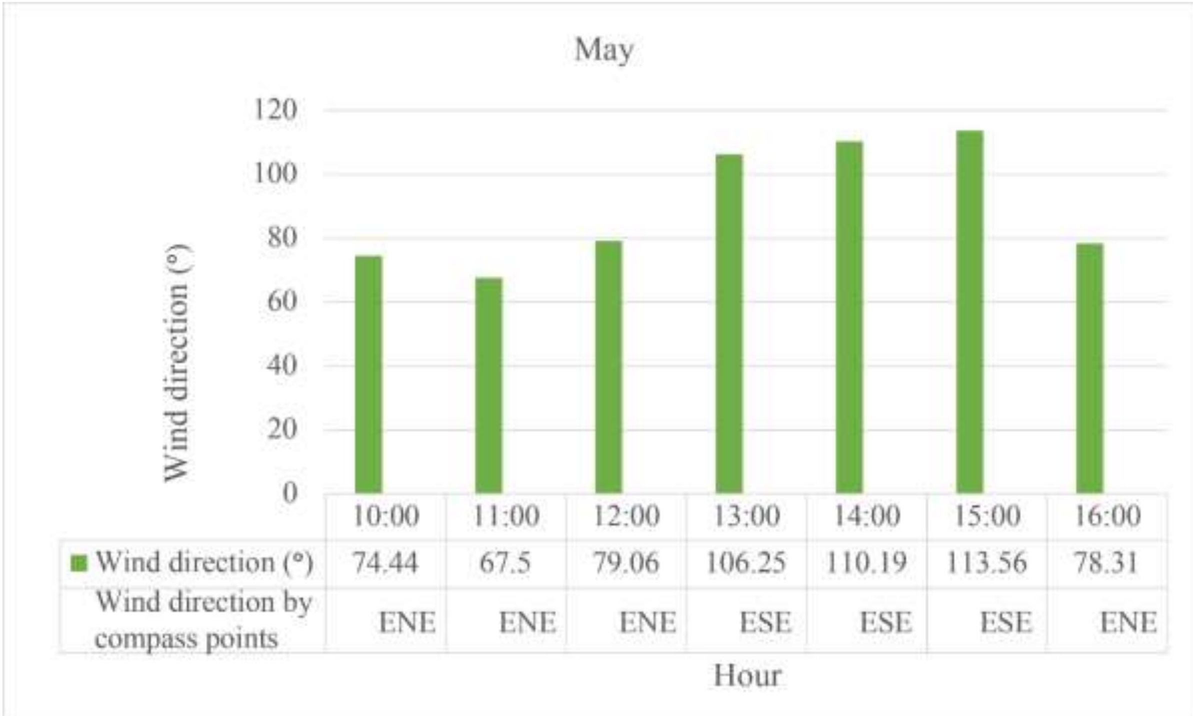

Figure 4.16 Hourly wind direction variation of May

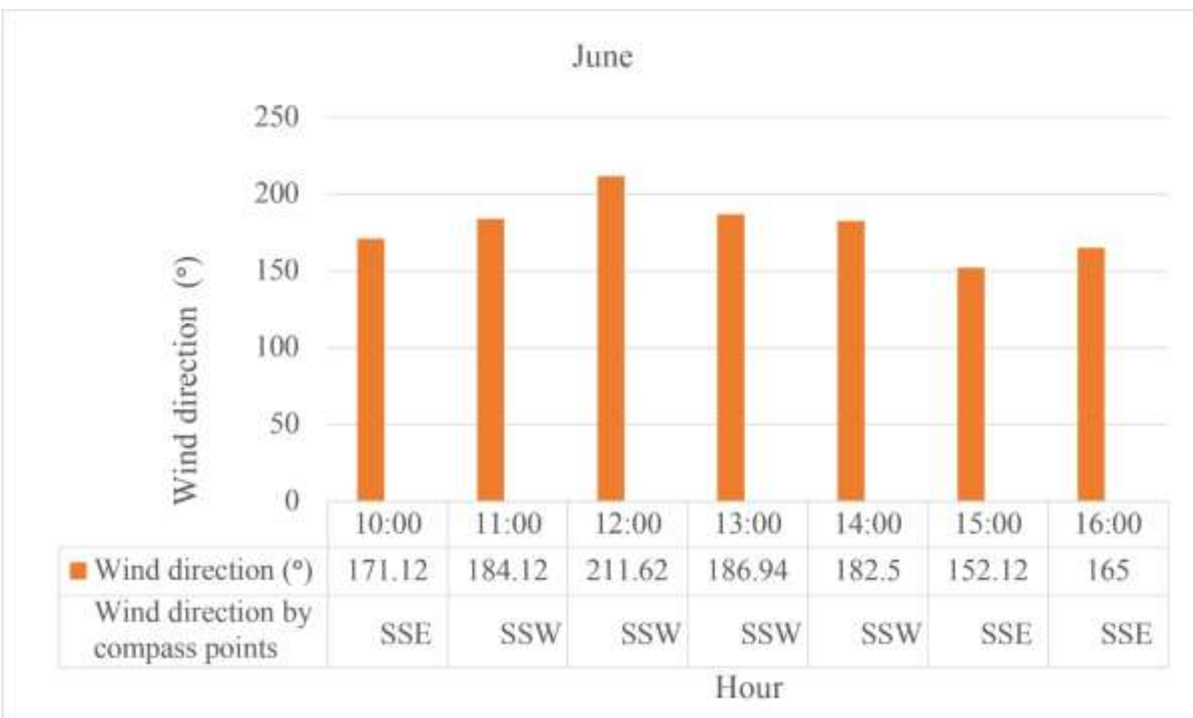

Figure 4.17 Hourly wind direction variation of June

According to the wind direction data on the figures 4.15, 4.16 and 4.17 above, Street-1 (East-West) orientation in April & May easterly winds (E, ENE) provide ventilation across the street axis, enhancing pedestrian thermal comfort. However, due to limited shading from north-side low-rise buildings, the comfort improvement is primarily through airflow. In June the transition to SSE/SSW winds reduces cross-street ventilation due to the alignment mismatch, potentially leading to stagnant conditions and higher heat stress.

Street-2 (North-South) orientation in April & May the alignment with ENE and E winds promotes effective longitudinal airflow, enhancing ventilation and reducing thermal stress. Shading from vegetation further supports comfort. For June winds from the SSE/SSW directions maintain airflow, although slightly oblique to the street axis. This configuration helps sustain pedestrian comfort, especially when combined with vegetation shading.

Street-3 (Northwest-Southeast) Orientation in the April & May ENE winds interact with the oblique street orientation, creating moderate cooling effects. At midday in May, ESE winds align with the street, promoting better ventilation. In June SSE/SSW winds flow parallel to the street axis, enhancing ventilation. However, the lack of shading infrastructure may limit thermal comfort improvements.

Street-4 (Northeast-Southwest) Orientation in April & May ENE winds face obstruction by building layouts, leading to reduced airflow and increased heat accumulation. ESE winds in May midday exacerbate stagnation in shaded areas. June SSE/SSW winds are creating somehow cooling effects, but mostly creating a warm and stagnant environment that significantly heightens pedestrian thermal discomfort.

4.4.5. Hourly Solar Radiation

Solar radiation is a major factor affecting pedestrian thermal comfort, especially in urban environments. The data provided in the figure 4.18 below illustrates the variation in solar radiation levels at different times of the day for the months of April, May and June. High levels of solar radiation can significantly impact pedestrian comfort, leading to increased heat stress and discomfort. Understanding these variations can help in designing strategies to enhance thermal comfort for pedestrians.

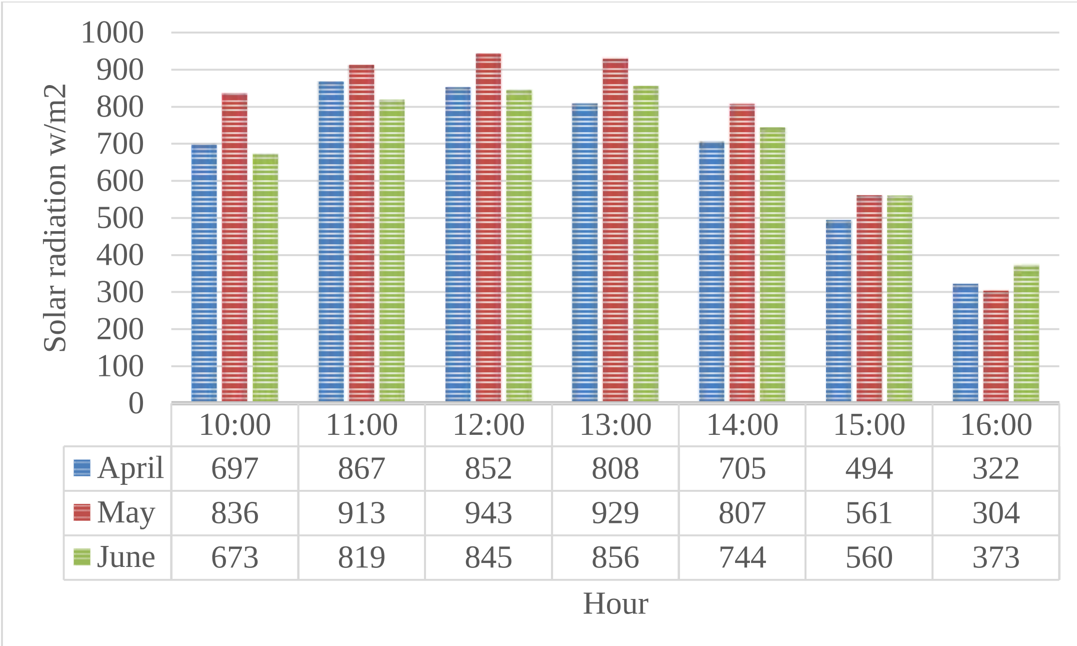

	10:00	11:00	12:00	13:00	14:00	15:00	16:00
April	697	867	852	808	705	494	322
May	836	913	943	929	807	561	304
June	673	819	845	856	744	560	373

Figure 4.18 Hourly solar radiation variation of the hottest months

Pedestrians thermal comfort implications in all three months during morning hours 10:00 solar radiation is relatively moderate; however May shows higher levels compared to April and June. During midday hours 11:00 – 13:00 peak solar radiation occurs for all months and discomfort for pedestrian; these suggest the need for effective shading and cooling solutions. Solar radiation decreases afternoon hours 14:00 – 16:00, but the heat accumulated throughout the day can still cause discomfort. The high radiation levels in May (943 w/m2) at 12:00 and lower radiation level May (304 w/m2) at 16:00 pm.

These variations can help in designing strategies to enhance thermal comfort for pedestrians. Street orientation can play a crucial role in mitigating heat stress. Street oriented in a way that minimizes direct solar exposure during peak hours can significantly improve pedestrian comfort. Therefore, one of the selected street orientation for this study is East- west (street-1) street. Buildings on the north side are single-story (G+0), while on the south side, some buildings are two or three stories (G+1 and G+2). According to table 4.2, 4.3 & 4.4 shadow width analysis of April, May and June, the buildings do not provide sufficient shade for pedestrian during peak hours since the shadows cast from the north side structures fall to the south. Additionally, there are not enough trees to minimize direct sunlight. Overall, the street has good air velocity, which helps reduce heat stress somehow.

Street - 2 (North - south) street, by considering the town hourly solar radiation the North – South oriented street is more comfortable compared to other street orientations. The street has enough trees to minimize direct sun light. But the buildings on the street are single story (G+0), so they do not provide sufficient shade for pedestrian during peak hours. The street has enough air velocity especially in May and June the direction of wind is mostly from the south to north. However, the street does not provide enough shade to achieve thermal comfort for pedestrians.

Street-3 (North West-South East) and Street-4 (North East-South west): These streets do not have sufficient shade from buildings during peak hours of the day because the buildings are G+0 story. Additionally the streets lack side trees for shade. Street-3 have good air velocity, but when come to street-4 the air velocity is blocked by the buildings on the North East side. Generally, stree-3 and street-4 are not comfortable for pedestrians.

4.4.6. Mean Daily Solar Radiation

The figure 4.19 below shows the highest mean daily solar radiation obtained in Metehara is 651 W/m2 in March and minimum is 368 W/m2 in July. When come to our emphasize the hottest months (April, May and June) the received solar radiation is high 529 w/m2, 552w/m2 and 487w/m2 respectively and the solar radiation needs for the town on these hottest month is zero. In case, on this month’s heat stress is increased for pedestrian, because of the received solar radiation is more than the needed solar radiation.

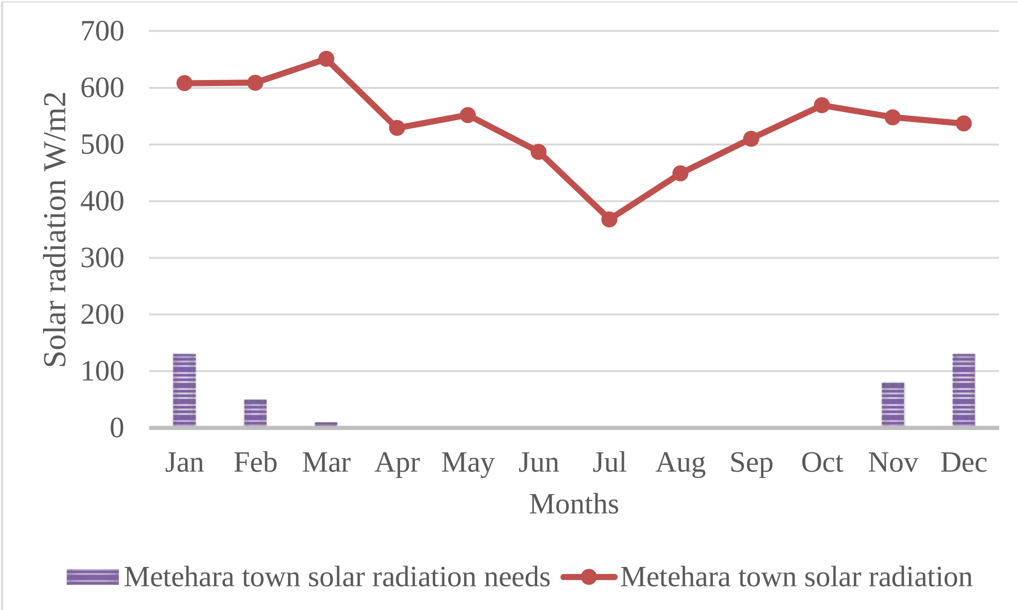

Figure 4.19 Mean daily solar radiation gains and the corresponding solar radiation need

During periods of high solar radiation, pedestrians are likely to experience increased heat stress, leading to heat stress. Pedestrians in the town must alter their outdoor activities, seeking shelter during peak solar radiation hours or modifying their clothing to stay cool. The varying solar radiation levels on the figure 4.19 above illustrates the need for adaptive design this could include designing streetscapes that provide shade and material selection for surface pavements and building facades these are reflective or cool materials that can help reduce heat absorption for ensuring pedestrian comfort is maintained.

4.5. Mean Radiant Temperature

It is a crucial factor in evaluating street orientation for pedestrian thermal comfort. It represents the average temperature of all surrounding surfaces that radiate heat and plays a significant role in the overall thermal sensation experienced by pedestrians. The quantities on the figures 4.20, 4.21 & 4.22 below sums up all short-wave and long-wave radiation fluxes absorbed by a human body and affecting its energy balance.

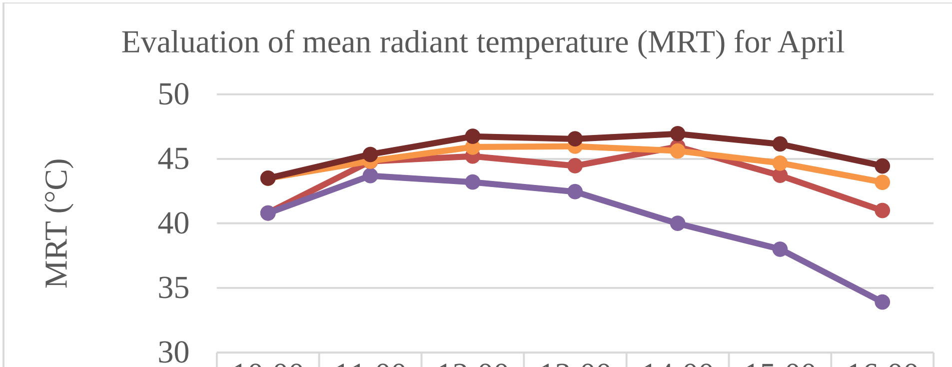

	10:00	11:00	12:00	13:00	14:00	15:00	16:00
street-1	40.81	44.8	45.21	44.47	45.95	43.72	41
street-2	40.8	43.7	43.2	42.46	40	38	33.9
street-3	43.5	44.83	45.92	45.98	45.62	44.67	43.19
street-4	43.5	45.35	46.75	46.55	46.95	46.15	44.45

Figure 4.20 April evaluation of mean radiant temperature for selected streets

The figure 4.20 above shows the MRT values vary throughout the day, showing higher values during midday hours (11:00 to 14:00) and lower value in the early morning and late afternoon. Street-4 consistently shows higher MRT values compared to the other streets, peaking 45.15^{o}c at 15:00 of the day. The higher MRT values of street indicate greater heat radiation exposure for pedestrians, negatively impacting thermal comfort. From these street-2 have lower MRT values compared to other street.

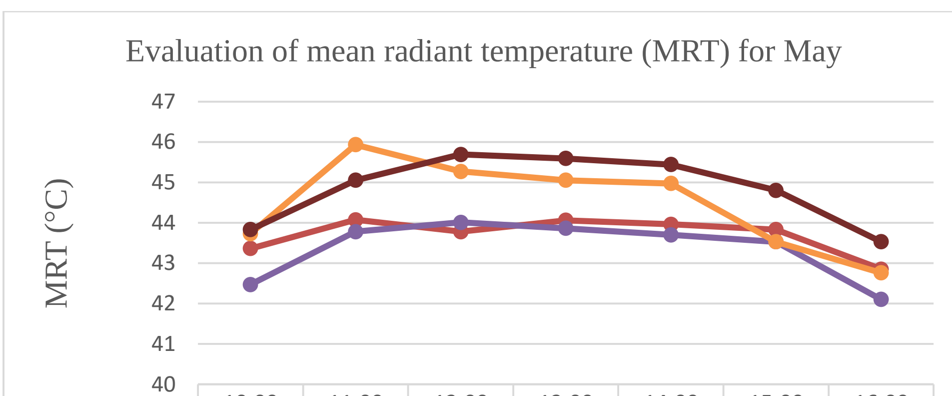

	10:00	11:00	12:00	13:00	14:00	15:00	16:00
street-1	43.36	44.07	43.78	44.06	43.96	43.83	42.85
street-2	42.47	43.78	44.01	43.86	43.7	43.53	42.1
street-3	43.73	45.93	45.27	45.05	44.97	43.53	42.76
street-4	43.83	45.05	45.69	45.59	45.44	44.8	43.53

Figure 4.21. May evaluation of mean radiant temperature for selected streets

The figure 4.21 above shows the MRT showing higher values during midday hours (11:00 to 14:00) and lower value in the early morning and late afternoon. Street-3 and street-4 consistently shows higher MRT values compared to the other streets, peaking at 45.93^{o}c at 11:00 of the day for street-3 and 45.69^{o}c at 12:00 for street-4. The higher MRT values of street indicate greater heat stress or thermal discomfort of pedestrians. From these street-1 and street-2 have lower MRT values compared to other street but they have still higher or thermally discomfort of pedestrian.

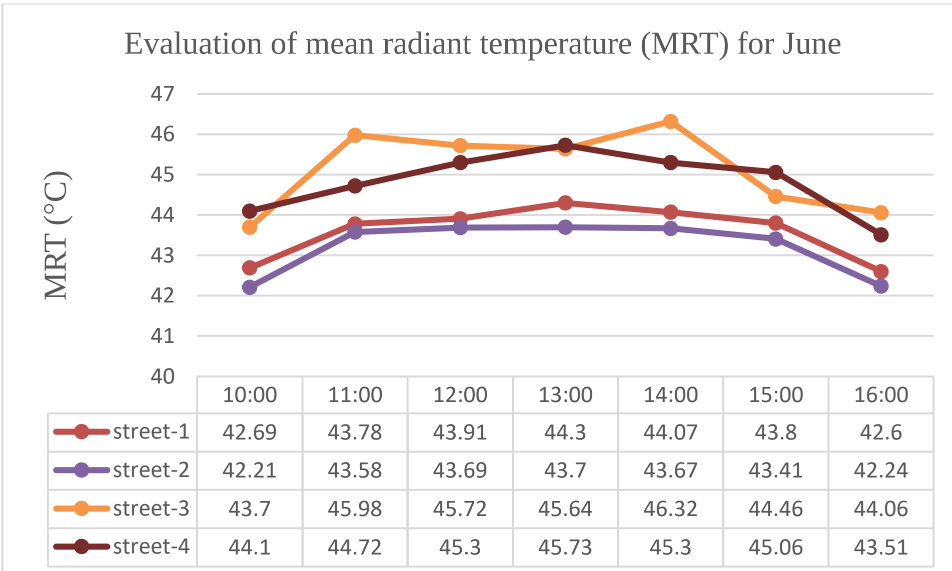

	10:00	11:00	12:00	13:00	14:00	15:00	16:00
street-1	42.69	43.78	43.91	44.3	44.07	43.8	42.6
street-2	42.21	43.58	43.69	43.7	43.67	43.41	42.24
street-3	43.7	45.98	45.72	45.64	46.32	44.46	44.06
street-4	44.1	44.72	45.3	45.73	45.3	45.06	43.51

Figure 4.22 June evaluation of mean radiant temperature for selected streets

On figure 4.22 above shows the MRT values of June for the critical time of the day, showing higher values during midday hours (11:00 to 14:00) and lower value in the early morning and late afternoon. Street-3 and street-4 consistently shows higher MRT values compared to the other streets, peaking 46.32^{o}c at 14:00 of the day for street-3 and 45.73 for street-4 at 13:00.

For all months (April, May and June) street-4 consistently shows the highest MRT values, this negatively impact pedestrian thermal comfort, as high MRT values correlate with higher thermal stress. Street-2 has the lowest MRT values when compared to other, suggesting better for pedestrians, but still higher. Street-1 and street-3 have intermediate MRT values but still shows noticeable peaks during the (11:00 to 14:00) hours.

Overall, MRT values for all streets of the hottest selected months are high and typically indicate thermal discomfort for pedestrians. Such high MRT values suggest intense radiant heat from the surrounding environment, which can cause significant thermal stress and discomfort for individuals. The streets needs shading, good air velocity for cooling the pedestrians, use different cooling strategies and using materials that reflect solar radiation and allow for better heat dissipation can help lower the thermal load on pedestrian.

4.6. Universal Thermal Climate Index

Universal thermal climate index (UTCI) is a valuable tool for evaluating street orientation in urban design to enhance pedestrian thermal comfort. It can be used by identify key parameters like air temperature, mean radiant temperature, relative humidity and wind speed. The UTCI values on figure 4.23, 4.24 & 4.25 below are calculated by using online UTCI calculator based on the collected key parameters for each street orientation.

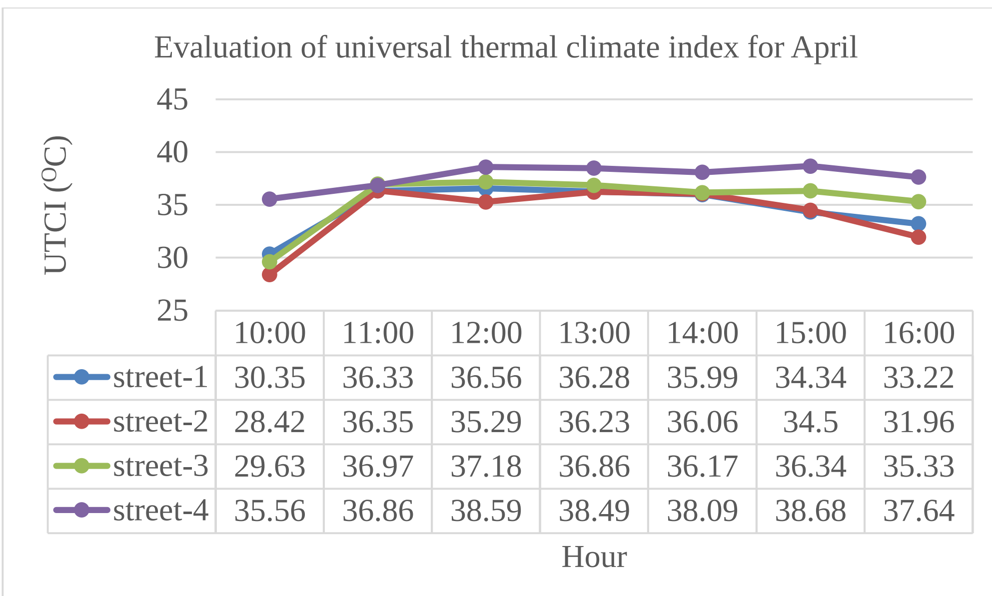

Figure 4.23 April evaluation of universal thermal climate index for selected streets

The figure 4.23 above indicates variations in UTCI values throughout the day for different streets. UTCI values fluctuate throughout the day, reflecting the influence of meteorological parameters. During morning at 10:00 lower UTCI values indicating thermal comfort for all street except street-4.the value of UTCI increased at 11:00 – 15:00 reflecting higher thermal stress due to peak UTCI. But street-4 have higher UTCI value compared to other street it indicate strong heat stress at morning (10:00 – 11:00) and afternoon at 16:00. And also at (12:00 – 15:00) there is very strong heat stress at street-4. For all street without morning at 10:00 of the day there is strong heat stress because the value of UTCI are increased at these critical time of the day.

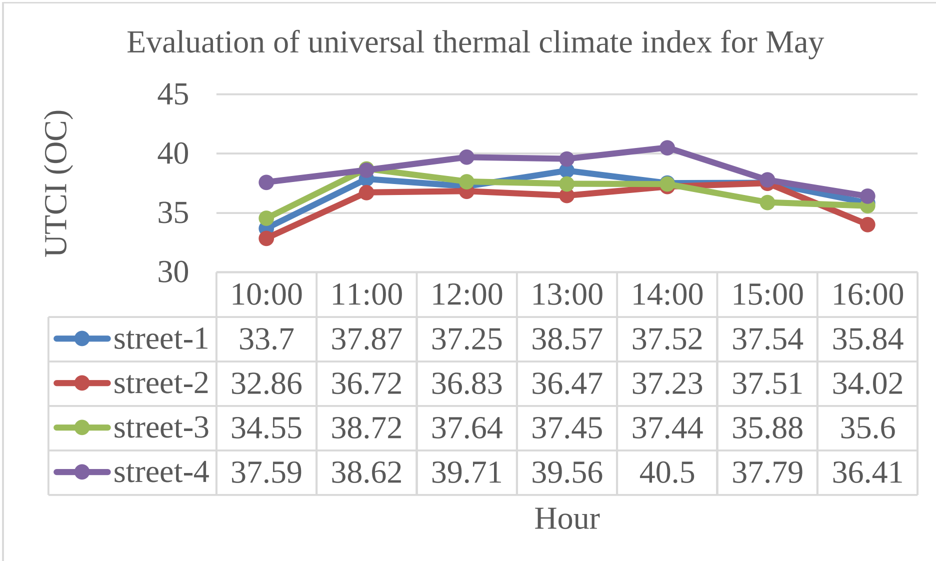

	10:00	11:00	12:00	13:00	14:00	15:00	16:00
street-1	33.7	37.87	37.25	38.57	37.52	37.54	35.84
street-2	32.86	36.72	36.83	36.47	37.23	37.51	34.02
street-3	34.55	38.72	37.64	37.45	37.44	35.88	35.6
street-4	37.59	38.62	39.71	39.56	40.5	37.79	36.41

Figure 4.24 May evaluation of universal thermal climate index for selected streets

According to the figure 4.24 above shows the values of UTCI are high in the month of May for all street without street-1 at 10:00 of the day; the values of UTCI indicates strong heat stress for street-1, street-2 and street-3 all over the day and also, Street-4 indicates under very strong heat stress in case of higher solar radiation in this month.

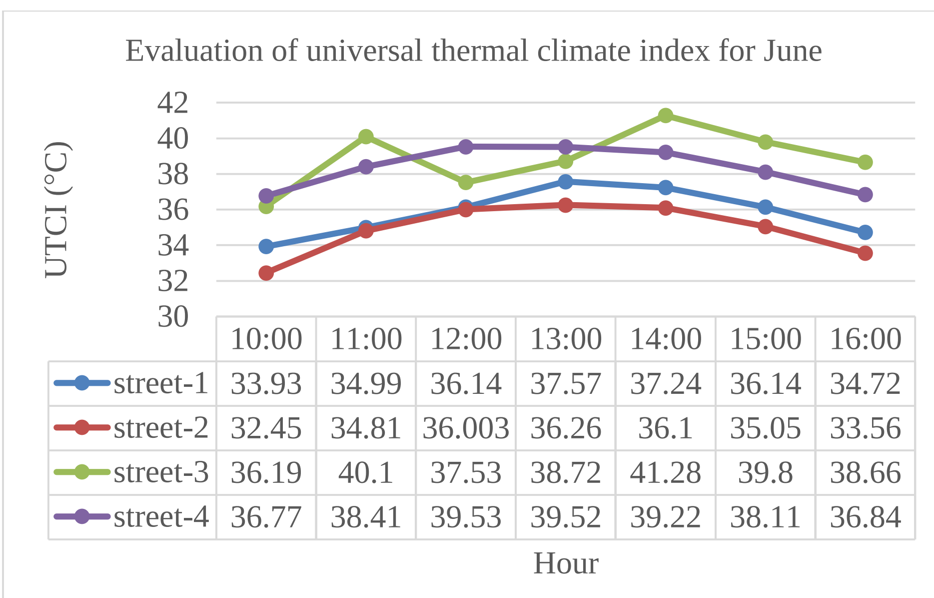

	10:00	11:00	12:00	13:00	14:00	15:00	16:00
street-1	33.93	34.99	36.14	37.57	37.24	36.14	34.72
street-2	32.45	34.81	36.003	36.26	36.1	35.05	33.56
street-3	36.19	40.1	37.53	38.72	41.28	39.8	38.66
street-4	36.77	38.41	39.53	39.52	39.22	38.11	36.84

Figure 4.25 June evaluation of universal thermal climate index for selected streets

The UTCI value in June on the figure 4.25 above indicates us higher compared to other month because the temperature in this month is very high. The UTCI values on street-1 and street-2 are between 32^{o}c UTCI 38^{o}c this indicate strong heat stress on the streets. And on street-3 and street-4 the value of UTCI is increased compared to other street, indicates the streets mostly under very strong heat stress. Generally on June all over the day the streets are thermally uncomfortable for pedestrian. In this month the pedestrians need shaded streets and other cooling strategies.

Overall, the UTCI values of the streets are high for all hottest months (April, May and June) especially from the hour (11:00 – 15:00) of the day; it's typically indicate the streets thermal discomfort for pedestrians. The streets needs shading, good air velocity for cooling the pedestrians, use different cooling strategies to get thermally comfortable streets.

4.7. Bioclimatic Chart and Strategies

Bioclimatic chart development enables to apply appropriate design strategies for different climate zones to restore thermal comfort. The bioclimatic charts that developed below on figure 4.26 and 4.27 were by using the measured data on the table 4.5 below. Accordingly the climate zone of Metehara town is assigned in warm dry climate zone. While Figure 4.26 delivers precise quantitative thresholds for interventions, Figure 4.27 offers broader qualitative insights into how urban designs can align with climatic conditions.

Table 4.5 Measured average maximum and minimum air temperature and relative humidity

Months	**Mean maximum temperature (^{O}C)**	**Mean minimum relative humidity (%)**	**Mean minimum temperature (^{O}C)**	**Mean maximum relative humidity (%)**
April	36.5	37.3	33.5	44.5
May	37.5	33.9	34.5	42
June	38	26.6	34.75	32.4

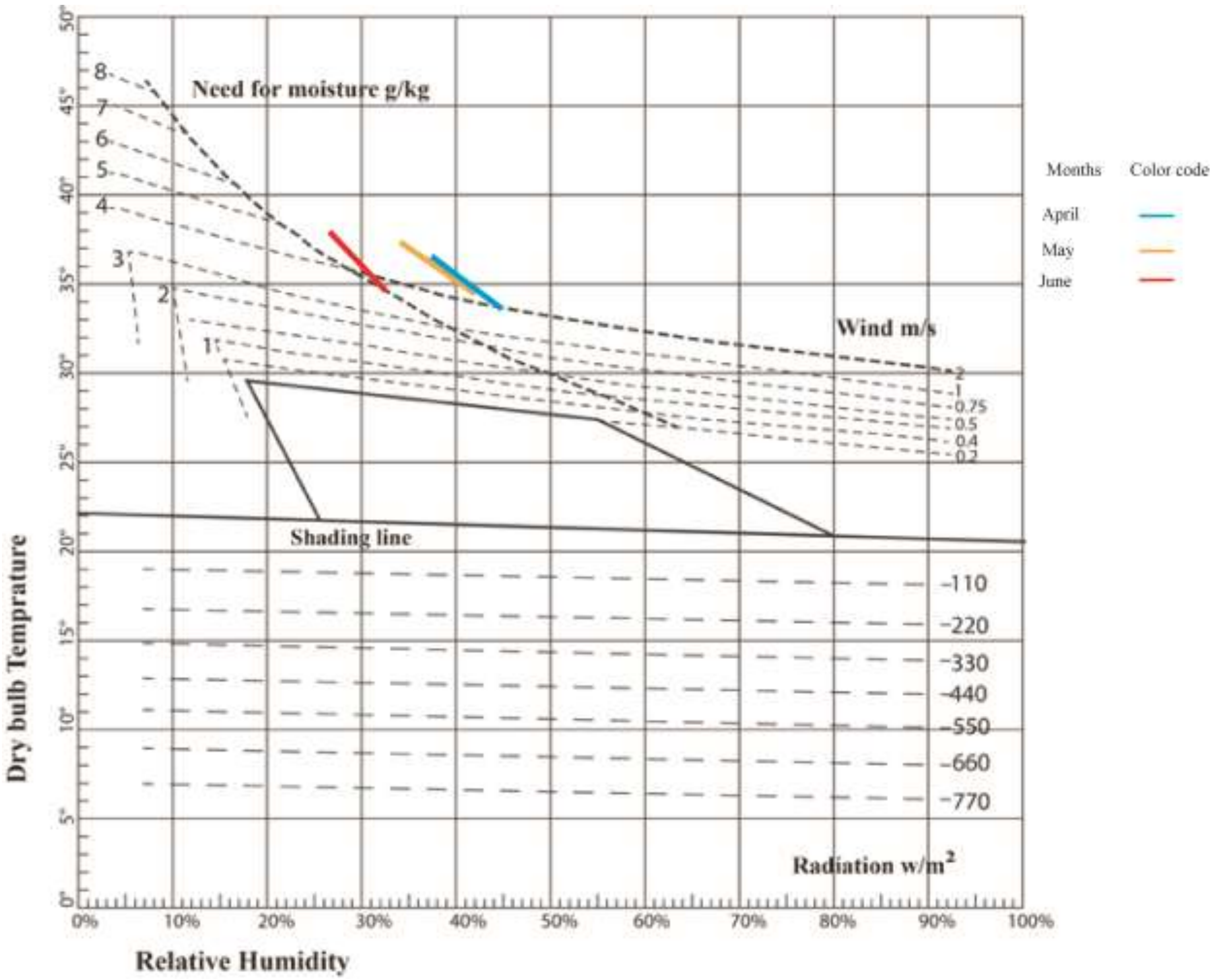

Figure 4.26 Quantitative bioclimatic chart analysis of Metehara town

The quantitative bioclimatic chart on the figure 4.26 above illustrates thermal conditions and strategies required to achieve thermal comfort. The mean maximum temperatures range from 36.5°C to 38°C, while minimum temperatures ranges between 33.5°C to 34.75°C. Relative humidity varies significantly, with minimum values as low as 26.6% and maximum values reaching 44.5%. When the humidity is low, moisture air is required to maintain the comfort of the space. The chart identifies the need for moisture levels between 4 to 5 g/kg during the hottest months (April, May, and June) to maintain pedestrian comfort. Air velocities exceeding 2 m/s are critical for pedestrian thermal comfort. Natural ventilation strategies, such as optimizing street orientations to channel prevailing winds, are essential for promoting airflow. In all hottest months shading is required for pedestrian during the day to avoid overheating during the high-temperature appearance by trapping harsh sunlight. Buildings, trees canopies and other techniques is critical to shade the pedestrian streets during critical time of the da

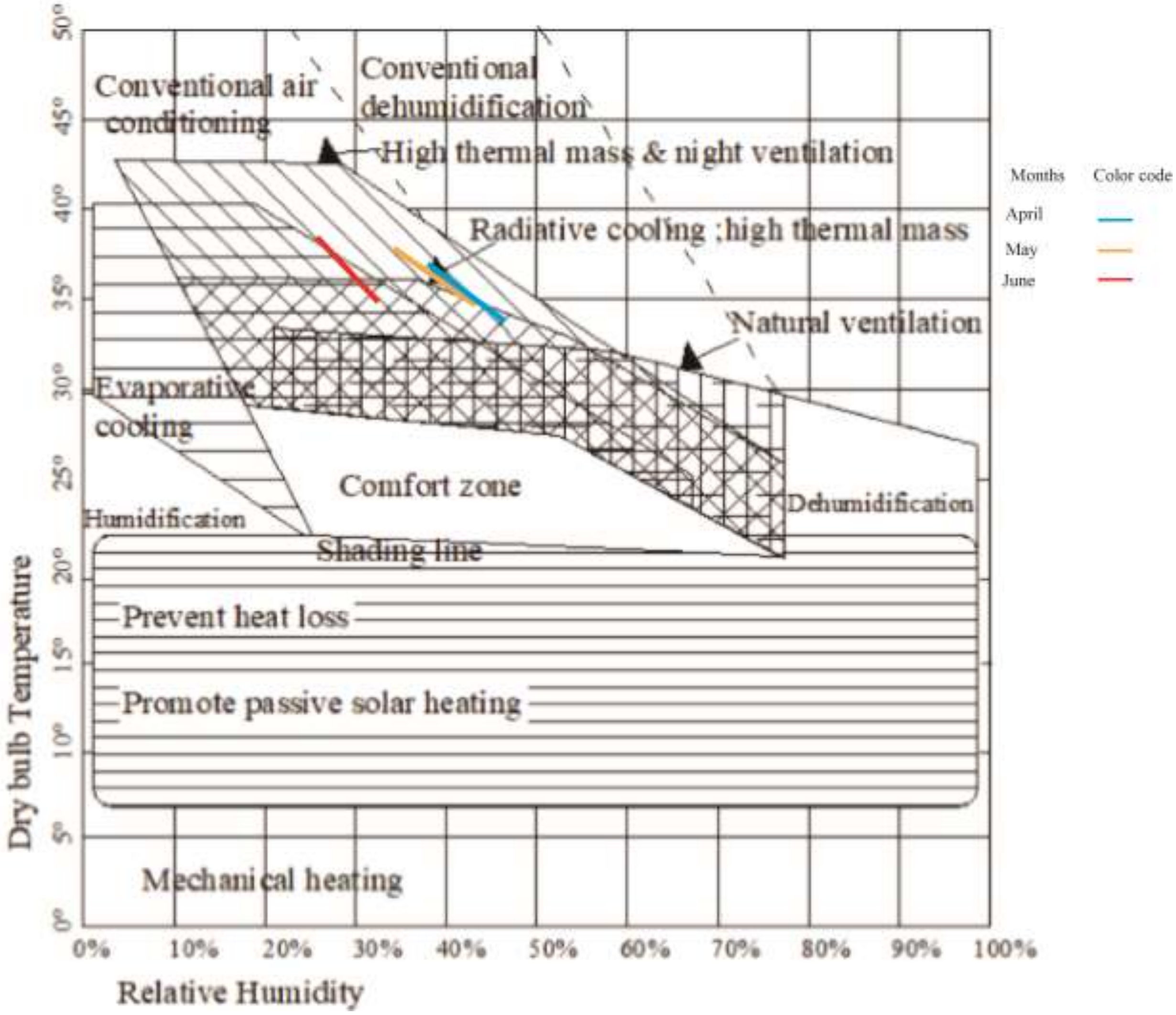

Figure 4.27 Qualitative bioclimatic chart analysis of Metehara town

The qualitative bioclimatic chart on the figure 4.27, shows the thermal conditions and strategies such as trees shading, arcaded buildings, and other canopies for pedestrians are recommended to protect from direct sunlight at critical periods. Shading is important during the hottest months to mitigate overheating. Improving street orientation enhances natural ventilation and minimize direct sunlight exposure. Adding gardens and vegetation's provide natural cooling and reduces heat accumulation. Thermal comfort strategies like radiative cooling, including high thermal mass, and remains are critical across all hottest months. On the chart evaporative cooling is recommended to address low humidity conditions of town streets, especially during the peak hour of the day. Fountains and artificial lakes create microclimates that cool surrounding areas and minimize urban heat island effects.

Comparative insights from both charts the data points reveal the thermal conditions that pedestrians experience throughout the year. The bioclimatic chart includes various zones indicating different thermal comfort strategies for pedestrians. For very warm and hot months of April, May and June urban design consideration such as shading by using trees, arcaded building and canopies to create areas that protect pedestrian from direct sunlight. Natural ventilation by optimize street orientation to enhance natural ventilation and minimize direct sunlight exposure and green spaces incorporate gardens to provide natural cooling and shade and also to promote reduce heat buildup. Water bodies by integrate fountains and artificial lakes to create microclimates that cool the surrounding areas and also water bodies help to reduce the urban heat island effect.

4.8. Summary of the Results

Pedestrian perception indicated strong dissatisfaction with thermal conditions across all selected street orientations particularly in streets lacking adequate shade. Respondents need shade and airflow as critical factors. N-S streets were perceived as slightly more comfortable due to better shading and alignment with prevailing wind directions. E-W streets, despite offering moderate ventilation and lacked sufficient shading from structures. Diagonal streets exhibited prolonged exposure to direct solar radiation resulting in high discomfort among pedestrians.

Sun path and solar shadow analyses demonstrated that street orientation significantly influences shading effectiveness. North-South (N-S) streets provided better shading conditions minimizing direct solar exposure. East-West (E-W) streets lacked consistent shade, especially from south-side buildings leading to elevated pedestrian heat stress. Diagonal streets (NE-SW and NW-SE) exhibited prolonged solar exposure, resulting in intensified discomfort. Sky View Factor (SVF) analysis confirmed that shading effectiveness varies across street orientations. N-S streets had lower SVF value (0.49) indicating reduced sky exposure and better shading. E-W streets had moderate SVF (0.66) but lacked sufficient vegetation coverage to mitigate heat stress. Diagonal streets (NW-SE & NE-SW) had high SVF values (0.68 & 0.96) respectively meaning greater exposure to direct solar radiation further worsening pedestrian discomfort.

Microclimate analysis demonstrated distinct temperature, humidity, wind speed and solar radiation variations among different street orientations. N-S streets benefited from relatively cooler conditions due to improved ventilation while E-W streets faced thermal stress during midday due to limited shading from buildings. Streets with NE-SW and NW-SE orientations exhibited the highest MRT and UTCI values, indicating extreme heat stress due to excessive solar exposure and poor wind flow.

Generally, the overall result of analysis showed that street-2 (N–S) oriented street is the best orientation for Metehara town while E–W oriented street and the diagonal oriented streets are the most uncomfortable street. Design solutions suited to warm-dry environments were highlighted by quantitative and qualitative bioclimatic chart studies. Shading, natural ventilation, and evaporative cooling proved to be critical treatments for rebalance of thermal equilibrium. High-albedo materials, reflective pavements, water bodies, and plants can help to significantly reduce pedestrian thermal discomfort.

CHAPTER FIVE

CONCLUSION AND RECOMMENDATION

5.1. Conclusion

The study concludes that street orientation plays a central role in shaping pedestrian thermal comfort especially during the hottest months April, May and June. Among the four orientations assessed street-2 (N–S) oriented street offered the most favorable thermal conditions benefiting from improved ventilation, vegetation cover and shading. Street-1 (E–W) street demonstrated some cooling advantages during certain periods due to better airflow but suffered from insufficient shading. Conversely, street-3 (NW–SE) and street-4 (NE-SW) consistently exhibited greater heat stress due to prolonged solar exposure limited for climate responsive urban design that aligns street orientation with thermal comfort goals.

Pedestrian perception results revealed a high level of thermal discomfort across all selected streets, with streets-3 and 4 (diagonally oriented) recording the lowest acceptability ratings. Respondents indicated a strong desire for cooler conditions, preferring increased wind speed, higher humidity and significant shading especially during the midday period. Street-2 (N-S) was indicated as the most tolerable environment due to better airflow and partial shading from trees. These subjective findings closely aligned with the measured MRT and UTCI values reinforcing that both environmental parameters and design elements shape pedestrian comfort perception.

Shading plays a critical role in moderating pedestrian thermal comfort in Metehara town. Streets with adequate shading particularly North-South (N-S) benefited from reduced solar exposure, lower mean radiant temperature (MRT) and improved Universal Thermal Climate Index (UTCI) values. Sun path and shadow analyses showed that the N-S orientation provided more consistent shade during peak hours of the day especially when enhanced by vegetation. In contrast, East-West (E-W) and diagonal orientations received high direct solar exposure intensifying heat stress. The effectiveness of shading was also closely linked to height to width ratios and vegetation coverage as validated through Sky View Factor (SVF) analysis.

Among street orientations analyzed the N-S street have better thermal performance. The N-S street offered improved ventilation aligned with prevailing winds, while the E-W and diagonal orientations (NE–SW and NW–SE) consistently underperformed, showing higher MRT and UTCI values and limited natural ventilation. Across all street types midday thermal stress remained elevated underscoring the importance of integrating climate responsive design strategies like shading, vegetation and reflective materials to improve walkability in Metehara town.

The qualitative and quantitative bioclimatic chart strengthened the need for climate responsive interventions. The strategies such as shading enhancement, increase vegetation planting and water bodies for cooling, and also the adoption of high-albedo materials were identified as essential measures for mitigating pedestrian thermal discomfort in Metehara town.

The study results finally demonstrated that street orientation is a critical factor challenging pedestrian thermal comfort in Metehara town. The feasibility of N-S oriented street when complemented with proper shading and ventilation strategies, to enhance thermal conditions of pedestrians. E-W, NW-SE and NE-SW oriented streets require significant design improvements, including shading techniques and enhanced ventilation corridors to address their inherent thermal discomfort. This study initiates a scientific framework for evaluating thermal comfort of the pedestrian in street environments. By considering climatic analysis with urban design strategies, it allocates actionable insights for urban planners, architects and policymakers aiming to create thermally comfortable and sustainable streetscapes in Metehara town warm-dry climates. The results reinforce the importance of climate responsive design strategies that coordinate street orientation, shading, ventilation, and material selection to mitigate thermal stress of the pedestrians in the town.

5.2. Recommendation

Metehara town experience significant challenges in managing pedestrian thermal comfort due to extreme solar radiation and limited natural cooling. Street orientation serves one of a major element affecting the microclimatic situations of urban areas that shapes the distribution of solar exposure, availability of shade, and flow of cooling breezes. Strategic optimizing street alignment can reduce heat stress, increase walkability, and improve the general living circumstances for the residents of the town.

For improving pedestrian thermal comfort Metehara town based on the analysis results, the following urban design approaches are recommended help to enhance pedestrian thermal comfort:

1. Street View Adjustment

- Give North-South and East-West Street alignments top priority to reduce direct solar exposure and thermic discomfort.

2. Inclusion of Shade Techniques

- Tree Canopies: Raise the density of shade-providing trees and correct placement along paths for pedestrians. Choose species suited for Metehara warm-dry environment for best performance.
- Arcades provide shaded areas that greatly cut down on direct solar radiation exposure, reducing temperatures of air and surface. It gives consistent shadow at peak sunlight hours.
- Create shaded rest zones every 100–150 meters along pedestrian streets help to relief from heat exposure and enable thermal recovery.
- Shade from built form: position walkways as near as feasible to the buildings to maximize building cover.

3. Improvement of Green Infrastructure

- Plant more trees along pedestrian pathways to increase cooling environment. Add green areas such like shrubbery and tiny urban parks near pathways to lower heat radiation from surrounding surfaces areas.

4. Heat reduced pavement materials for pedestrian and building facades.

- Use high albedo pavement materials to decrease solar radiation.
- Use light colored pavement materials such like granite, concrete and brick to get thermal comfort of the pedestrians.
- Use grid field stone with grass pedestrian side walk design for natural cooling.

5. Provide natural ventilation

- Design streets to elevate ventilation for pedestrian aligned street direction to the prevailing wind direction. Remove things that obstacles wind flow; especially on the Northeast-Southwest oriented street where wind flow is typically low.

6. Design water bodies

- Incorporate fountains, ponds and artificial lakes near pedestrian’s walkway to increase evaporative cooling and enhance pedestrian thermal comfort.

Those recommended strategies are used to assist urban planners and designer and also policymakers to develop thermally comfortable pedestrian environment in Metehara town. They are well founded in guidelines of sustainable urban design and evidence based strategies to decrease heat stress.

REFERENCES

Abbaszaden, R., & Koichi, T. (2006). Poor thermal conditions in pedestrian areas and emotional well-being. International Journal of Bioclimatic Research, 32, 5–20.

Ahmed, K., Khare, M., & Chaudhry, S. (2005). Street configuration and air velocity: Implications for thermal comfort. Journal of Urban Design, 18(2), 112–127.

Akshay, K. (2023). Solar shadow analysis for improving thermal comfort in urban design. Environmental Design Studies Journal, 45(2), 215–230.

Al- Azri ,Al-Rawahi, Zuriget (2012) Development of Bioclimatic Chart for Passive Building Design in Muscat-Oman Oman, Sultan Qaboos University

Aljawabra, F., & Nikolopoulou, M. (2010). Shade structures and urban microclimates: Implications for pedestrian comfort. Journal of Urban Sustainability, 12(4), 87–101.

Andreou, E. (2013). Effect of urban canopy shading on outdoor thermal comfort. Energy and Buildings, 62, 123–135.

Ariane, B. (2016). Recommendations for urban shading strategies to improve pedestrian thermal comfort. Journal of Urban Sustainability.

ASHRAE Standard 55. (2010–2017). Thermal Environmental Conditions for Human Occupancy. Atlanta, USA: American Society of Heating, Refrigerating and Air-conditioning Engineers Inc.

Asimakopoulos, D. N., et al. (2001). Energy and Climate in the Urban Built Environment. London: James & James.

Balling, R. C. (1992). Urban surfaces and increasing temperatures. Journal of Environmental Studies, 67(3), 98–109.

Błażejczyk, K., et al. (2013). Universal thermal climate index: Assessment and application. International Journal of Biometeorology, 56(5), 571–580.

Broderick, B., et al. (2012). Urban thermal stress and pedestrian comfort: A case study analysis.

Journal of Environmental Studies, 67(3), 98–109.

Çengel, Y. A., & Boles, M. A. (2015). Thermodynamics: An Engineering Approach (8th ed.). McGraw-Hill Education.

Chali, Y., Dante, S., & Esayas, A. (2016). Human thermal comfort in residential house building of Jimma town, south-west Ethiopia. International Journal of Scientific & Technology Research.

Chen, N., & Ng, E. (2011). Urban livability and vitality: The importance of outdoor spaces. Journal of Urban Design, 18(2), 112–127.

Co. KGaA, Titisee-Neustadt, Germany. (2019). Standard meteorological measurements for urban comfort studies. Instrument Specifications Manual.

de Dear, R., & Brager, G. (1998). Developing an adaptive model of thermal comfort and preference. ASHRAE Transactions.

De Jong, A. (2013). Urban design and pedestrian environments. Cambridge University Press.

Dines, N., & Kyle, B. (2001). Landscape Architects Portable Handbook. McGraw-Hill Companies.

Di Nunzio, A. (2020). Online Universal Thermal Climate Index (UTCI) Calculator. UTCI Research Tools. Available from: [Insert official source, if necessary].

Djekic, J. (2018). Investigating material effects on urban thermal comfort: Field observations in Nis, Serbia. International Journal of Environmental Studies, 34(2), 109–122.

Emmanuel, M. (2005). Climate-responsive urban planning: Lessons from vernacular architecture. Energy Policy, 33(9), 1223–1232.

Emmanuel, M., & Johansson, E. (2006). Urban climate studies in tropical cities. Urban Ecology, 12(3), 19–31.

Enteria, N., et al. (2019). Urban thermal comfort dynamics: Clothing, activity, and environmental parameters. Environmental Research Journal.

Fanger, P. O. (1982). Thermal Comfort: Analysis and Applications in Environmental Engineering. McGraw-Hill Education.

Fiala, D., Bröde, P., & Jendritzky, G. (2012). Mean Radiant Temperature (MRT): A critical tool in thermal comfort studies. International Journal of Biometeorology, 56(5), 571–580.

Gehl, J., & Svarre, B. (2013). Public spaces and their impact on urban safety and comfort. Washington, DC: Island Press.

Ghosouri, A. (2020). The influence of street shading and H/W ratio on pedestrian thermal comfort. Environmental Research, 78(5), 321–340.

Givoni, B. (1998). Climate considerations in urban design. New York: Wiley.

Golany, G. (1996). Urban Design for an Urban Climate. Wiley.

Grimmond, C. S. B. (1999). Urban canyon surface energy balance: Sensitivity to the street canyon geometry. Boundary-Layer Meteorology, 94(3), 489–495.

Hakimiefaez, K. (2010). Evaluation of air temperature effects on pedestrian comfort. Environmental Climate Studies Journal, 28(4), 223–240.

Han, M. (2024). Building height-to-width ratios and shading strategies in warm climates. Urban Planning and Design Journal.

Hegazy, T., & Qurnfulah, M. (2020). Enhancing pedestrian thermal comfort through microclimate modifications. Energy and Buildings, 78, 86–98.

International Organization for Standardization (ISO). ISO 7726 (1998). Ergonomics of the Thermal Environment - Instruments for Measuring Physical Quantities. Geneva, Switzerland: ISO.

Jauregui, E. (1991). The human climate of tropical cities. International Journal of Biometeorology.

Johansson, E., et al. (2012). Shading impacts on mean radiant temperature in urban settings. Applied Urban Ecology, 32, 147–161.

Jendritzky, G., Bröde, P., & Fiala, D. (2012). Human-biometeorology and urban climates: Impacts of radiant temperature. International Journal of Biometeorology, 56(5), 571–580.

Kariminia, S., Nikpour, A., & Gholipour, M. (2016). The relationship between shading and thermal comfort in urban squares: Case study of Isfahan. International Journal of Urban Climates, 45(3), 789–798.

Katafygiotou, M., & Serghides, D. (2014). Bioclimatic design principles for urban environments. Renewable and Sustainable Energy Reviews, 38, 551–560.

Kenny, N., et al. (2009). The role of radiant temperature in outdoor thermal comfort assessments. International Journal of Biometeorology, 53(2), 121–130.

Khodakarami, J. (2020). Urban thermal comfort analysis: Exploring radiant and convective heat exchanges. Energy and Buildings, 215, 109875.

Kim, J., & Baik, J. (2005). Street configurations and wind flow optimization. Journal of Environmental Design, 89(1), 44–61.

Kleerekoper, L., van Esch, M., & Salcedo, T. B. (2012). Addressing urban heat island effect in city planning. Resources, Conservation and Recycling, 64, 30–38.

Koichi, T. (1996). Thermal comfort and architectural adaptation in warm climates. Energy Policy, 24(3), 253–260.

Krishan, A., Baker, N., Yannas, S., & Szokolay, S. V. (2001). Climate responsive architecture: A design handbook for energy-efficient buildings. McGraw-Hill.

Krüger, E., & Pearlmutter, D. (2015). Reflective urban surfaces: Benefits for pedestrian thermal comfort. Energy and Buildings, 78, 86–98.

Kumar, S. (2023). Solar shadow analysis for pedestrian comfort: Formulas and applications. Environmental Design Studies Journal.

Landsberg, H. E. (1981). The urban climate. Academic Press.

Lee, J. W., & Cheung, K. K. (2019). Urban street design strategies for effective shading and ventilation. International Journal of Urban Design, 23(4), 241–258.

Lin, T.-P., Matzarakis, A., & Hwang, R.-L. (2010). Pedestrian comfort in different climates: A systematic analysis. Urban Climate, 23, 24–36.

Lindberg, F., & Grimmond, C. S. B. (2010). Continuous sky view factor maps from high-resolution urban digital elevation models. Climate Research, 42(1), 177–183.

Littlefair, P. (2000). Environmental Site Layout Planning: Solar Access, Microclimate and Passive Cooling in Urban Areas. Thomas Telford.

Marsh, A. (2015). Urban shading and its impact on thermal conditions. Journal of Environmental Design, 58(2), 112–119.

Masons, B. (2021). Solar shading and pedestrian cooling in arid cities. Urban Ecology Review, 32(5), 19–31.

Masoud, M. (2021). Urban cooling strategies in semi-arid climates: The Jeddah perspective. Saudi Arabian Climate Review, 15(2).

Mataram, R., et al. (2007). Bioclimatic chart interpretation in sustainable urban planning. Energy Policy, 33(9), 1223–1232.

Matzarakis, A., & Endler, C. (2010). Climate-responsive urban design: Applications of bioclimatic indices in Europe. Meteorological Applications, 17(3), 241–251.

Matzarakis, A., & Mayer, H. (1996). Another kind of environmental stress: Thermal stress. WHO Collaborating Centre for Air Quality Management and Air Pollution Control.

Matzarakis, A., & Mayer, H. (2007). Heat stress in urban environments: Evaluation using UTCI. International Journal of Biometeorology, 51(5), 437–444.

Mayer, H. (1987). Thermal comfort in diverse urban environments. Theoretical and Applied Climatology, 38(1), 43–49.

Middel, A., & Ariane, B. (2016). Urban heat island mitigation strategies for sustainable cities. Journal of Urban Planning and Development, 42(1), 73–92.

Michael, A., et al. (2015). Thermodynamics: An Engineering Approach (8th Ed.). McGraw-Hill Education, New York.

Ministry of Agriculture (MOA). (2000). Traditional Climate Zones of Ethiopia. Addis Ababa, Ethiopia.

Mohammad Taleghani. (2019). optimizing outdoor thermal comfort: Guidelines for warm climates. In Urban Microclimate Design for Warm Climates (pp. xx–xx).

Oke, T. R. (1982). The urban heat island phenomenon. Atmospheric Environment, 16(1), 19–33.

Olgyay, V. (1963). Design with Climate: Bioclimatic Approach to Architectural Regionalism. Princeton University Press.

Sanaieian, H., Tenpierik, M., van den Dobbelsteen, A., Mehdigholi, A., & Sariyildiz, S. (2014). Review of the impact of urban block form on thermal performance, solar access and ventilation. Renewable and Sustainable Energy Reviews, 38, 551–560.

Santamouris, M. (2001). Cities and urbanization: Climatic implications. Cambridge University Press.

Schell, L. M., & Smith, M. T. (1993). Effects of urbanization on environmental quality and population health. Annual Review of Anthropology, 22, 125–149.

Shamir, H. (2003). Urban climatic interactions in tropical cities. Journal of Urban Ecology, 15(2), 129–144.

Shashua-Bar, L., & Hoffman, M. E. (2003). Geometry and orientation aspects in passive cooling of canyon streets with trees. Energy and Buildings, 35, 61–68.

Shishegar, N. (2013). Orientation strategies in urban design: Impacts on solar access. Journal of Clean Energy Technologies, 1(1), 54–63.

Tapies, E., & Schmitt, G. (2014). Climate-sensitive urban growth: Outdoor thermal comfort as an indicator for the design of urban spaces. WIT Press.

Taleghani, M. (2020). Bioclimatic indices in urban planning. Urban Climate, 32(5), 19–31.

Tinz, B. (2012). Universal Thermal Climate Index (UTCI): Thermal stress classification. Meteorological Applications, 19(3), 303–313.

Toy, S., & Yilmaz, S. (2010). Impacts of urban surfaces on thermal comfort: Bioclimatic analysis. Building and Environment, 45(3), 850–860.

United Nations (2014) Department of Economic and Social Affairs, Population Division, Urban Agglomerations

Van Esch, M., Looman, R., & de Bruin-Hordijk, G. (2012). Climate-sensitive urban design: Principles and practices. Resources, Conservation and Recycling, 64, 30–38.

Wolkoff, P., et al. (2007). Indoor air humidity: Environmental health perspectives. International Journal of Biometeorology, 51(2), 124–134.

Yang, W., Qian, L., & Lau, S. (2013). Orientation and ventilation strategies in urban streets. Journal of Clean Energy Technologies, 1(1), 54–63.

Zhang, L., & Deng, X. (2020). Effects of wind velocity and direction on pedestrian thermal comfort in a hot climate. Sustainable Cities and Society, 55, 102049.

Zhang, T. (2019). Analysis of microclimatic parameters in urban street canyons. International Journal of Biometeorology, 63(4), 315–326.

APPENDIX

Appendix 1: Sun Path and Solar Shadow Analysis Parameters

The sun path and shadow analysis involves understanding solar angles and shadow lengths to optimize pedestrian thermal comfort.

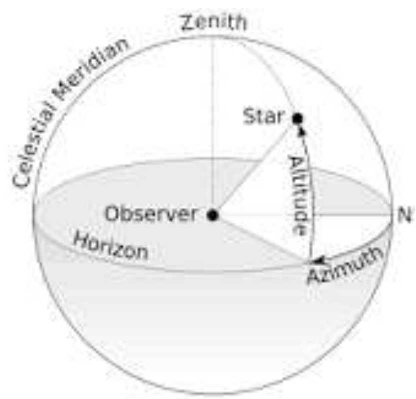

Figure: Altitude and azimuth angles (Mukesh Pandey, 2020).

1. Declination (δ):

The angle between the rays of the sun and the equatorial plane varies with the day of the year:

$$\delta = 23.45 * \sin\left(360/365\ (N+284)\right)$$

Where N is the Julian day, starting from January 1 (Arvind Krishan et al., 2001).

2. Solar Altitude (A):

Determines shadow angles, crucial for designing shading strategies. The vertical angle of the sun above the horizon at a given time and location:

$$\mathrm{Sin}(A) = \sin(\delta) * \sin(\varnothing) + \cos(\delta) * \cos(\varnothing) * \cos(H)$$

Where Ø = Latitude of location and H = hour angle (degree difference from solar noon) (United Nations Environment Programme, 1997)

3. Azimuth (AZI):

The horizontal angle between the sun and the north direction, measure clockwise.

$$AZI = \arcsin\left(\cos(\delta) * \sin(H) / \cos(A)\right)$$

(Source: Kumar, 2023)

4. Shadow Length (L):

The length of shadow cast by objects (e.g., buildings, trees) on pedestrian paths.

Shadow length is calculated as:

$$L = H / \tan(A)$$

Where H is the height of the object, and A is the solar altitude angle (Source: Ghosouri, 2020).

Appendix 2: Sky View Factor (SVF) Reference Values

SVF describes the fraction of visible sky from a point on the ground for quantifying solar exposure and radiant heat.

Table 1. Sky view factor values and description (source: Oke, T.R., 1988)

SVF Range	Shading Condition	Implication
0.1 – 0.3	Dense shading	Ideal for minimizing solar gain
0.3 – 0.5	Moderate shading	Balances daylight and thermal relief
0.5 – 0.7	Light shading	Higher solar exposure
0.7 – 1.0	Minimal or no shading	High radiant heat load

Appendix 3: Interview Questionnaires for Pedestrians

Date: ____ / ____ / ____ Time: ________ Gender: (1) Male (2) Female Age: ______

2. The position pedestrian are in:

a. street-1 b.street-2 c.street-3 d.street-4

3. Your current clothing includes (multiple choices):

Upper: …..…....Vest ……Underwear …..Short sleeve T-shirt …….Long sleeve T-shirt ….……Pullover …….Shirt …….Sweater ……Jacket

Bottom: ....Shorts ……..Short skirt ……Trousers ……..Long skirt

Footwear: …….Sandals ……..Shoes ……..Boots ………Cotton-padded shoes ……..Pantyhose ………..Ankle-length socks ……….low-cut liners socks

Others: ____________________________

4. Your activity in outdoor is:

(1) Light exercising (walking, etc.)

(2) Medium exercising (Jogging, etc.)

(3) Heavy exercising (ball games, sports, etc.)

(4) Standing (viewing, etc.)

(5) Sitting (Chatting, playing mobile phone, reading, playing chess, etc.)

5. Please choose your overall comfort level at present:

a. −1 Uncomfortable b. 0 Neutral c. 1 Comfortable

6. Please choose your acceptable level for current thermal environment at present:

a. −3 extremely unacceptable b. −2 unacceptable c. -1 slightly Unacceptable d. 0 Neutral e. 1 slightly acceptable f. 2 acceptable g. 3 extremely acceptable

7. What changes do you expect from the following meteorological data at present?

Air temperature: a. higher b. unchanged c. lower

Relative humidity: a. higher b. unchanged c. lower

Wind speed: a. stronger b. unchanged c. weaker

Solar Radiation: a. stronger b. unchanged c. weaker

Appendix 4: Global Horizontal Irradiation Map of Fentale Woreda and Metehara Town

Global horizontal irradiation (GHI) significantly impacts pedestrian thermal comfort by contributing to the mean radiant temperature (MRT), a key factor in evaluating thermal conditions (Wang & Akbari, 2016). High GHI levels can elevate MRT, making outdoor spaces feel warmer and less comfortable for pedestrians (Santamouris, 2020)

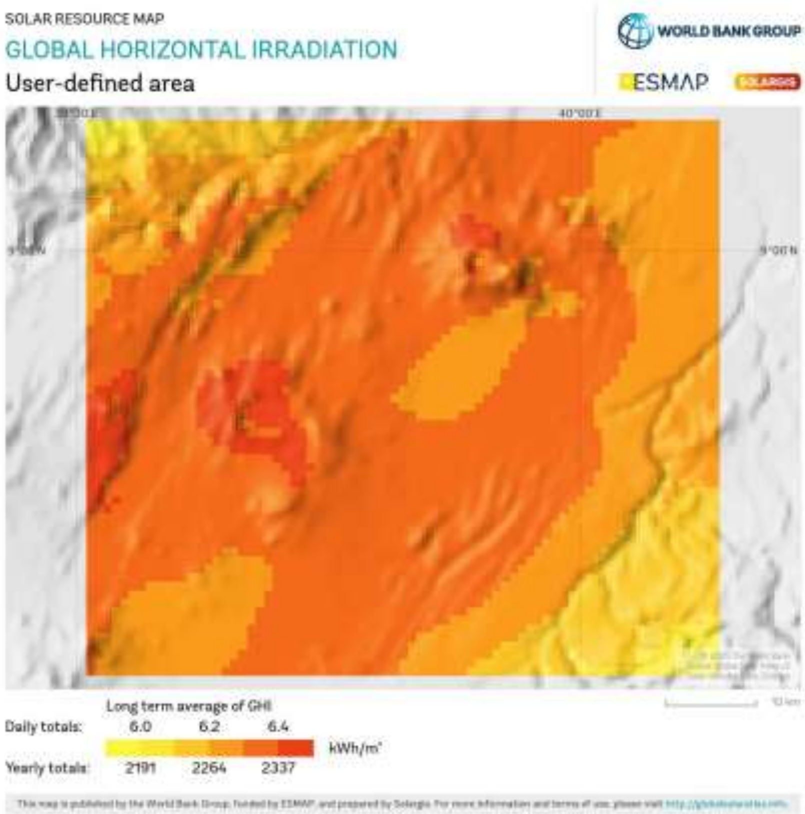

Figure 2. Fentale Woreda Global horizontal irradiation map (source: Global solar atlas, 2025)

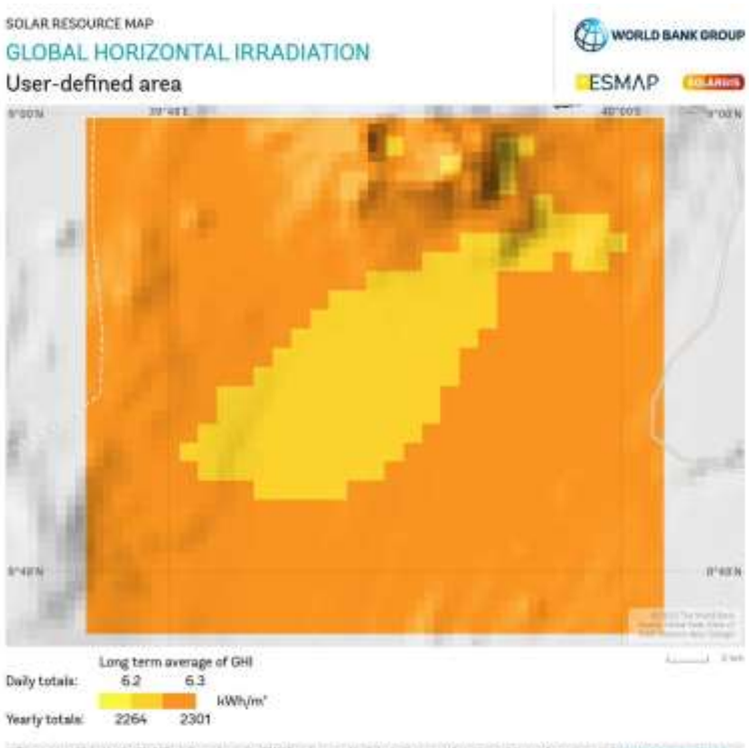

Figure 3. Metehara town global horizontal irradiation map (source: Global solar atlas, 2025)

ANNEX: Publishable Manuscript

EVALUATING STREET ORIENTATION FOR PEDESTRIAN THERMAL COMFORT THE CASE OF METEHARA TOWN

Rorisa Eshetu and Nebyou Yonas (Ass.Prof)
Addis Ababa University

Abstract

Street orientation significantly influences pedestrian thermal comfort in warm dry urban climates. This study evaluates the thermal comfort performance of four selected street orientations North-South (N-S), East-West (E-W), Northwest-Southeast (NW-SE) and Northeast-Southwest (NE-SW) in Metehara town Ethiopia, during the peak hottest months (April-June) of the year. A mixed method approach integrates field measurements (air temperature and relative humidity), satellite data (wind speed and solar radiation) and calculated thermal indices including mean radiant temperature (MRT) and the universal thermal climate index (UTCI). Shading effectiveness was assessed using sky view factor (SVF) and solar geometry calculations while pedestrian perceptions were captured through standardized surveys. Results identify that N-S streets as optimal offering lower heat stress due to shading and alignment with prevailing wind patterns. In contrast E-W and diagonal (NW-SE and NE-SW) street orientations experienced higher thermal stress due to poor shading geometry and disrupted airflow. The findings highlight the importance of climate responsive urban design strategies in warm dry regions.

Keywords: Street orientation, Thermal comfort, Shading, Sky view factor and Warm dry climate

1. Introduction

Rapid urbanization in Ethiopia's warm dry regions has heightened pedestrian thermal discomfort. Rapid population growth and expanding urban areas demand innovative approaches to enhance urban livability while addressing the critical issue of thermal comfort in pedestrian environments (United Nations, 2014). In towns like Metehara, insufficient shading, poorly aligned street orientation and limited climate sensitive planning practices exacerbate urban heat exposure. Street orientation by influencing solar radiation, shading and airflow is a critical yet under examined variable in shaping outdoor thermal comfort (Hoffman, 2003).

Street orientation is a key determinant in shaping the microclimatic conditions and pedestrian thermal comfort (Shishegar, 2013). By influencing exposure to solar radiation, shading potential, ventilation and wind patterns; street orientation has a significant impact on the thermal environment experienced by pedestrians. Strategic urban planning, which takes into account local climatic conditions is essential for creating thermally comfortable spaces. In particular, optimizing street orientation and incorporating shading and ventilation mechanisms are vital for reducing heat stress, especially in arid and semi-arid regions where extreme temperatures are prevalent (Shashua-Bar & Hoffman, 2003). Despite its significance urban planning in many fast growing towns often overlooks these critical considerations resulting in environments that exacerbate thermal discomfort (Kleerekoper, 2012).

Metehara town, located in Oromia, Ethiopia at 08°54′N, 39°55′E with an elevation of 947m, presents high temperatures average of 29°C during hot months and minimal rainfall, it provides a credible context for exploring the relationship between street orientation and pedestrian thermal comfort. The town is characterized by its warm dry climate with high temperatures during its hottest months April, May and June increasing significant challenges for outdoor activities and pedestrian comfort (MOA, 2000). Despite the urgency of addressing these challenges the existing urban layout of Metehara often lacks strategic shading, effective ventilation corridors and climate responsive designs making it imperative to investigate potential urban design solutions.

This study aims to evaluate the thermal comfort performance of major street orientations in Metehara town by assessing microclimatic conditions, pedestrian perception, sky view factor and solar geometry, through a comprehensive analysis of microclimatic variables and urban geometry. By employing methodologies such as field measurements, sky view factor calculation and thermal indices like the universal thermal climate index (UTCI) and mean radiant temperature (MRT) the research identifies the microclimatic variations across selected street orientations. The findings emphasize the importance of integrating shading mechanisms, vegetation, reflective materials and optimized street orientations in urban planning to mitigate thermal discomfort.

2. Materials and Methods

From 197 mapped streets, four streets were purposively selected for the study based on orientation, street width, pedestrian flow and physical geometry. The selected streets orientation are shown below on (Figure 1 and Table 1) Street 1 (E-W), Street 2 (N–S), Street 3 (NW-SE) and Street 4 (NE-SW) were sampled to evaluate thermal comfort of the pedestrians.

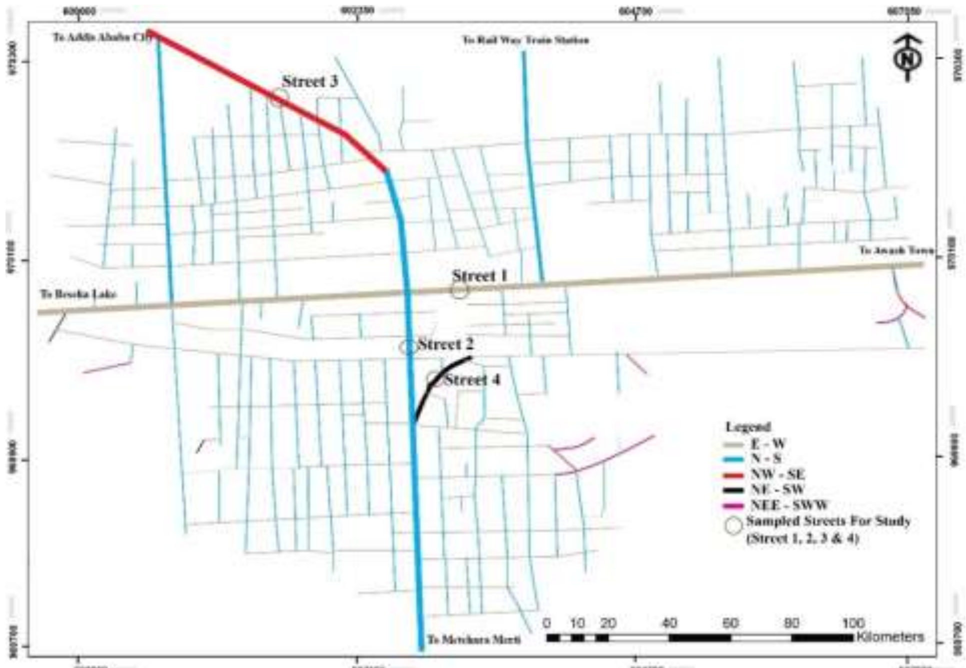

Figure 1 Streets orientations of Metehara town by cardinal direction

Table 1 Sampled street geometry and description

Name	Street orientation	Street width	Building height	Street section
Street-1	E-W	20m	G+0 on the north side of street G+2 on the south side	
Street-2	N-S	20m	G+0 both side	
Street-3	NW-SE	20m	G+0 both side	
Street-4	NE-SW	15m	G+0 both side	

A mixed methods approach was employed integrating environmental measurements, pedestrian surveys and geometric analysis of four representative streets. The data collection period focused on the hottest months of the year April, May and June between 10:00 AM and 16:00 PM when pedestrian thermal stress is typically elevated.

Air temperature and relative humidity were measured hourly using ISO 7726 compliant digital hygrometers positioned at 1.5 m above ground. Wind speed and solar radiation data were sourced from NASA power and refined to pedestrian height using the logarithmic wind profile equation.

$$U(z) = U_{ref} \times (\ln(Z/Z_0) / \ln(Z_{ref} / Z_0))$$

Where: U (z) is the pedestrian-level wind speed, U_{ref} is the NASA power wind speed at reference height Z_{ref} typically 10m, Z is pedestrian height (1.5–2m) and Z_O is the surface roughness length (varies by terrain ~0.1m-1m for urban areas)

The pedestrian perception interview questionnaire was administered to 80 participants (20 per street). The sample size was determined by using Cohen's effect size formula for one way ANOVA, ensuring 95% confidence and 80% statistical power to evaluate thermal comfort vote (TCV) of the sampled streets orientation.

Sun shade analyses are an important tool for studying thermal comfort of the pedestrian at different street orientation. Sun shade was analyzed using trigonometric formula used to calculate shadow width based on solar altitude angles, azimuth angle and building height and also the equations; Sun shade length (L) = H/tan θ Where H = height of buildings or trees and θ = Sun altitude

Sky View Factor (SVF) was estimated using geometric and adjusted for tree canopy transmissivity. Symmetrical urban canyon according to Oke (1981)

$$SVF = 1/ 1 + (H/W)^2 \quad (1)$$

Where: H is average building height and W is street width; used when both side height are same

Asymmetrical canyon (two different heights) according to Grimmond (1999)

$$SVF = ½ [\cos^2 (\arctan (H_1/W)) + \cos^2 (\arctan (H_2/W))] \quad (2)$$

Where: H1, H2 are building heights on each side and W is street width; for uneven urban geometry.

Vegetation adjustment according to Lindberg & Grimmond (2010)

$$SVF_{adjusted} = SVF_{geometric} \times T_f \quad (3)$$

Where: T_f is tree canopy transmissivity (typically, dense tree canopy using $T_f = 0.3 - 0.5$ and sparse trees with gaps use $T_f = 0.7 – 0.9$).

According to Fanger (1982), Mean radiant temperature analyses are an important tool for studying thermal comfort of the pedestrian at different street orientation. Universal Thermal Climate Index (UTCI) was calculated using an established online calculator, integrating measured temperature, wind, humidity, and MRT.

3. Result and Discussion

3.1 Shading and Solar Geometry

Table 2 Altitude, Azimuth and Sun shade length of hottest months.

Hour		**10:00**	**11:00**	**12:00**	**13:00**	**14:00**	**15:00**	**16:00**
April,	Altitude(θ) (°)	55.73	70.36	84.44	79.47	65.00	50.34	35.68
21,	Azimuth(β) (°)	81.85	79.42	56.61	-72.4	-80.84	-82.01	-81.65
2024	Sun shade length	0.6812H	0.36H	0.1H	0.19H	0.47H	0.83H	1.4H
Hour		**10:00**	**11:00**	**12:00**	**13:00**	**14:00**	**15:00**	**16:00**
May,	Altitude(θ) (°)	55.06	68.18	77.79	74.47	62.59	49.04	35.09
22,	Azimuth(β) (°)	66.89	56.02	18.97	-40.93	-62.29	-69.00	-71.24
2024	Sun shade length	0.7H	0.4H	0.22H	0.28H	0.52H	0.87H	1.423H
Hour		**10:00**	**11:00**	**12:00**	**13:00**	**14:00**	**15:00**	**16:00**
June,	Altitude(θ) (°)	53.05	65.56	74.53	72.89	62.47	49.61	36.08
21,	Azimuth(β) (°)	62.53	51.09	19.43	-30.79	-55.23	-64.09	-67.43
2024	Sun shade length	0.752H	0.455H	0.277H	0.31H	0.521H	0.851H	1.372H

Table 3 Selected streets shadow analysis of April, 21 (10:00 AM - 16:00 PM)

Hour	**North – South**	**East -West**	**North East to South West**	**North West to South East**
10:00	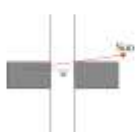 W = Sinβ*SHL W= 0.7 x 3m = 2.1m	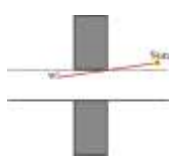 W = Cosβ*SHL W = 0.3m	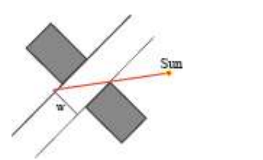 W = Sin(90 - β + 45)*SHL W = 1.65m	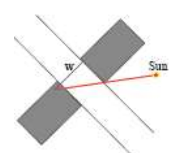 W = Cos(90 - β + 45)*SHL W =1.2m
11:00	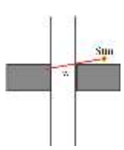 W = Sinβ*SHL W = 1.062m	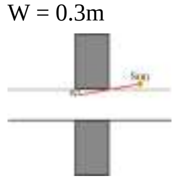 W = Cosβ*SHL W = 0.21m	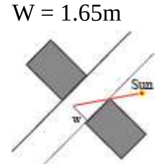 W = Sin(90 - β + 45)*SHL W = 0.9m	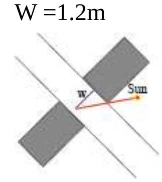 W = Cos(90 - β + 45)*SHL W= 0.612m

12:00	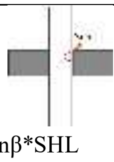 W = Sinβ*SHL W = 0.1H = 0.3m	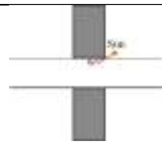 W = Cosβ*SHL W = 0.165m	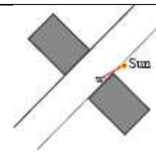 W = Sin(90 - β + 45)*SHL W = 0.1H = 0.3m	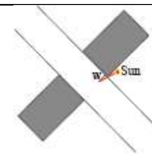 W = Cos(90 - β + 45)*SHL W = 0.02H = 0.06m
13:00	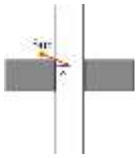 W = Sinβ*SHL W = -0.6m	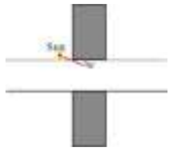 W = Cosβ*SHL W = 0.174m	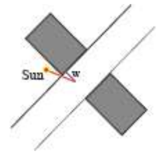 W = Sin(90 - β + 45)*SHL W = -027m	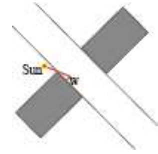 W = Cos(90 - β + 45)*SHL W = -1.2m
14:00	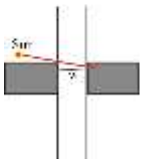 W = Sinβ*SHL W = -0.464H = -1.392m	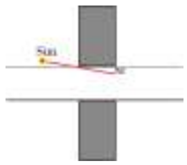 W = Cosβ*SHL W = 0.225m	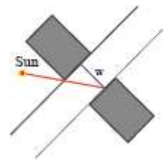 W = Sin(90 - β + 45)*SHL W = -0.9m	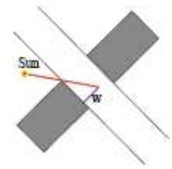 W = Cos(90 - β + 45)*SHL W = -1.2m
15:00	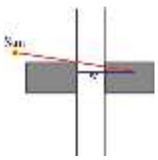 W = Sinβ*SHL W = -2.466m	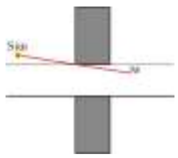 W = Cosβ*SHL W = 0.14H = 0.42m	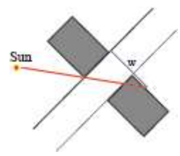 W = Sin(90 - β + 45)*SHL W = -0.5H = -1.5m	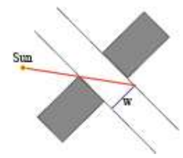 W = Cos(90 - β + 45)*SHL W = -0.663H = -1.989m
16:00	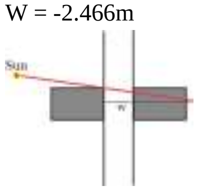 W = Sinβ*SHL W = -4.17m	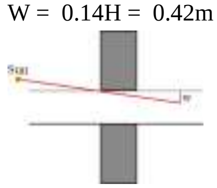 W = Cosβ*SHL W = 0.609m	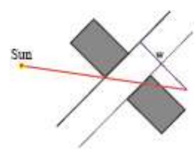 W = Sin(90 - β + 45)*SHL W = -2.52m	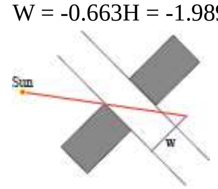 W = Cos(90 - β + 45)*SHL W = -3.369m

Table 4 Selected streets shadow analysis of May, 22 (10:00 AM - 16:00 PM)

Hour	**North – South**	**East -West**	**North East to South West**	**North West to South East**
10:00	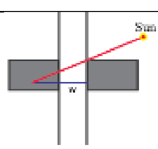 W = Sinβ*SHL W = 0.644H = 1.932m	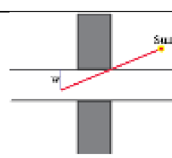 W = Cosβ*SHL W = 0.3H = 0.9m	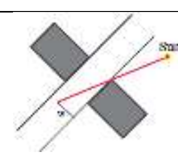 W = Sin(90 - β + 45)*SHL W = 0.65H = 1.95m	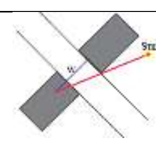 W = Cos(90 - β + 45)*SHL W = 0.261H = 0.783m
11:00	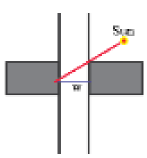 W = Sinβ*SHL W = 0.332H = 0.996m	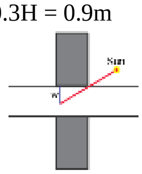 W = Cosβ*SHL W = 0.224H = 0.672m	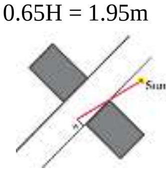 W = Sin(90 - β + 45)*SHL W = 0.4H = 1.2m	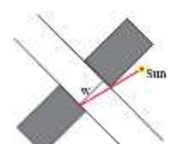 W = Cos(90 - β + 45)*SHL W = 0.1H = 0.3m

12:00	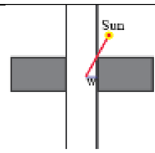 W = Sinβ*SHL W = 0.1H = 0.3m	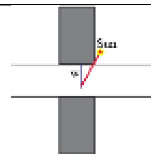 W = Cosβ*SHL W = 0.21H = 0.63m	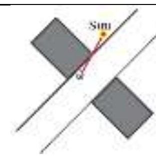 W = Sin(90 - β + 45)*SHL W = 0.2H = 0.6m	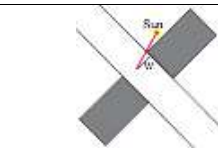 W = Cos(90 - β + 45)*SHL W = -0.09H = -0.27m
13:00	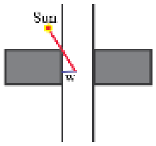 W = Sinβ*SHL W = -0.184H = -0.552m	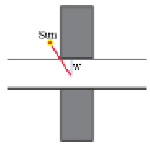 W = Cosβ*SHL W = 0.212H = 0.636m	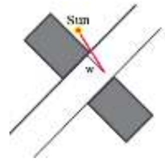 W = Sin(90 - β + 45)*SHL W = 0.02H = 0.06m	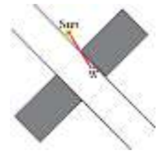 W = Cos(90 - β + 45)*SHL W = -0.28H = -0.84m
14:00	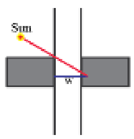 W = Sinβ*SHL W = -0.5H = -1.5m	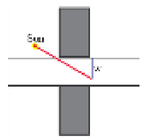 W = Cosβ*SHL W = 0.242H = 0.726m	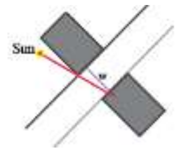 W = Sin(90 - β + 45)*SHL W = -0.155H = -0.465m	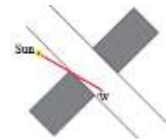 W = Cos(90 - β + 45)*SHL W = -0.5H = -1.5m
15:00	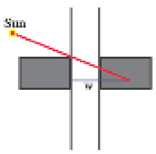 W = Sinβ*SHL W = -0.812H = -2.436m	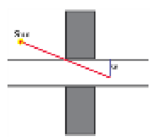 W = Cosβ*SHL W = 0.312H = 0.936m	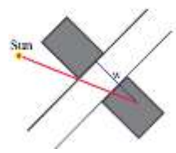 W = Sin(90 - β + 45)*SHL W = -0.354H = -1.062m	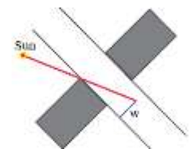 W = Cos(90 - β + 45)*SHL W = -0.795H = -2.385m
16:00	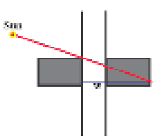 W = Sinβ*SHL W = -1.35H = -4.05m	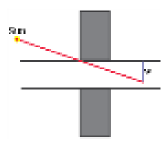 W = Cosβ*SHL W = 0.46H = 1.38m	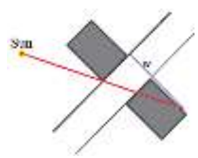 W = Sin(90 - β + 45)*SHL W = -0.63H = -1.89m	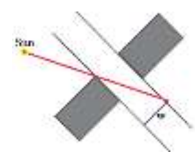 W = Cos(90 - β + 45)*SHL W = -1.28H = -3.84m

Table 5 Selected streets shadow analysis of June, 21 (10:00 AM - 16:00 PM)

Hour	North – South	East -West	North East to South West	North West to South East
10:00	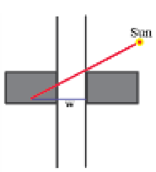 W = Sinβ*SHL W = 0.67H = 2.01m	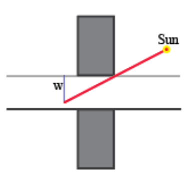 W = Cosβ*SHL W = 0.35H= 1.05m	 W = Sin(90 - β + 45)*SHL W = 0.72H = 2.16m	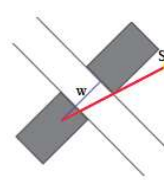 W = Cos(90 - β + 45)*SHL W = 0.23H = 0.69m

11:00	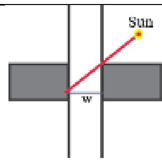 W = Sinβ*SHL W = 0.354H = 1.062m	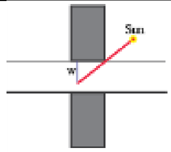 W = Cosβ*SHL W = 0.29H = 0.87m	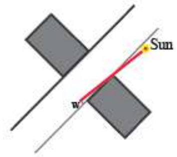 W = Sin(90 - β + 45)*SHL W = 0.452H = 1.356m	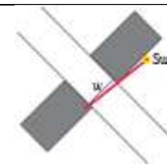 W = Cos(90 - β + 45)*SHL W = 0.05H = 0.15m
12:00	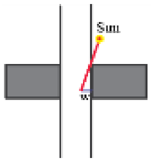 W = Sinβ*SHL W = 0.092H = 0.276m	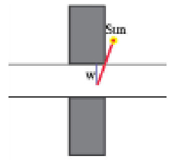 W = Cosβ*SHL W = 0.261H = 0.783m	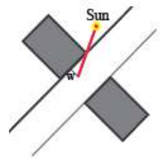 W = Sin(90 - β + 45)*SHL W = 0.25H = 0.75m	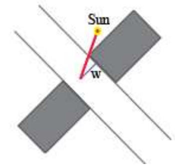 W = Cos(90 - β + 45)*SHL W = -0.12H = -0.36m
13:00	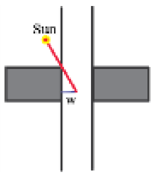 W = Sinβ*SHL W = -0.16H = -048m	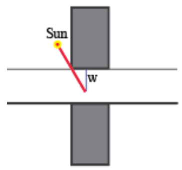 W = Cosβ*SHL W = 0.27H = 0.81m	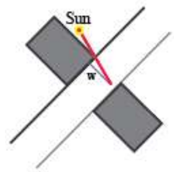 W = Sin(90 - β + 45)*SHL W = 0.08H = 0.24m	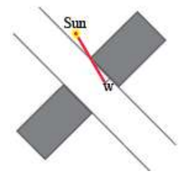 W = Cos(90 - β + 45)*SHL W = -0.3H = -0.9m
14:00	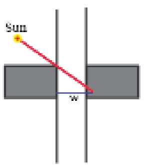 W = Sinβ*SHL W = -0.43H = -1.29m	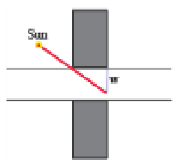 W = Cosβ*SHL W = 0.3H = 0.9m	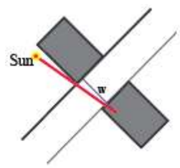 W = Sin(90 - β + 45)*SHL W = -0.1H = -0.3m	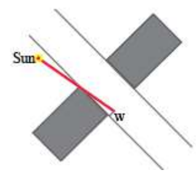 W = Cos(90 - β + 45)*SHL W = -0.513H = -1.539m
15:00	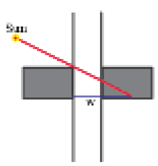 W = Sinβ*SHL W = -0.77H = -2.31m	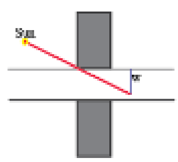 W = Cosβ*SHL W = 0.372H = 1.116m	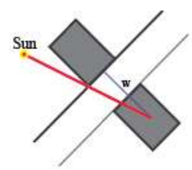 W = Sin(90 - β + 45)*SHL W = -0.3H = -0.9m	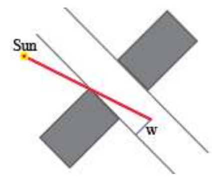 W = Cos(90 - β + 45)*SHL W = -0.804H = -2.412m
16:00	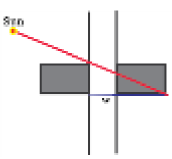 W = Sinβ*SHL W = -1.27H = -3.81m	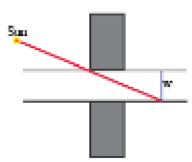 W = Cosβ*SHL W = 0.53H = 1.59m	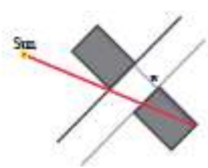 W = Sin(90 - β + 45)*SHL W = -0.524H = -1.572m	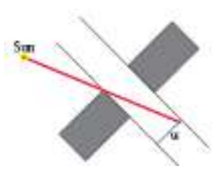 W = Cos(90 - β + 45)*SHL W = -1.27H = -3.81m

Tables 3,4 & 5 illustrates how buildings shadow on the streets vary across April, May, and June between 10:00 AM and 16:00 PM, with direct implications for pedestrian thermal comfort along selected street orientations. As solar altitude peaks around 12:00 and 13:00, the sun shade length (SHL) reaches its minimum, resulting in reduced shadow width to the streets. In all three hottest months, the shading from buildings on North-South (N-S) oriented streets consistently achieve longer and effective shading coverage throughout the day compared to East-West and diagonal streets due to favorable sun angles and it providing critical relief during walking. In contrast, E-W streets have minimal shading from north side buildings, but south side buildings never cast shadow to street all over three hottest months at the critical hours when solar exposure is most intense and diagonal orientations (NW-SE and NE-SW) struggle with inconsistent building shade due to angular misalignment with solar paths. Overall, the analyses show how strategic alignment especially preferring the N-S orientation can meaningfully mitigate direct solar exposure and improve pedestrian thermal conditions in warm dry climates of Metehara town.

3.2 Sky View Factor (SVF)

In warm dry climates, a sky view factor of less than 0.5 with careful design considerations is generally recommended for pedestrian thermal comfort promoting cooler conditions during the day and reducing heat stress. SVF between 0.3 and 0.5 is considered moderately shaded, while an SVF above 0.5 is considered less shaded and can lead to higher daytime temperatures and heat stress, according to Mohammad Taleghani (2019).

Table 6 Sky view factor values of the selected streets

No	Name	orientation	Sky view factor (SVF) value
1	Street-1	E–W	0.66
2	Street-2	N–S	0.49
3	Street-3	NE–SW	0.68
4	Street-4	NW–SE	0.96

A high SVF value results in high solar exposure, increasing pedestrian heat stress. In addition, minimal shading leads to elevated MRT intensify discomfort and lack of vegetation further increase thermal stress. Generally, street-2 (N-S) have good shade and comfortable for pedestrian than other selected streets orientations according to sky view factor value of all selected streets shows on table 6 above.

3.3 Pedestrian Perception

Thermal comfort vote as illustrated in the figure 2 below majority of respondents (55-90%) voted discomfort for all selected streets. Street-2 (N-S) had the highest percentage of pedestrian feeling neutral and comfortable indicating better thermal conditions likely due to good shading and natural ventilation. This suggests N-S oriented street provide good thermally pleasant experience for pedestrians during the hottest months in Metehara town.

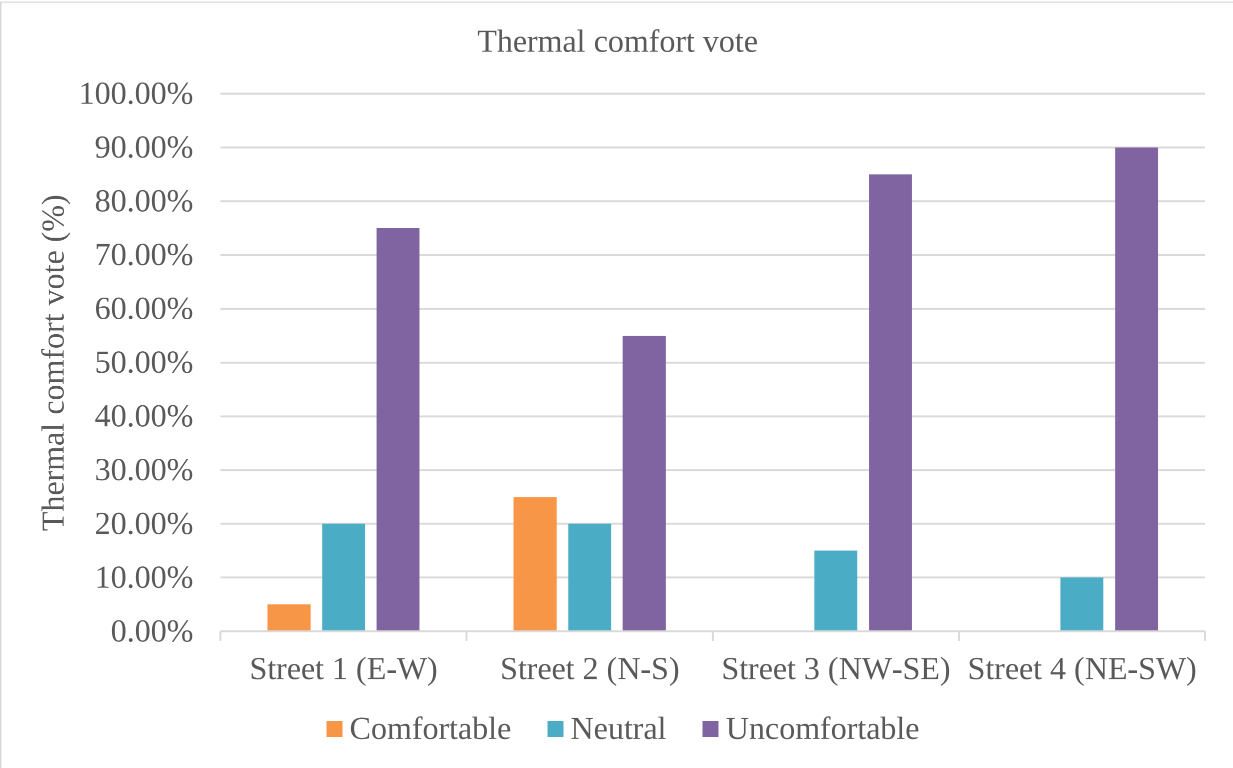

Figure 2 Thermal comfort vote percentage of respondents for the selected street orientation

3.4 Existing Microclimate Analysis

The hourly microclimatic data was taken as the real feeling of day to day human activities. In warm dry climate like Metehara town, tolerable air temperature for pedestrians generally falls within the range of 20^{o}c to 35^{o}c depending on like humidity, wind speed and solar radiation (Mohammad Teleghani, 2020). For the four selected streets the hourly air temperature was measured at one hour interval as shown in figure 3 for April, figure 4 for May and figure 5 for June below. Among the selected streets, the North-South (N-S) oriented street (Street-2) demonstrated relatively lower peak temperatures attributed to enhanced airflow and shading from vegetation. Conversely, the North East-South West (NE-SW) oriented street (Street-4) exhibited the highest temperatures due to reduced shading mechanisms and impeded ventilation, thereby posing high thermal stress to pedestrians.

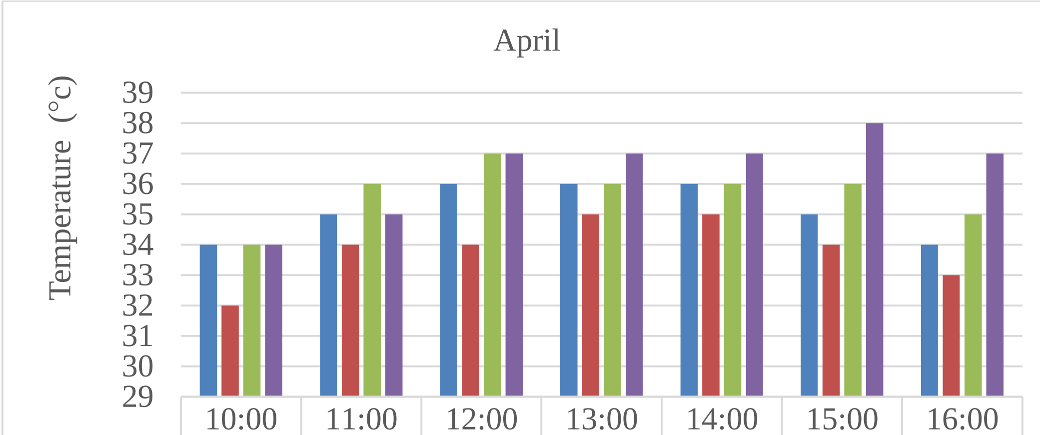

	10:00	11:00	12:00	13:00	14:00	15:00	16:00
street 1	34	35	36	36	36	35	34
street 2	32	34	34	35	35	34	33
street 3	34	36	37	36	36	36	35
street 4	34	35	37	37	37	38	37

Figure 3 April hourly selected streets temperature variation

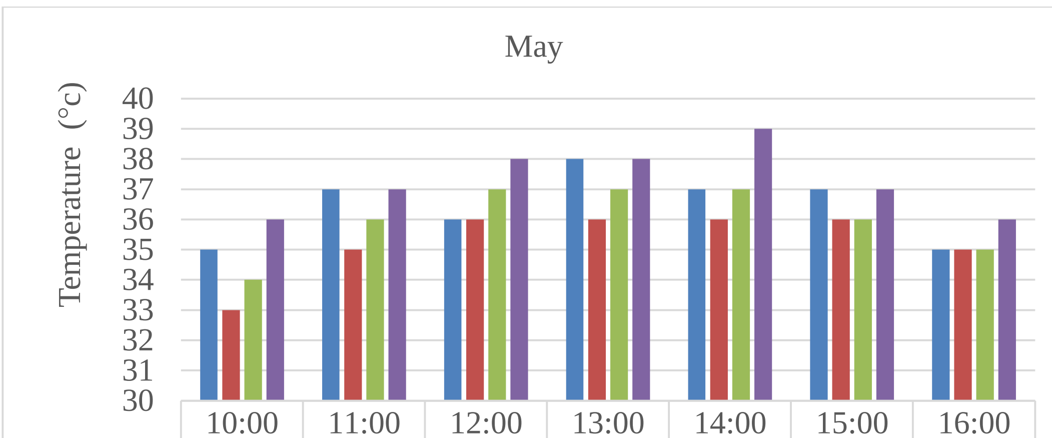

	10:00	11:00	12:00	13:00	14:00	15:00	16:00
street 1	35	37	36	38	37	37	35
street 2	33	35	36	36	36	36	35
street 3	34	36	37	37	37	36	35
street 4	36	37	38	38	39	37	36

Figure 4 June hourly selected streets temperature variation

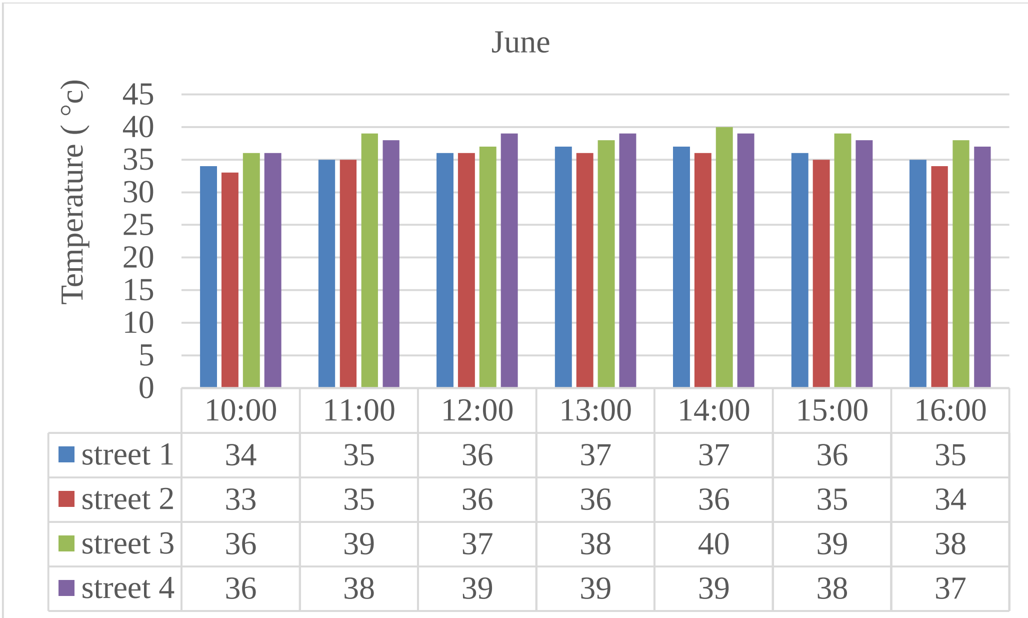

Figure 5 June hourly selected streets temperature variation

Wind speed according to Zhang & deng x. (2020) in warm dry climate tolerable wind speed for pedestrian thermal comfort typically range between 1 to 3.5 m/s, depending on factors such as air temperature, solar radiation and humidity. Wind speed data was obtained from NASA Power at hourly intervals for April, May, and June.

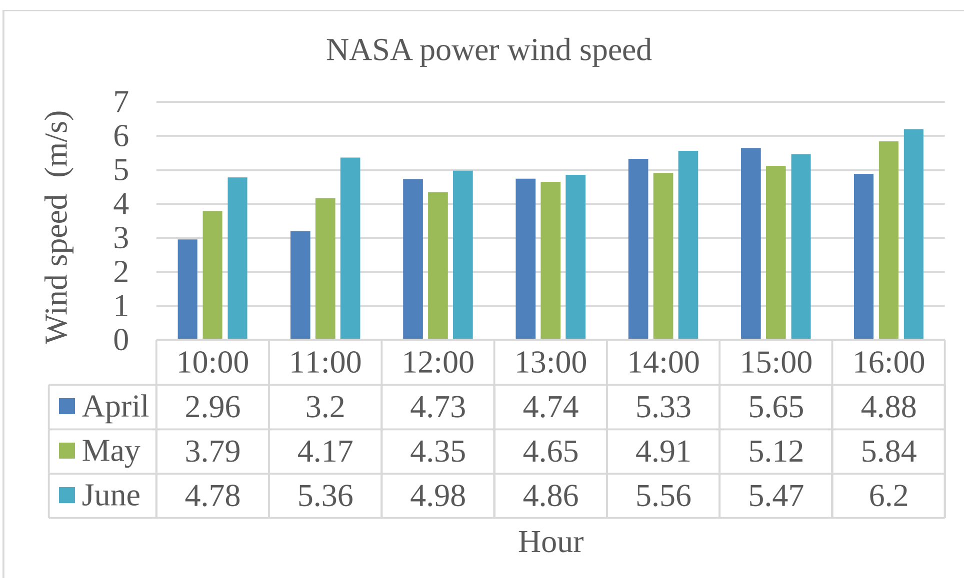

Figure 6 Hourly NASA power wind speed (April-June, 10:00-16:00)

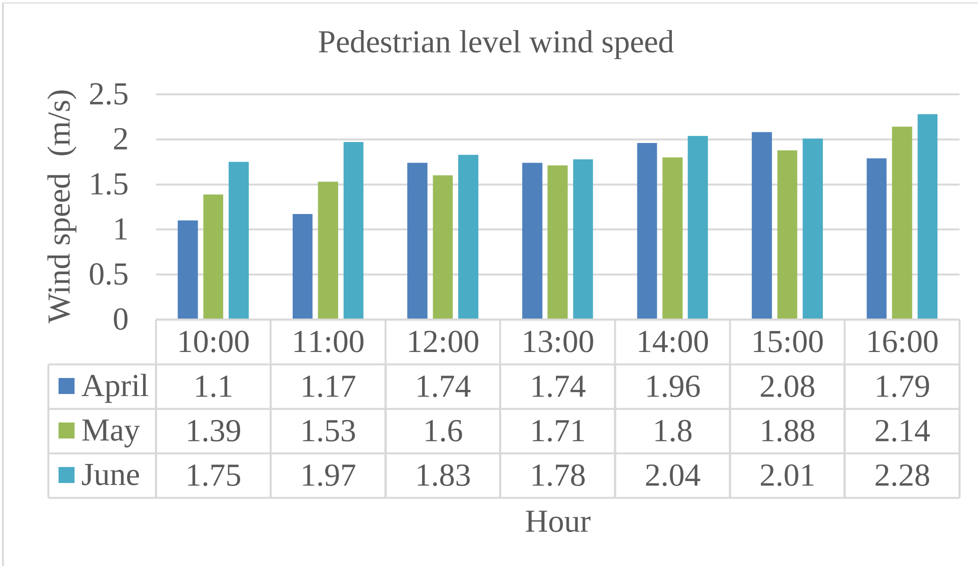

Figure 7 Hourly pedestrian level wind speed (April-June, 10:00-16:00)

The pedestrian level wind speed calculated by logarithmic wind profile equation value shows on the figure 7 above can be tolerable for pedestrians but it depends on the wind direction and street orientation. The data illustrates that wind speeds generally rise during the afternoon across all months, with June exhibiting the highest overall values. Higher wind speeds contribute significantly to pedestrian thermal comfort by enhancing airflow and reducing heat stress. Streets aligned with prevailing wind patterns benefit most, emphasizing the need for strategic urban planning to maximize ventilation potential. Conversely, areas with obstructed airflow should prioritize shading and vegetation to alleviate heat related discomfort in the town.

3.5 Mean Radiant Temperature

MRT is a critical factor in evaluating street orientation for pedestrian thermal comfort. It represents the average temperature of all surrounding surfaces that radiate heat and plays a significant role in the overall thermal sensation experienced by pedestrians. In warm dry urban environments, mean radiant temperature (MRT) values below 40 - 45 °C are generally tolerable for adapted pedestrians especially when aligned with moderate wind speeds and relative humidity (Krüger & Pearlmutter, 2015). Figure 8 illustrates the hourly variation of mean radiant temperature for the selected street orientations averaged across the hottest months (April-June).

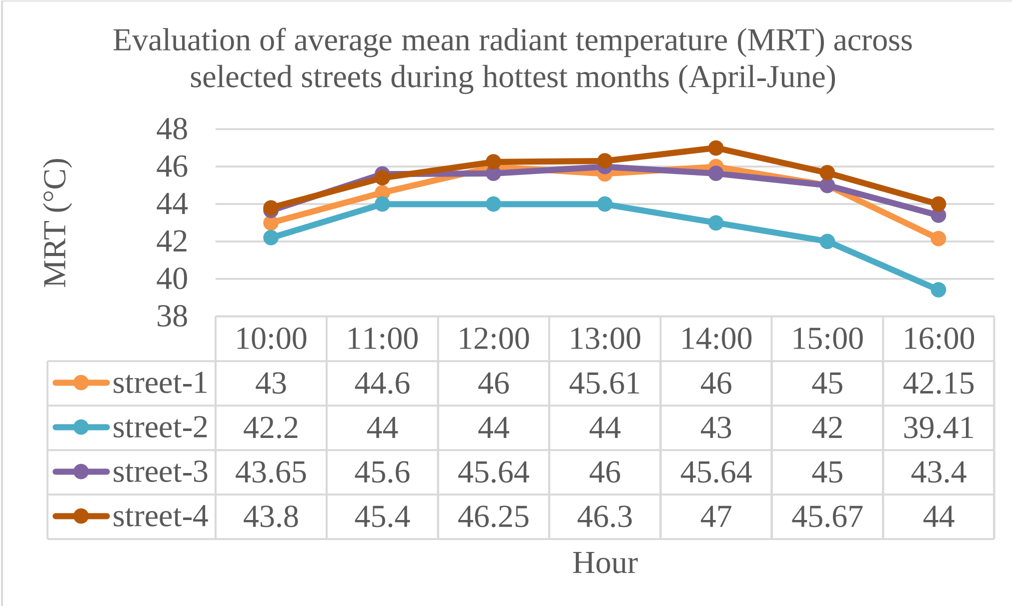

	10:00	11:00	12:00	13:00	14:00	15:00	16:00
street-1	43	44.6	46	45.61	46	45	42.15
street-2	42.2	44	44	44	43	42	39.41
street-3	43.65	45.6	45.64	46	45.64	45	43.4
street-4	43.8	45.4	46.25	46.3	47	45.67	44

Figure 8 Evaluation of average mean radiant temperature for selected streets

Across all orientations the figure 8 above illustrates MRT peaked between 11:00 AM and 14:00 PM reflecting the hours of maximum solar intensity and minimal shading exist. Street-4 (NE-SW) registered the highest MRT values 47 °C at 14:00 PM likely due to lack of shading, vegetation, wind flow and high SVF (0.96), which expose pedestrians to prolonged solar gain particularly between 11:00-14:00. In contrast, the N-S street maintained MRTs generally 1-4 °C lower than diagonal streets and E-W street by partial tree shading and more effective wind flow and lower SVF (0.49). These findings shows the importance of climate responsive urban geometry to mitigate radiant heat stress in pedestrian area.

3.6 Universal Thermal Climate Index

Figure 9 illustrates the average hourly universal thermal climate index (UTCI) across the four selected streets in Metehara, combined data from the peak thermal stress months of April to June. The UTCI integrates key parameters these are air temperature, relative humidity, wind speed & mean radiant temperature to estimate outdoor thermal comfort. The UTCI values on figure 9 below are calculated by using online UTCI calculator based on the collected key parameters for each street orientation.

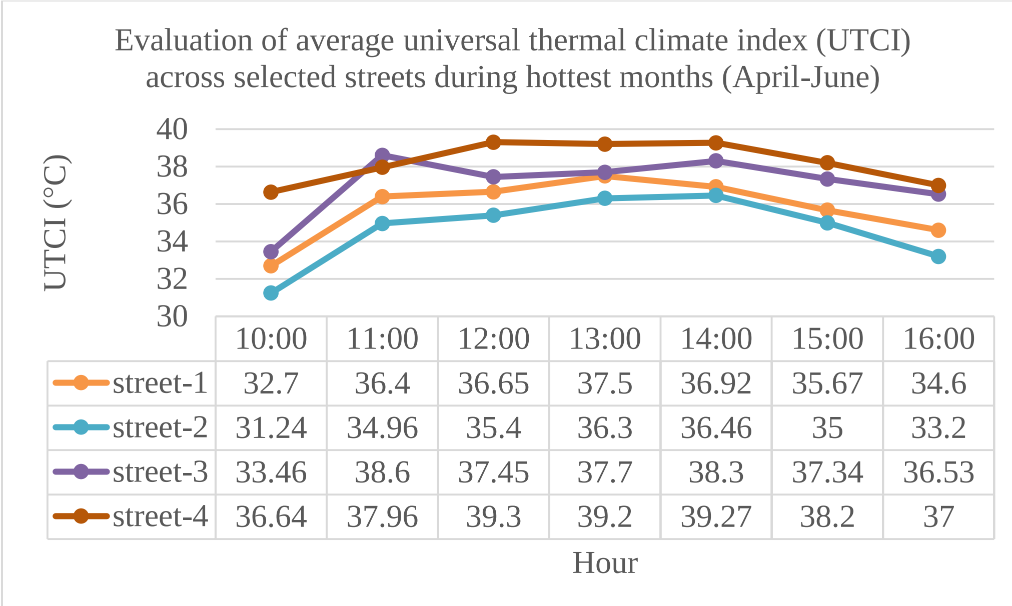

	10:00	11:00	12:00	13:00	14:00	15:00	16:00
street-1	32.7	36.4	36.65	37.5	36.92	35.67	34.6
street-2	31.24	34.96	35.4	36.3	36.46	35	33.2
street-3	33.46	38.6	37.45	37.7	38.3	37.34	36.53
street-4	36.64	37.96	39.3	39.2	39.27	38.2	37

Figure 9 Evaluation of average universal thermal climate index for selected streets

The figure 9 above illustrates, all streets experienced strong to very strong thermal stress during critical hours. Street-4 (NE-SW) registered the highest UTCI values throughout the day 39.3 °C at 13:00 PM, due to lack of shading elements and also wind flow in case of wind break by buildings. In contrast the street-2 (N-S) maintained relatively lower UTCI values, peak values approximately 1-4 °C lower than E-W and diagonal streets, but still it falls in strong heat stress. Overall, the UTCI values of the selected streets are high especially at the hour of 11:00 AM-15:00 PM of the day; it's typically indicate the streets thermal discomfort for pedestrians. The streets needs shading, air velocity for cooling the pedestrians to get thermally comfortable streets.

4. Conclusion

The study concluded that street orientation plays critical role in shaping thermal comfort for pedestrians. Among the four selected street orientations examined in Metehara, N-S streets consistently provided more favorable microclimatic conditions due to better alignment with prevailing winds and more effective shading. The N-S street demonstrate lower mean radiant temperatures and sky view factors (0.49) and also well thermal perception among pedestrians when compared to other selected streets. In contrast East-West and diagonally oriented streets showed higher thermal stress driven by poor solar geometry and limited airflow. The findings point out the need for planners and designers to prioritize climate responsive street layouts, vegetation strategies and shading is essential to support walkability in rapidly urbanizing warm dry of Metehara town.

References

(1) Antonello, D. N. (2020). UTCI online calculator. Retrieved from https://www.utci.org

(2) Fanger, P. O. (1982). Thermal comfort: Analysis and applications in environmental engineering. New York: McGraw-Hill.

(3) Grimmond, C. S. B. (1999). Urban canyon surface energy balance: Sensitivity to the street canyon geometry. Boundary-Layer Meteorology, 94(3), 489–495.

(4) Kleerekoper, L., van Esch, M., & Salcedo, R. (2012). How to make a city climate-proof, addressing the urban heat island effect. Resources, Conservation and Recycling, 64, 30–38.

(5) Krüger, E. L., & Pearlmutter, D. (2015). Thermal comfort and outdoor urban spaces: Design and climate considerations in hot-humid regions. Building and Environment, 94, 544–553.

(6) Lindberg, F., & Grimmond, C. S. B. (2010). Continuous sky view factor maps from high-resolution urban digital elevation models. Climate Research, 42(1), 177–183.

(7) Ministry of Agriculture (MOA). (2000). Climate data analysis for Ethiopian regions. Addis Ababa, Ethiopia.

(8) Mohammad Taleghani. (2019). optimizing outdoor thermal comfort: Guidelines for warm climates. In Urban Microclimate Design for Warm Climates (pp. xx–xx).

(9) NASA. (1993–2023). POWER project climate data. Retrieved from https://power.larc.nasa.gov/

(10) Oke, T. R. (1981). Canyon geometry and the nocturnal urban heat island: Comparison of scale model and field observations. Journal of Climatology, (3), 237–254.

(11) Shashua-Bar, L., & Hoffman, M. E. (2003). Geometry and orientation effects on outdoor thermal comfort in hot arid zones. Energy and Buildings, 35(1), 27-37.

(12) Shishegar, N. (2013). Street geometry in improving pedestrian thermal comfort in urban areas. Procedia - Social and Behavioral Sciences, 85, 108–117.

(13) Taleghani, M. (2020). Outdoor thermal comfort in urban design: Application of climate indices in hot climates. In Urban Microclimate Design

(14) United Nations. (2014). World Urbanization Prospects: The 2014 Revision. United Nations Department of Economic and Social Affairs.

(15) Zhang, L., & Deng, X. (2020). Effects of wind velocity and direction on pedestrian thermal comfort in a hot climate. Sustainable Cities and Society, 55, 102049.